INFLAMMATION OF PERIPHERAL TISSUES AND INJURY TO PERIPHERAL NERVES INDUCE DIFERRING EFFECTS IN THE EXPRESSION OF THE CALCIUM-SENSITIVE ANANDAMIDE-SYNTHESISING ENZYME AND RELATED MOLECULES IN RAT PRIMARY SENSORY NEURONS

Journal:	*Journal of Comparative Neurology*
Manuscript ID	JCN-15-0306.R1
Wiley - Manuscript type:	Research Article
Keywords:	cannabinoid type 1 receptor, transient receptor potential vanilloid type 1 ion channel, fatty acid amide hydrolase, pain, inflammation, neuropathy

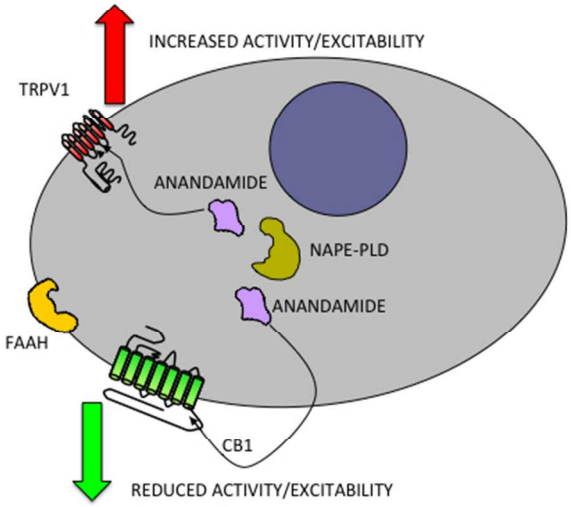

254x190mm (72 x 72 DPI)

The anandamide-synthesising NAPE-PLD, together with the anandamide-responding CB1 receptor and TRPV1, and the anandamide-hydrolysing FAAH, forms a signalling system, which responds to peripheral pathological processes and regulates the activity of a sub-population of nociceptive primary sensory neurons. Hence, NAPE-PLD could be the target for the development of novel analgesics.

INFLAMMATION OF PERIPHERAL TISSUES AND INJURY TO PERIPHERAL NERVES INDUCE DIFERRING EFFECTS IN THE EXPRESSION OF THE CALCIUM-SENSITIVE ANANDAMIDE-SYNTHESISING ENZYME AND RELATED MOLECULES IN RAT PRIMARY SENSORY NEURONS

Dr João Sousa-Valente[1], Dr Angelika Varga[1,2], Mr Jose Vicente Torres Perez[1], Dr Agnes Jenes[1,2], Dr John Wahba[1], Professor Ken Mackie[3], Professor Benjamin Cravatt[4], Professor Natsuo Ueda[5], Dr Kazuhito Tsuboi[5], Dr Peter Santha[6], Professor Gabor Jancso[6], Dr Hiren Tailor[1], Dr António Avelino[7] and Hon Professor Istvan Nagy[1]

[1]Section of Anaesthetics, Pain Medicine and Intensive Care, Department of Surgery and Cancer, Imperial College London, Chelsea and Westminster Hospital, 369 Fulham Road, London, SW10 9NH, United Kingdom; [2]Department of Physiology, University of Debrecen, Medical and Health Science Center, Nagyerdei krt. 98, Debrecen, H-4012, Hungary; [3]Department of Psychological & Brain Sciences, Gill Center for Biomedical Sciences, Indiana University, Bloomington, IN 47405, USA; [4] The Skaggs Institute for Chemical Biology and Department of Chemical Physiology, The Scripps Research Institute, La Jolla, California, USA; [5]Department of Biochemistry, Kagawa University School of Medicine, 1750-1 Ikenobe, Miki, Kagawa 761-0793, Japan [6] Department of Physiology, University of Szeged, Dóm tér 10, 6720, Szeged, Hungary; [7]Departamento de Biologia Experimental, Faculdade de Medicina do Porto, Rua, Plácido Costa, 4200-450 Porto, Portugal and I3S - Instituto de Investigação e Inovação em Saúde, IBMC - Instituto de Biologia Molecular e Celular, Rua Alfredo Allen, 208 4200-135 Porto, Portugal

Abbreviated title: NAPE-PLD in DRG

Associate Editor: Prof. Gert Holstege

Keywords: cannabinoid type 1 receptor, transient receptor potential vanilloid type 1 ion channel, fatty acid amide hydrolase, pain, inflammation, neuropathy

RRID: Aviva Systems Biology Cat# ARP55927_P050 RRID:AB

Correspondence: Istvan Nagy, MD, PhD, Section of Anaesthetics, Pain Medicine and Intensive Care, Department of Surgery and Cancer, Imperial College London, Chelsea and Westminster Hospital, 369 Fulham Road, London, SW10 9NH, United Kingdom, Phone: (0)20-33158897, Fax: (0)2033155109, email: i.nagy@imperial.ac.uk

Acknowledgements: Part of this work has been supported by a project grant from the Wellcome Trust (061637/Z/06/Z) and the NIH (DA011322 and DA021696). João Sousa-Valente has been supported by a PhD studentship from Fundação para a Ciência e a Tecnologia (Portugal). Angelika Varga has been supported by a European Union Marie Curie Intra-European Fellowship (254661) and by a Hungarian Social Renewal Operation Program (TÁMOP 4.1.2.E-13/1/KONV-2013-0010). Jose Vicente Torres Perez has been supported by a capacity building grant provided by the Chelsea and Westminster Health Charity. Agnes Jenes has been supported by a British Journal of Anaesthesia / Royal College of Anaesthetists Project Grant. Peter Santha has been supported by a Janos Bolyai Research Fellowship from the Hungarian Academy of Sciences.

ABSTRACT

Elevation of intracellular Ca^{2+} concentration induces the synthesis of N-arachydonoylethanolamine (anandamide) in a sub-population of primary sensory neurons. N-acylphosphatidylethanolamine phospholipase D (NAPE-PLD) is the only known enzyme, which synthesises anandamide in a Ca^{2+}-dependent manner. NAPE-PLD mRNA, as well as anandamide's main targets, the excitatory transient receptor potential vanilloid type 1 ion channel (TRPV1) and the inhibitory cannabinoid type 1 (CB1) receptor and the main anandamide-hydrolysing enzyme fatty acid amide hydrolase (FAAH) are all expressed by sub-populations of nociceptive primary sensory neurons. Thus, NAPE-PLD, TRPV1, the CB1 receptor and FAAH could form an autocrine signalling system, which could shape the activity of a major sub-population of nociceptive primary sensory neurons, hence contribute to the development of pain. While the expression patterns of TRPV1, the CB1 receptor and FAAH have been comprehensively elucidated, little is known about NAPE-PLD expression in primary sensory neurons under physiological and pathological conditions. We report that NAPE-PLD is expressed by about a third of primary sensory neurons, the overwhelming majority of which also express nociceptive markers as well as the CB1 receptor, TRPV1 and FAAH. Inflammation of peripheral tissues and injury to peripheral nerves induce differing but concerted changes in the expression pattern of NAPE-PLD, the CB1 receptor, TRPV1 and FAAH. Together these data indicate the existence of the anatomical basis for an autocrine signalling system, in a major proportion of nociceptive primary sensory neurons, and that alterations in that autocrine signalling by peripheral pathologies could contribute to the development of both inflammatory and neuropathic pain.

INTRODUCTION

N-arachidonoylethanolamine (anandamide) is a lipid signalling molecule (Devane et al., 1992), which is synthesised both in a Ca^{2+}-insensitive and Ca^{2+}-sensitive manner through respective multiple enzymatic pathways and a single pathway which involves the activity of N-acylphosphatidylethanolamine phospholipase D (NAPE-PLD) (Ueda et al., 2001; Okamoto et al., 2004; Wang et al., 2006; Wang et al., 2008). Although, anandamide acts on a series of molecules, the transient receptor potential vanilloid type 1 ion channel (TRPV1) (Caterina et al., 1997) and the cannabinoid 1 (CB1) receptor (Matsuda et al., 1990) are believed to be anandamide's main targets (Devane et al., 1992; Zygmunt et al., 1999). While activation of TRPV1 results in the opening of this non-selective cationic channel and subsequent excitation of nociceptive primary sensory neurons, activation of the CB1 receptor is believed to produce an inhibitory effect, which includes the inhibition of L-, P/Q-, and N-type voltage-gated Ca^{2+} channels in neurons including primary sensory neurons (Mackie and Hille, 1992; Mackie et al., 1995; Caterina et al., 1997; Twitchell et al., 1997; Tominaga et al., 1998). Intriguingly, the CB1 receptor and TRPV1 are co-expressed by various neurons including a great proportion of nociceptive primary sensory neurons (Ahluwalia et al., 2000; Binzen et al., 2006; Mitrirattanakul et al., 2006; Agarwal et al., 2007). This anatomical arrangement enables exogenous anandamide to control the activity of neurons including a major group of nociceptive primary sensory neurons (Ahluwalia et al., 2003).

Anandamide is synthesised in sub-populations of primary sensory neurons both in Ca^{2+}-sensitive and Ca^{2+}-insensitive manners (van der Stelt et al., 2005; Vellani et al., 2008; Varga et al., 2014). In agreement with the ability of a group of primary sensory

neurons to synthesise anandamide in a Ca^{2+}-sensitive manner (van der Stelt et al., 2005) and the role of NAPE-PLD in such anandamide synthesis (Ueda et al., 2001; Okamoto et al., 2004; Wang et al., 2006; Wang et al., 2008), NAPE-PLD mRNA is expressed by primary sensory neurons (Nagy et al., 2009). Importantly, the majority of the NAPE-PLD mRNA-expressing cells are capsaicin sensitive (Nagy et al., 2009), therefore, they should also express TRPV1, and the CB1 receptor (Ahluwalia et al., 2000; Binzen et al., 2006; Mitrirattanakul et al., 2006; Agarwal et al., 2007). Thus, in addition to exogenous anandamide, anandamide of primary sensory neuron origin could also be able to control TRPV1 and CB1 receptor activity in a major sub-population of nociceptive primary sensory neurons in an autocrine manner (van der Stelt and Di Marzo, 2005; van der Stelt et al., 2005).

In addition to NAPE-PLD and the CB1 receptor, the great majority of TRPV1-expressing primary sensory neurons also express the main anandamide-hydrolysing enzyme, fatty acid amide hydrolase (FAAH) (Cravatt et al., 1996; Lever et al., 2009). Blocking FAAH activity, through increasing the level of anandamide, also results in regulating the activity of a proportion of nociceptive primary sensory neurons through the CB1 receptor and TRPV1 (Lever et al., 2009). Based on the co-expression pattern of TRPV1, the CB1 receptor, NAPE-PLD and FAAH, and the effects of those molecules, the presence of an endocannabinoid/endovanilloid autocrine signalling system built by those molecules has been proposed in a major sub-population of nociceptive primary sensory neurons (van der Stelt and Di Marzo, 2005; van der Stelt et al., 2005; Sousa-Valente et al., 2014b). That autocrine signalling system, through TRPV1- and CB1 receptor-mediated changes in the intracellular Ca^{2+} concentration and subsequent NAPE-PLD-mediated anandamide synthesis, as well as FAAH-

mediated anandamide hydrolysis is considered to be prominently suitable to provide a significant control over TRPV1 and CB1 receptor activity in, hence over the excitation of, a major group of nociceptive primary sensory neurons (van der Stelt and Di Marzo, 2005; Sousa-Valente et al., 2014b; Varga et al., 2014).

The excitation level of nociceptive primary sensory neurons is pivotal for the initiation and maintenance of pain experiences including those which are associated with peripheral pathologies, such as inflammation of peripheral tissues and injury to peripheral nerves (Nagy et al., 2004; Sousa-Valente et al., 2014a). Therefore, the control provided by the endocannabinoid/endovanilloid autocrine signalling system built by the CB1 receptor, TRPV1, NAPE-PLD and FAAH in a major group of nociceptive primary sensory neurons may play an important role in the development and maintenance of pain. While the expression patterns, and the changes in those expression patterns by pathological conditions, of the CB1 receptor, TRPV1 and FAAH have comprehensively been elucidated (Hudson et al., 2001; Ji et al., 2002; Zhou et al., 2003; Amaya et al., 2004; Bar et al., 2004; Luo et al., 2004; Amaya et al., 2006; Mitrirattanakul et al., 2006; Yu et al., 2008; Lever et al., 2009; Malek et al., 2015), little is known about those properties and changes of NAPE-PLD. Accordingly, in order to improve our understanding of the putative autocrine cannabinoid/endovanilloid signalling in primary sensory neurons, here we describe the co-expression patterns of NAPE-PLD with TRPV1, the CB1 receptor and FAAH in naive condition and changes those expression patters by pathological conditionas. Preliminary findings have been reported earlier (Valente et al., 2011).

METHODS

Forty two male Wistar rats (250-300 g), 10 C57BL/6 wild type (WT) and 10 NAPE-PLD$^{-/-}$ (Leung et al., 2006; Tsuboi et al., 2011) adult mice were used in this study. NAPE-PLD$^{-/-}$ mice were generated by the deletion of a sequence (from amino acid 99 to amino acid 313), which contains the catalytic domain of the enzyme (Leung et al., 2006; Tsuboi et al., 2011). Both WT and NAPE-PLD$^{-/-}$ mice have been used for antibody control purposes. All quantitative assessments on NAPE-PLD expression pattern have been performed on rat tissues.

All procedures were performed according to the UK Animals (Scientific Procedures) Act 1986, the revised National Institutes of Health *Guide for the Care and Use of Laboratory Animals*, the Directive 2010/63/EU of the European Parliament and of the Council on the Protection of Animals Used for Scientific Purposes and the guidelines of the Committee for Research and Ethical Issues of IASP published in Pain, 16 (1983) 109-110. Further, we fully obeyed to Good Laboratory Practice and ARRIVE guidelines. Every effort was taken to minimize the number of animals used.

Rat models of inflammatory and neuropathic pain

Tissue inflammation was induced by injecting 50µl of 50% complete Freund's adjuvant (CFA, Thermo Scientific, USA) or incomplete Freund's adjuvant (IFA, Thermo Scientific, USA) subcutaneously into the plantar aspect of the left hindpaw of adult rats. The injection was performed under isoflurane-induced anaesthesia.

Nerve injury was produced according to previously published protocols (Kim and Chung, 1992). Briefly, rats were deeply anaesthetised by isoflurane and the fifth lumbar (L5) spinal nerve was exposed and identified after partial laminectomy. A

tight 4.0 ligature was then placed around the nerve. The nerve was cut about 5mm distal from the ligature and the wound was closed in layers. The sham operation consisted of exposing the L5 spinal nerve without placing the ligature or cutting the nerve.

Testing pain-related behaviour

Inflammation- or nerve injury-induced changes in responses to mechanical stimuli were assessed by using an electrical von Frey apparatus (Ugo Basile, Italy). Briefly, rats were placed in a Perspex chamber with a 0.8 cm-diameter mesh flooring and allowed to acclimatize for 15 min. The tip of the probe was pressed against the plantar surface of the paw at a steadily increasing pressure, until the animal voluntarily withdrew the paw. The paw-withdrawal threshold was defined as the average weight in grams over three applications. Care was given not to repeat testing on the same paw within 5 minutes. Responses to mechanical stimuli were assessed every day for two days prior to, and three days after, the injection of either CFA or IFA. In animals which were subjected to nerve injury, changes in the sensitivity to mechanical stimulation was assessed every day for two days prior to, and then on the second, fourth and seventh day after, the surgery.

Inflammation- or nerve injury-induced changes in responses to noxious heat stimuli were assessed by the Hargreaves test (Hargreaves et al., 1988). Briefly, rats were placed in a Perspex box. After a fifteen minutes acclimatisation period, an infrared beam (Ugo Basile, Italy), which is able to deliver a constantly increasing thermal stimulus, was directed to the plantar surface of the paw. The time until the animal voluntarily withdrew the paw was measured. Again, attention was given not to repeat

testing on the same paw within 10 minutes. Responses to heat and mechanical stimuli were assessed on the same days.

Reverse transcriptase polymerase chain reaction (RT-PCR)

Rats were terminally anaesthetised with isoflurane and L4 and L5 DRGs were collected in RNAlater (Sigma-Aldrich, USA) and homogenised using QIA shredder columns (QIAGEN, UK). Total RNA was extracted using RNeasy Plus Mini Kit (QIAGEN, UK) according to the manufacturer's instruction. RNA was reverse-transcribed using SuperScript II cDNA synthesis reagents (Invitrogen, USA). Sequences of the primers (Eurofins MWG Operon, Germany) designed to amplify rat NAPE-PLD (NM_199381.1) are: forward: TACCAACATGCTGACCCAGA; reverse: ATCGTGACTCTCCGTGCTTC. Sequences of primers designed to amplify the housekeeping gene, glyceraldehyde-3- phosphate dehydrogenase (GAPDH, NC_005103) are: forward: ACCCATCACCATCTTCCA; reverse: CATCACGCCACAGCTTTCC. The annealing temperature was 57^{o}C and product sizes were 199bp for NAPE-PLD and 380bp for GAPDH. The PCR mixture was composed of cDNA, primers, 1.5 mM $MgCl_2$, 1× Green Go-Taq Reaction buffer (Promega, USA), 0.2 mM deoxynucleotide mix (Promega, USA) and 1.25 U Go-Taq DNA polymerase (Promega, USA), the number of cycles was 30. After amplification, PCR products were separated by electrophoresis on 2% agarose gels and visualized with ethidium bromide using Syngene G:BOX (Synoptics Ltd, UK). Images were analysed by Syngene's GeneTools software (Synoptics Ltd, UK).

Western-blotting

Rats and mice were terminally anaesthetised with isoflurane and L4 and L5 DRGs

were collected and homogenized on ice in NP40 cell lysis buffer (Invitrogen, USA) supplemented with protease inhibitors cocktail (Sigma, USA). The protein content of the samples was determined with the BCA Protein Assay Reagent (Pierce Biotechnology, IL, USA). Proteins were denatured at 95 ºC for 10 minutes with 4-times concentrated NuPAGE LDS sample buffer (Invitrogen, USA) after which they were run in a NuPAGE Novex 4-12% Bis-Tris gel (Invitrogen, USA) and blotted onto PVDF membrane using the iBlot® Dry Blotting System (Invitrogen, USA). To visualise NAPE-PLD, the membrane was first incubated in 5% non-fat milk and then in an anti-NAPE-PLD antibody (1:1000, Aviva Systems Biology, USA), overnight at 4 ºC. The anti-NAPE-PLD antibody has been raised against the 71-130 amino acid sequence of the protein (TWKNPSIPNVLRWLIMEKDHSSVPSSKEELDKELPVLKPYFITNPEEAGV). Forty four % of this sequence is missing in NAPE-PLD-/- mice (Leung et al., 2006; Tsuboi et al., 2011).

Following the incubation of the membranes in the anti-NAPE-PLD antibody, they were incubated with Horseradish peroxidase-conjugated goat anti-rabbit secondary antibody (1:1000, Cell Signaling, USA) for an hour at room temperature. Western blotting luminol reagent (Santa Cruz, USA) was used for visualization. Images were captured using Syngene G:BOX (Synoptics Ltd, UK) and were analysed by Syngene's GeneTools software (Synoptics Ltd, UK). Membranes were then stripped with 0.2 M glycine stripping buffer supplemented with 0.5% Tween-20 (pH 3.0) at room temperature for 30 minutes and re-probed with rabbit anti-β-actin as a loading control (1:1000, Cell Signaling Technology, Danvers, MA).

Immunostaining

Animals were terminally anaesthetised by intraperitoneal injection of sodium pentobarbital (60 mg/kg) and perfused through the ascending aorta with 100 ml of 0.9% saline followed by 300 ml of 4% paraformaldehyde in 0.1 M phosphate buffer (PB; pH 7.4). The cerebellum and L4 and L5 DRGs were identified and collected bilaterally. Tissues were post-fixed for 4h-24h at 4°C in 4% paraformaldehyde in 0.1 M PB, cryoprotected in 30% sucrose in 0.1 M PB for 1-2 days at 4°C, embedded in a mounting medium and cut with a cryostat into either 10µm sections for DRG tissue or 30 µm for cerebella which were mounted on Superfrost slides.

Slides were washed with PBS containing 0.3% Triton X-100 (PBST) and then incubated with PBST containing 10% normal donkey serum (Jackson ImmunoResearch Labs, USA) for 1 hour at room temperature. Slides were then incubated in PBST containing 2% NDS and the appropriate primary antibody/antibodies for 24 hours at room temperature. The antibodies, in addition to the anti-NAPE-PLD antibody described above included: anti-NF200 (200kD neurofilament) andibody (Sigma-Aldrich): clone NE14; anti-CGRP (calcitonin gene-related peptide) antibody Abcam: AB22560; anti-TRPV1 antibody (A. Avelino laboratory): EDAEVFKDSMVPGEK; anti-CB1 receptor antibody (K. Mackie laboratory): SCNTATCVTHRLAGLLSRSGGVVKDNFVPTNVGSEAF; anti-FAAH antibody (B. Cravatt laboratory): GAATRARQKQRASLETMDKAVQRFRLQNPDLDSEALLTLPLLQLVQKLQSG ELSPEAVFFTYLGKAWEVNKGTNCVTSYLTDCETQLSQAPRQGLLYGVPVSL KECFSYKGHDSTLGLSLNEGMPSESDCVVVQVLKLQGAVPFVHTNVPQSMLS FDCSNPLFGQTMNPWKSSKSPGGSSGGEGALIGSGGSPLGLGTDIGGSIRFPSA

FCGICGLKPTGNRLSKSGLKGCVYGQTAVQLSLGPMARDVESLALCLKALLC EHLFTLDPTVPPLPFREEVYRSSRPLRVGYYETDNYTMPSPAMRRALIETKQR LEAAGHTLIPFLPNNIPYALEVLSAGGLFSDGGRSFLQNFKGDFVDPCLGDLIL ILRLPSWFKRLLSLLLKPLFPRLAAFLNSMRPRSAEKLWKLQHEIEMYRQSVI AQWKAMNLDVLLTPMLGPALDLNTPGRATGAISYTVLYNCLDFPAGVVPVT TVTAEDDAQMELYKGYFGDIWDIILKKAMKNSVGLPVAVQCVALPWQEELC LRFMREVEQLMTPQKQPS. In the majority of the experiments, NAPE-PLD immunostaining was amplified by the tyramide signal amplification (TSA) system (PerkinElmer Life and Analytical Sciences, USA) instructions. The immunostaining was visualised by 488nm or 568nm alexa fluor-conjugated streptavidin (1:1000) Invitrogen, USA) or a fluorophore-conjugated secondary antibodies for an hour. Previously we have extensively tested the specificity and selectivity of the anti-TRPV1-, anti-CB1 and anti-FAAH antibodies (Cruz et al., 2008; Lever et al., 2009; Veress et al., 2013).

For the TSA amplification, following incubation of sections in the primary antibody, a biotinylated secondary antibody (1:500 biotin donkey anti-rabbit, Jackson ImmunoResearch Labs, USA) was applied. Slides were then incubated with peroxidase containing avidin-biotin complex (1:200, ABC kit, PerkinElmer Life and Analytical Sciences, USA) for an hour. The biotinylated tyramide was detected with fluorescent streptavidin (see above). In order to control for the combined use of two antibodies raised in the same species in combination with the TSA amplification, the following experiments were conducted: a) the primary antibody was omitted; b) a fluorescent secondary antibody, recognising the species the primary antibody was produced in, was added at the end of the TSA reaction to check if any unoccupied

primary antibody could generate signal; c) for the same primary antibody, a TSA reaction and primary-fluorescent secondary antibody reaction were done in tandem in adjacent sections to verify whether both types of reactions yield similar results.

In addition to the antibodies, fluorescein-labelled *Griffonia simplicifolia* isolectin B4 (IB4) (Sigma-Aldrich, USA) was used to identify the non-peptidergic sub-population of nociceptive primary sensory neurons (Silverman and Kruger, 1990). This was performed by incubating sections in 1:1000 dilution of the fluorochrome-conjugated IB4 for 1 hour during the final incubation step for NAPE-PLD staining. Slides were mounted in Vectashield medium (Vector Laboratories, USA).

Control experiments

For testing the specificity and selectivity of the anti-NAPE-PLD antibody, first we studied proteins identified by the anti-NAPE-PLD antibody in protein samples prepared from the cerebella of WT and NAPE-PLD-/- mice. Further, we also studied the immunostaining generated by the anti-NAPE-PLD antibody in sections cut from DRG and cerebellum of WT and NAPE-PLD-/- mice. Finally, we also studied the proportion and size distribution of cells expressing NAPE-PLD mRNA as well as the co-expression pattern between NAPE-PLD mRNA and NAPE-PLD protein (*vide infra*).

Fluorescent in situ hybridisation

Fluorescent *in situ* hybridization was carried out using a Custom Stellaris FISH Probe Kit, which contains 48 fluorescent dye-conjugated NAPE-PLD mRNA complementary short probes (Biosearch Technologies). All material and stock

solutions were treated with diethyl pyrocarbonate (DEPC; Sigma), RNase ZAP (Sigma), or kept at -80 ^{o}C for 8 hours in order to prevent RNA degradation. The DEPC treatment included adding 2.5 mM of DEPC to all solutions and autoclaving. DRG sections mounted onto coverslips were washed with PBS then permeabilized with 70% ethanol for 1 hour at room temperature. After rinsing in washing buffer, which contained 20% formamide and 2 times concentrated saline sodium citrate (SSC) buffer (which contained sodium chloride and trisodium citrate), slides were incubated with the NAPE-PLD probe (2.5 μM) in hybridization buffer (2 times SSC buffer, 10 % formamide and 100 mg/ml dextran sulphate) at room temperature for 24 h. The following day, after 1-hour incubation in the washing buffer, slides were immunoreacted with the NAPE-PLD antibody as described above. For control, sections were incubated as described above, but the NAPE-PLD probes were omitted from the hybridisation buffer. Control sections were run in parallel with sections incubated in the presence of the NAPE-PLD probes.

Image analysis and quantification of immunofluorescent DRG cells

Immunofluorescent images were examined using a Leica DMR Fluorescence, a Zeiss Axioscope 40, or a Zeiss LSM 700 Confocal Laser Scanning microscope. With the Leica microscope, images were taken by a Hamamatsu CCD camera connected to a PC running the QWIN software package (Leica, Germany). The PC connected to the Zeiss Axioscope 40 ran the AxioVision 4.6 software, whereas the PC connected to the ZEISS LSM 700 microscope ran the ZEN software package.

With each microscope, respective identical acquisition parameters were used and raw, unprocessed images were used for analysis with Image J (NIH). Images selected for

figures however were subject to contrast and brightness adjustments if we felt they were necessary.

Neurons, which displayed a visible nucleus were identified, and the cytoplasm together with the nucleus of these cells were marked as regions of interest (ROI). The area and mean pixel intensity of the ROIs were then measured. At least 200 cells were sampled in each side of each animal, in serial sections at a distance of ± 10 sections (i.e.100μm) apart from each other to make sure that each cell with a given staining was included in the analysis only once.

The threshold staining intensity was established using three independent methods. First, with visual inspections we confirmed that sections contained both immunopositive and immunonegative cells. The presence of the 2 types of neurons was also confirmed by the non-normal distribution of the staining intensities in each section (Shapiro-Wilk test). k-clustering is able to separate variables into a defined number of clusters which then exhibit the greatest possible distinction. Therefore, we used k-clustering to define 2 clusters and the intensity values which separate the two groups of neurons in each section.

In the second method, raw intensity values were transformed using a logarithmic equation (LOG(255/(255-value)). These values were ranked and displayed on a scatter plot. The initial and last linear parts of the plots were then fitted with a tangent, and the intensity value at the intersection of the two fitted lines were used as a threshold to separate labelled and non-labelled cells. This initial separation was then used in a discriminant analysis as prediction. This statistical probe also confirmed that

the accuracy of the prediction was between 95% and 100%.

Finally, one blinded experimenter examined images of randomly chosen sections from naive animals, and the immunopositivity or immunonegativity judged by that experimenter was noted. These notes were than associated with the staining intensity values measured by Image J. These combined data were then used to determine the threshold of immunopositivity by the receiver operating curve. Importantly, the ratio of immunopositive and immunonegative cells determined by the three methods did not differ more than 5%. Data presented throughout the manuscript are obtained with the second method.

In addition to establishing the immunopositive and immunonegative cells, intensity values were also used for studying pathology-induced changes in staining intensities of NAPE-PLD-, TRPV1-, CB1 receptor- and FAAH-immunopositivity, as well as pathology-induced changes in the correlation between staining intensities of NAPE-PLD and TRPV1-, CB1 receptor- or FAAH-immunopositivity.

Statistics

In naive animals, data from both the left and right sides were analysed, and used for further statistical analysis. In treated animals, data obtained from the ipsilateral and contralateral sides of the same treatment group were respectively averaged, tested for normal distribution (Shapiro-Wilk test) and analysed for statistical differences. The statistical analysis of behavioural data was performed between withdrawal responses (on different testing days or between different animal groups on the same testing day) using ANOVA followed by Tukey's test, or using 2-tailed Student's t-test as

appropriate. Statistical comparisons between the number of immunostained cells identified in different experimental groups was performed by 2-tailed Fisher's exact test. Differences between sizes of neurons belonging to various populations were compared using 2-tailed Mann-Whitney U test. All data are expressed as a mean ± SEM. "n" refers to the number of repeated measurements in each of the experimental groups. A difference was regarded as statistically significant at $p<0.05$.

RESULTS

NAPE-PLD is expressed in primary sensory neurons of DRG

Gel images of RT-PCR products exhibited detectable levels of NAPE-PLD mRNA in L4-5 rat DRG (Figure 1A). The size of the PCR product was indistinguishable from the expected product size of 199 bp (Figure 1A). These findings support previous data that a sub-population of primary sensory neurons expresses NAPE-PLD (Nagy et al., 2009; Bishay et al., 2010).

To confirm that the NAPE-PLD mRNA is expressed in neurons in DRG, we performed fluorescent *in situ* hybridisation in sections cut from rat L4-5 DRG. Analysis of the staining confirmed that NAPE-PLD mRNA is expressed in DRG and that only a sub-population of neurons expresses this transcript (Figure 1B and C).

To find whether the NAPE-PLD protein is also expressed in rat DRG, we performed Western-blotting. The anti-NAPE-PLD antibody (Aviva Systems Biology) we used throughout this study recognised, in addition to some unknown proteins, a protein with the predicted size of NAPE-PLD (~46kDa) in samples prepared from rat DRG (Figure 2A). In addition, the anti-NAPE-PLD antibody also recognised a protein with

the predicted size of (~46kDa) in WT mouse brain (together with the apparently same unknown proteins; Figure 2A). However, while the antibody recognised the unknown proteins, it did not recognise the specific ~46kDa protein in samples prepared from the brain of NAPE-PLD$^{-/-}$ mice (Figure 2A).

To confirm that the NAPE-PLD protein is expressed exclusively by neurons in DRG, we incubated sections cut from rat L4-5 DRGs with the anti-NAPE-PLD antibody and visualised the staining using TSA. Analysis of the immunostaining revealed that the antibody produced a homogenous staining in the cytoplasm of DRG neurons (Figure 2B). In addition to DRG neurons, a fluorescent signal was also seen in some satellite cells (Figure 2B). However, our control experiments revealed that this staining is produced by the TSA reaction if the postfixation time is less than 24h hours (data not shown).

To obtain evidence that the anti-NAPE-PLD antibody produces a selective and specific immunostaining, we immunoreacted cerebellum and DRG sections of WT and NAPE-PLD$^{-/-}$ mice (Figure 3A-D). As expected (Suarez et al., 2008; Nagy et al., 2009) WT mouse Purkinje cells (Figure 3A$_{1-4}$) as well as a sub-population of WT mouse DRG neurons (Figure 3C$_{1-4}$) exhibited strong NAPE-PLD immunoreactivity. In contrast, the immunoreaction produced by this antibody was lost in both cerebella and DRG dissected from NAPE-PLD$^{-/-}$ mice (Figure 3B$_{1-4}$ and 3D$_{1-4}$).

To provide further evidence that the anti-NAPE-PLD antibody produces a specific and selective staining, we also combined the immunostaining with *in situ* hybridisation using fluorescent NAPE-PLD probes (Figure 4). Analysis of this

combined staining revealed that 73 of 231 cells (31.6%) showed positivity for the *in situ* probes. The number of cells showing NAPE-PLD immunopositivity was not significantly different from this value (75 of 231 (32.5%), p=0.9, Fischer's exact test). The proportion of immunopositive neurons was not significantly different from that found in naive animals in the rest of the study (37.6±0.17%, p=0.13, n=18; Fischer's exact test). The combined fluorescent *in situ* hybridisation and immunofluorescent staining also revealed that fifty-nine of the total number of neurons showed double staining (25.6%), which represented 80.8% and 78.7% of the *in situ*- and immuno-positive cells, respectively.

NAPE-PLD is expressed in small DRG neurons

Next we analysed the morphology and neurochemical properties of NAPE-PLD-expressing primary sensory neurons. Of the 8129 DRG neurons we analysed, 3056 were NAPE-PLD-immunoreactive (37.60±0.17%, 3056 of 8129 cells in the "ipsilateral" and "contralateral" sides of 9 animals, n=18 repeated measurements; Table 1). The cell-size distribution of NAPE-PLD-immunostained neurons revealed that most of the NAPE-PLD-expressing cells were small neurons, though some large NAPE-PLD-immunopositive cells were also found (Figure 5). The area of perikarya of the NAPE-PLD-immunoreactive cells was 923±9 μm^2 (n=3056). This value was significantly smaller than the average area of perikarya of unlabelled cells (1315±10 μm^2, n=5073, 2-tailed Mann Whitney U test, p=0.01).

NAPE-PLD is expressed by both peptidergic and non-peptidergic nociceptive neurons

The great majority of small diameter primary sensory neurons are nociceptive in function (Nagy et al., 2004). While nociceptive primary sensory neurons either

contain neuropeptides such as calcitonin gene-related peptide (CGRP) or express the binding site for the lectin IB4, non-nociceptive neurons express the heavy (200kDa) neurofilament NF200 (Lawson et al., 1984; Lawson and Waddell, 1991). Therefore, to confirm that NAPE-PLD-expressing DRG neurons are indeed nociceptive, we used combined immunofluorescent staining using the anti-NAPE-PLD antibody, an anti-NF200, and an anti-CGRP antibody as well as fluorescein-conjugated isolectin B4 (IB4) on sections cut from L4-5 DRGs. Results of these combined immunoreactions are shown in Table 1 and Figure 6. In summary, 31.28±3.89% (n=6) of the NAPE-PLD immunoreactive neurons expressed NF200 (154 of 502 cells in the left and right sides of 3 animals), (Figure 6A-C; Table 1). In contrast, 52.05±2.02% (n=6) of the cells bound IB4 (267 of 512 cells in the left and right sides of 3 animals; Figure 6D-F, Table 1), and 34.58±2.67% (n=6) of the cells exhibited immunopositivity for the neuropeptide, CGRP (174 of 509 cells in the left and right sides of 3 animals; Figure 6G-I, Table 1). Importantly, more NAPE-PLD-expressing cells bound IB4 than contained CGRP ($p<0.001$ Fisher's exact test).

NAPE-PLD shows a high level of co-expression with TRPV1, the CB1 receptor and FAAH

To find whether NAPE-PLD could indeed be involved in the formation of an autocrine endocannabinoid/endovanilloid signalling system in a sub-population of primary sensory neurons, we next assessed the co-expression of NAPE-PLD and FAAH, or the CB1 receptor or TRPV1. Data from the analysis of these combined immunoreactions are shown in Figure 7 and Table 1. In summary, we found a very high level of co-expression between NAPE-PLD and all the endocannabinoid/endovanilloid signalling-related molecules (Figure 7; Table 1).

However, significantly more (p=0.029 Fisher's exact test) NAPE-PLD-immunopositive neurons expressed the CB1 receptor (72.71±1.47%, n=6; 349 of 480 cells in 3 animals) than TRPV1 (59.89±1.33%, n=6; 304 of 546 cells in the left and right sides of 3 animals).

We also assessed the correlation between the intensities of NAPE-PLD- and the CB1 receptor-, TRPV1- or FAAH-immunostaining, respectively. While NAPE-PLD- and CB1 receptor-immunostaining exhibited a high correlation (R=0.76±0.02, n=3; Figure 8A), essentially, no correlation was found between NAPE-PLD- and TRPV1-immunostaining (R=0.14±0.07, n=3; Figure 8B). Further, a weak correlation (R=0.34±0.06, n=3; data not shown) was found between the intensities of NAPE-PLD- and FAAH-immunoreactivity.

Both CFA and IFA injection induce changes in NAPE-PLD, TRPV1 and the CB1 receptor immunolabelling pattern

In primary sensory neurons, one of the main functions of anandamide's excitatory target, TRPV1, is to signal peripheral inflammatory events to the central nervous system (White et al., 2011; Nagy et al., 2014). To determine whether peripheral inflammation induces changes in NAPE-PLD expression that may be associated with increased TRPV1 activity, following the assessment of behavioural changes, we studied the expression pattern of NAPE-PLD, TRPV1, the CB1 receptor and FAAH after the induction of inflammation in the hind paw.

CFA injection into the hind paw produced hypersensitivity to both thermal and mechanical stimuli, 3 days after injection which was significantly greater than that

induced by IFA (data not shown). The proportion of NAPE-PLD immunostained neurons was significantly reduced by both CFA and IFA injections on the ipsilateral side (from 37.60±0.17% (3056/8129 cells in the left and right sides of 9 animals; n=18) to 35.18±0.64% (1363/3872 in the ipsilateral side of 3 animals) p=0.01, Fisher's exact test, by IFA, and to 35.40±0.60% (1483/ 4181 cells in the ipsilateral side of 3 animals) p=0.02, Fisher's exact test, by CFA, Figure 9; Table 2) but not on the contralateral side. The cell-size distribution of the NAPE-PLD immunopositive cells was not changed either on the ipsilateral side or the contralateral side (data not shown). The high correlation between NAPE-PLD and CB1 receptor immunostaining intensity was significantly reduced both by CFA injection (from 0.76±0.02 (n=3) to 0.48±0.03 (n=3), p<0.001, Student's t-test; Figure 8C) and by IFA injection (from 0.76±0.02 (n=3) to 0.57±0.02 (n=3), p<0.001, Student's t-test; data not shown) on the ipsilateral but not on the contralateral side. Further, the ipsilateral/contralateral ratio of NAPE-PLD-, CB1 receptor- and FAAH-immunostaining were not changed (Figure 8D). However, the ipsilateral/contralateral ratio for TRPV1-immunolabelling was increased by both IFA injection (from 1±0.03, n=3 in naive to 1.21±0.07 n=3 in IFA-injected; p=0.02, Student's t-test; data not shown) and CFA injection (from 1±0.03, n=3 in naive to 1.16±0.05 in CFA injected, n=3; p=0.03, Student's t-test; Figure 8D).

Spinal nerve ligation results in a pronounced reduction of NAPE-PLD immunoreactivity in injured DRG neurons

Nerve injury has been associated with changes in the expression in a large number of proteins including various components of the endocannabinoid/endovanilloid system(s) as well as in anandamide levels in DRG (Michael and Priestley, 1999; Hudson et al., 2001; Costigan et al., 2002; Agarwal et al., 2007; Zhang et al., 2007;

Lever et al., 2009). Therefore, next we assessed nerve injury-induced alterations in NAPE-PLD, FAAH, TRPV1 and the CB1 receptor expression.

In agreement with previous data (Kim et al., 2012) ligation and transection of the 5th lumbar spinal nerve, but not sham surgery, resulted in the development of reflex hypersensitivity to mechanical and thermal stimuli from two to seven days after the surgery (data not shown). Both the nerve injury and the sham surgery resulted in a significant reduction in the number of NAPE-PLD-immunostained neurons, in the injured DRG (from 37.60±0.17% (3056 of 8129 cells in the left and right sides of of 9 animals; n=18) to 33.71±2.19% (653 of 1932 cells in 3 sets of samples (i.e. 3 different combined staining) from the ipsilateral side of 3 animals, n=9, p=0.002 Fischer's exact test) by sham surgery, and to 18.50±1.42 (653 of 1932 cells in 3 sets of samples from the ipsilateral side of 3 animals, n=9, p<0.001, Fischer's exact test by SNL; Figure 10; Table 3) tough the SNL-induced reduction was significantly greater than that produced by the sham injury (p<0.001, Fischer's exact test). SNL but not the sham injury also reduced the number of TRPV1-immunolabelled (from 42.14±0.69% (569 of 1350 cells in the ipsilateral and contralateral sides of 3 animals, n=6) to 6.38±6.15% (41 of 695 cells in the ipsilateral side of 3 animals, n=3, p<0.001, Fischer's exact test) and CB1 receptor immunolabelled neurons (from 33.64±0.59% (426 of 1267 cells in the ipsilateral and contralateral sides of 3 animals, n=6) to 24.64±8.46% (96 of 653 cells in the ipsilateral side of 3 animals, n=3, p<0.001, Fischer's exact test) and increased the number of FAAH-immunolabelled neurons (from 34.39±1.24% (501 of 1464 cells in the ipsilateral and contralateral sides of 3 animals, n=6) to 50.81±6.49% (307 of 614 cells in the ipsilateral side of 3 animals, n=3, p<0.001, Fischer's exact test) in the injured DRG (Figure 10; Table 3). Both the

sham injury (data not shown) and SNL significantly reduced the correlation between the intensities of NAPE-PLD and CB1 receptor immunolabelling both on the ipsilateral (Figure 8C) and contralateral sides (data not shown). While the number of TRPV1-immunopositive cells was reduced, the ipsilateral/contralateral ratio of TRPV1 immunolabelling was increased (from 1±0.03 (n=3) to 1.29 (n=2, Figure 8D), though due to absence of TRPV1-immunolabelled neurons in one animal the significance could not be assessed..

Previous data show that primary sensory neurons in the DRG adjacent to the injured DRG also show phenotypic changes (Hudson et al., 2001; Hammond et al., 2004). Therefore, we also assessed NAPE-PLD, TRPV1, CB1 receptor and FAAH immunostaining in the ipsilateral L4 DRG. We found no significant change in the ratio of immunopositive cells for NAPE-PLD ($p=0.415$), FAAH ($p=0.454$) and TRPV1 ($p=0.166$; 2-tailed Fisher's exact test; Table 4). For the CB1 receptor, the significance level for the reduction in the ratio of immunopositive cells was $p=0.051$ (Fisher's exact test; Table 4).

DISCUSSION

We have found in the present study that about a third of primary sensory neurons in lumbar DRGs expresses NAPE-PLD. Our present data also show that about 2/3 - 3/4 of the NAPE-PLD-expressing neurons could be nociceptive, because the majority of the NAPE-PLD-immunopositive cells are small diameter neurons which are nociceptive in function (Nagy et al., 2004), and ~35%, ~50% and ~60% of the NAPE-PLD-expressing cells also express, respectively, the nociceptive markers, CGRP, IB4-binding site and TRPV1 (*nota bene*, CGRP, IB4-binding site and TRPV1 exhibit significant co-expression in DRG (Nagy et al., 2004)), whereas only ~30% of the

cells express the non-nociceptive cell marker heavy weight neurofilament NF200. These data are consistent with recent findings, which show that NAPE-PLD mRNA is expressed in primary sensory neurons, and that the majority of those neurons are sensitive to the archetypical TRPV1 activator, capsaicin (Nagy et al., 2009; Bishay et al., 2010).

Between the two major types of nociceptive primary sensory neurons, NAPE-PLD exhibits preference for IB4-binding cells. IB4-binding and peptidergic primary sensory neurons differ in their peripheral tissue targets, spinal projections, membrane protein expression, responses to painful events, and even in the brain areas where the information they convey is transmitted (Bennett et al., 1996; Perry and Lawson, 1998; Breese et al., 2005; Todd, 2010). Functionally, IB4-binding neurons are associated primarily with responses to noxious mechanical stimuli and the development of mechanical pain, though they may also significantly contribute to the development of thermal pain following nerve injury (Cavanaugh et al., 2009; Vilceanu et al., 2010). Hence, if NAPE-PLD is involved in nociceptive processing in primary sensory neurons, its activity could contribute, among others, to the regulation of mechanosensitivity and the development of mechanical pain.

Among the putative enzymatic pathways, which are implicated in converting NAPE into N-acylethanolamine (NAEA), including anandamide (Okamoto et al., 2004; Liu et al., 2006; Simon and Cravatt, 2006; Liu et al., 2008; Simon and Cravatt, 2008), the NAPE-PLD-catalysed pathway is the only one known to be Ca^{2+}-sensitive (Ueda et al., 2001; Okamoto et al., 2004; Wang et al., 2006; Wang et al., 2008; Tsuboi et al., 2011). van der Stelt and colleagues have reported that increasing the intracellular Ca^{2+}

concentration results in anandamide synthesis in cultured primary sensory neurons (van der Stelt et al., 2005). These data therefore, indicate that NAPE-PLD is functional in cultured primary sensory neurons.

In addition to anandamide, related molecules including palmitoylethanolamine (PEA) and oleoylethanolamine (OEA) are also synthesised by NAPE-PLD. Both PEA and OEA (and anandamide) activate the peroxisome proliferator-activated receptor alpha (PPARα; (Fu et al., 2003; Lo Verme et al., 2005; Sun et al., 2006), and the G protein coupled receptor 119 (GPR119; (Overton et al., 2006; Ryberg et al., 2007). Further, PEA (and anandamide) also activates GPR55 (Ryberg et al., 2007; Lauckner et al., 2008). While PPARα is expressed in both small and large diameter cells, GPR55 is primarily expressed in NF200-expressing large diameter cells (Lo Verme et al., 2005; Lauckner et al., 2008). Hence, the expression pattern of NAPE-PLD we found in the present study suggests that NAPE-PLD in addition to signalling through the CB1 receptor and TRPV1, could also be involved in signalling through PPARα and GPR55 in sub-populations of primary sensory neurons.

Consistent with the view that an autocrine signalling system, which involves anandamide, the CB1 receptor and TRPV1, could exist in a sub-population of nociceptive primary sensory neurons (Sousa-Valente et al., 2014b), we have shown here that NAPE-PLD exhibits a high degree of co-expression with both TRPV1 and the CB1 receptor. We have also demonstrated here that NAPE-PLD also shows a high degree of co-expression with FAAH, which is expressed in the majority of TRPV1-expressing primary sensory neurons (Lever et al., 2009). Considering the co-expression patterns we found in the present study, together with those published

previously on TRPV1 and CB1 receptor-, and on TRPV1 and FAAH co-expression (Ahluwalia et al., 2000; Binzen et al., 2006; Mitrirattanakul et al., 2006; Agarwal et al., 2007; Lever et al., 2009), it appears that the anatomical basis for an anandamide-, TRPV1-, CB1 receptor- and FAAH-mediated autocrine signalling system indeed exists in the majority of nociceptive primary sensory neurons. Importantly, our recent finding that TRPV1 shows a high degree of co-expression with some of the enzymes implicated in Ca^{2+}-insensitive anandamide synthesis (Varga et al., 2014) suggests that anandamide could be synthesised both in Ca^{2+}-sensitive and Ca^{2+}-insensitive manners in at least some of those primary sensory neurons.

While TRPV1 activation by anandamide results in excitation (Zygmunt et al., 1999; Ahluwalia et al., 2003; Potenzieri et al., 2009), CB1 receptor activation by this agent is generally considered as inhibitory in nociceptive primary sensory neurons (Calignano et al., 1998; Richardson et al., 1998; Kelly et al., 2003; Clapper et al., 2010; Chen et al., 2016). The CB1 receptor-mediated inhibitory effect, in those neurons, results *inter alia* in the reduction of TRPV1-mediated responses (Binzen et al., 2006; Mahmud et al., 2009; Santha et al., 2010). By hydrolysing anandamide, FAAH could serve as a brake both in the anandamide-induced TRPV1- and CB1 receptor-mediated effects.

We found recently that while anandamide produced in a Ca^{2+}-insensitive fashion in cultured primary sensory neurons induces TRPV1-mediated excitation, it does not produce a CB1 receptor-mediated inhibitory effect, when the inhibitory effect is assessed by measuring TRPV1-mediated responses (Varga et al., 2014). The finding that Ca^{2+}-sensitive anandamide production in primary sensory neurons results in

TRPV1-mediated excitatory effects (van der Stelt et al., 2005) suggests that NAPE-PLD activity could also be associated with TRPV1 activation. However, while we found a strong correlation between NAPE-PLD- and CB1 receptor-immunostaining intensities, the correlation between NAPE-PLD- and TRPV1-immunostaining intensities is very low. These data suggest that NAPE-PLD activity, at least in intact DRG, may be linked to CB1 receptor, rather than to TRPV1 activation. If anandamide produced by Ca^{2+}-sensitive and Ca^{2+}-insensitive manner has indeed differing primary targets in primary sensory neurons, the anandamide-, CB1 receptor-, TRPV1- and FAAH-formed putative autocrine signalling system could exert a very delicate control over the activity of a major proportion of nociceptive cells, hence over the development of pain. Consequently, any change in the expression or activity of any members of that system could disturb balanced signalling, which may contribute to the development of pain.

Our data indicate that various types of painful disturbances of the homeostasis of peripheral tissues are able to produce such perturbation. While CFA is used to induce a painful inflammatory reaction, IFA is used as its control, though IFA injection itself induces some inflammatory reaction and even hypersensitivity (Billiau and Matthys, 2001). Indeed, IFA injection induced a transient hypersensitivity in the present study. Further, similarly to CFA injection it also induced a small nevertheless significant reduction in the number of NAPE-PLD-immunolabelled cells as well as in the high correlation of intensities between NAPE-PLD and CB1 receptor immunolabelling. Both IFA and CFA increased the ipsilateral/contralateral intensity ratio of TRPV1 immunolabelling (i.e. increased in intensity of TRPV1 immunolabelling on the ipsilateral side). The slight but significant reduction in the number of CB1 receptor-

expressing cells produced by CFA and IFA is surprising as they are opposite to those reported previously (Amaya et al., 2006). Further, the lack of increase in the number of TRPV1-expressing cells is also surprising as it differs from data reported earlier (Ji et al., 2002; Amaya et al., 2004; Luo et al., 2004; Amaya et al., 2006; Yu et al., 2008) but see (Zhou et al., 2003; Bar et al., 2004). These differences could be due to the use of different analysing techniques in the different studies. Nevertheless, the combined effects of the changes we observed suggest that a balanced signalling between anandamide of NAPE-PLD origin and TRPV1 and the CB1 receptor is tipped towards a signalling with increased excitatory and reduced inhibitory components. However, the contribution of this unbalanced signalling could be negligible because while the CFA injection-induced hypersensitivity is significantly greater than that produced by IFA injection, the changes in the expression pattern of the molecules are not.

A different type of perturbation of balanced endocannabinoid/endovanilloid signalling occurs following peripheral nerve injury, because SNL reduces the number of NAPE-PLD-and CB1 receptor-expressing neurons, whereas it increases the number of FAAH-immunolabelled cells. These changes are expected to result in a dramatic reduction of inhibitory signalling between anandamide of NAPE-PLD origin and the CB1 receptor in the affected neurons. The nerve injury-induced down-regulation of NAPE-PLD expression agrees with a recent report which shows that NAPE-PLD mRNA expression is reduced in the injury-affected DRG in another neuropathic pain model, the so called spared nerve injury model (Bishay et al., 2010). Importantly, nerve injury-induced down-regulation of NAPE-PLD expression is associated with a reduction in NAEA content, including that of anandamide, of the affected DRG (Mitrirattanakul et al., 2006; Bishay et al., 2010; Bishay et al., 2013). The nerve

injury-induced up-regulation of FAAH expression is also in agreement with previous reports (Bishay et al., 2010), though in our earlier study (Lever et al., 2009), the increase in the proportion of FAAH-expressing neurons did not reach the level of significance. This discrepancy between our present and previous data could be due to the transient nature of up-regulation of FAAH expression, which reaches its peak on the 7th day after the injury (Bishay et al., 2010). Although we assessed nerve injury-induced changes 7 days after the surgery in both studies, due to possible slight differences in surgery techniques used by different persons, the time course of changes could be different. Nevertheless, the changes we found in CB1 receptor expression is generally in agreement with previous reports (Costigan et al., 2002; Mitrirattanakul et al., 2006; Zhang et al., 2007). Finally, in addition to changes in the proportions of NAPE-PLD-, CB1 receptor- and FAAH-expressing neurons, the proportion of TRPV1-expressing DRG neurons are also dramatically reduced by the spinal nerve ligation. This change is similar to that reported earlier by others using the same neuropathic model (Hudson et al., 2001; Lever et al., 2009). This reduced TRPV1 expression is in agreement with the limited role of this ion channel in the development of pain following peripheral nerve injury (Caterina et al., 2000).

In summary, we have shown here that a major proportion of primary sensory neurons express NAPE-PLD. We have also shown that NAPE-PLD exhibits a high degree of co-expression with TRPV1, the CB1 receptor and FAAH, which indicates that NAPE-PLD indeed could be involved in an autocrine regulatory mechanism in a major proportion of nociceptive primary sensory neurons. Finally, we have shown that while peripheral inflammation and injury to peripheral nerves induce differing changes in the expression pattern of NAPE-PLD, the CB1 receptor, TRPV1 and FAAH, both sets

of changes are highly likely to produce unbalanced signalling in that autocrine regulatory system, and that unbalanced signalling is characterised primarily by reduced anandamide-induced and CB1 receptor-mediated activity hence, reduced inhibition on the activity and excitability of primary sensory neurons. Similar unbalanced endocannabinoid/endovanilloid signalling due to reduction in CB1 receptor-mediated inhibitory effects in primary sensory neurons as well as in the spinal cord has been reported and shown to contribute to the development of pain in various animal models of persistent pain (Jhaveri et al., 2006; Khasabova et al., 2008; Guasti et al., 2009; Bishay et al., 2010; Khasabova et al., 2012; Starowicz et al., 2012; Starowicz and Przewlocka, 2012; Khasabova et al., 2013; Starowicz et al., 2013).

Importantly, the findings we present here provide the first insight into an autocrine signalling system, which is highly likely to play an important role in regulating the excitability of a major group of nociceptive primary sensory neurons. This insight is important because it suggests that pharmacological manipulation of this system may provide a significant reduction in spinal nociceptive input hence reduction in pain associated with peripheral pathologies. However, full utilisation of the putative analgesic potential of this system requires further elucidation of the signalling mechanism. For example, we have shown recently that spatial proximity and protein-protein interactions between TRPV1 and the CB1 receptor may determine how the CB1 receptor affects TRPV1 activity (Chen et al., 2016). Similarly, the spatial relationship between FAAH and TRPV1 and/or the CB1 receptor, which is currently unknown, is of high importance as it determines whether FAAH activity directs anandamide away from the CB1 receptor or TRPV1. Further, although our data

suggest that anandamide synthesised by NAPE-PLD may preferentially activate the CB1 receptor, this assumption requires further support.

It is also important to note that in order to avoid inducing undesirable effects, manipulation of the endocannabinoid/endovanilloid autocrine signalling system even outside the blood-brain-barrier should occur in a cell specific manner (i.e. in nociceptive primary sensory neurons), because several components of the endocannabinoid/endovanilloid system exhibit widespread expression pattern. Hence, while the CB1 receptor and TRPV1, outside the central nervous system, are expressed almost exclusively by nociceptive primary sensory neurons (Caterina et al., 1997; Tominaga et al., 1998; Ahluwalia et al., 2000; Binzen et al., 2006; Mitrirattanakul et al., 2006; Agarwal et al., 2007; Veress et al., 2013; Sousa-Valente et al., 2014a), both NAPE-PLD and FAAH are expressed by various cells and involved in various physiological functions (Paria et al., 1999; Guo et al., 2005; Rossi et al., 2009; Alhouayek and Muccioli, 2012; Geurts et al., 2015). Nevertheless, our data indicate that NAPE-PLD could be another important molecule of the endocannabinoid/endovanilloid system(s) which controls nociceptive processing in primary sensory neurons. Therefore, we propose that NAPE-PLD in nociceptive primary sensory neurons could be a valuable novel target for the development of new analgesics.

Conflict of Interest Statement
The authors report no conflict of interest associated with this work.

Role of Authors
Dr João Sousa-Valente: Majority of immunolabellig and data analysis, behavioural experiments, writing up
Dr Angelika Varga: Immunolabelling, Western blotting, PCR, writing up
Mr Jose Vicente Torres Perez: In situ hybridisation-immunolabelling
Dr Agnes Jenes: immunolabelling, statistical analysis, writing up
Dr John Wahba: PCR
Professor Ken Mackie: writing up, finalising the manuscript
Professor Benjamin Cravatt: FAAH antibody, finalising manuscript
Professor Natsuo Ueda: NAPE-PLD-/- mice, finalising manuscript
Dr Kazuhito Tsuboi: NAPE-PLD-/- mice, finalising manuscript
Dr Peter Santha: imaging, statistics, writing up
Professor Gabor Jancso: imaging, statistics, writing up
Dr Hiran Tailor: immunolabelling
Dr António Avelino: project management, writing up
Hon Professor Istvan Nagy: project management, writing up

REFERENCES

Agarwal N, Pacher P, Tegeder I, Amaya F, Constantin CE, Brenner GJ, Rubino T, Michalski CW, Marsicano G, Monory K, Mackie K, Marian C, Batkai S, Parolaro D, Fischer MJ, Reeh P, Kunos G, Kress M, Lutz B, Woolf CJ, Kuner R. 2007. Cannabinoids mediate analgesia largely via peripheral type 1 cannabinoid receptors in nociceptors. Nat Neurosci 10(7):870-879.

Ahluwalia J, Urban L, Bevan S, Nagy I. 2003. Anandamide regulates neuropeptide release from capsaicin-sensitive primary sensory neurons by activating both the cannabinoid 1 receptor and the vanilloid receptor 1 in vitro. Eur J Neurosci 17(12):2611-2618.

Ahluwalia J, Urban L, Capogna M, Bevan S, Nagy I. 2000. Cannabinoid 1 receptors are expressed in nociceptive primary sensory neurons. Neuroscience 100(4):685-688.

Alhouayek M, Muccioli GG. 2012. The endocannabinoid system in inflammatory bowel diseases: from pathophysiology to therapeutic opportunity. Trends Mol Med 18(10):615-625.

Amaya F, Shimosato G, Kawasaki Y, Hashimoto S, Tanaka Y, Ji RR, Tanaka M. 2006. Induction of CB1 cannabinoid receptor by inflammation in primary afferent neurons facilitates antihyperalgesic effect of peripheral CB1 agonist. Pain 124(1-2):175-183.

Amaya F, Shimosato G, Nagano M, Ueda M, Hashimoto S, Tanaka Y, Suzuki H, Tanaka M. 2004. NGF and GDNF differentially regulate TRPV1 expression that contributes to development of inflammatory thermal hyperalgesia. Eur J Neurosci 20(9):2303-2310.

Bar KJ, Schaible HG, Brauer R, Halbhuber KJ, von Banchet GS. 2004. The proportion of TRPV1 protein-positive lumbar DRG neurones does not increase in the course of acute and chronic antigen-induced arthritis in the knee joint of the rat. Neurosci Lett 361(1-3):172-175.

Bennett DL, Averill S, Clary DO, Priestley JV, McMahon SB. 1996. Postnatal changes in the expression of the trkA high-affinity NGF receptor in primary sensory neurons. Eur J Neurosci 8(10):2204-2208.

Billiau A, Matthys P. 2001. Modes of action of Freund's adjuvants in experimental models of autoimmune diseases. J Leukoc Biol 70(6):849-860.

Binzen U, Greffrath W, Hennessy S, Bausen M, Saaler-Reinhardt S, Treede RD. 2006. Co-expression of the voltage-gated potassium channel Kv1.4 with transient receptor potential channels (TRPV1 and TRPV2) and the cannabinoid receptor CB1 in rat dorsal root ganglion neurons. Neuroscience 142(2):527-539.

Bishay P, Haussler A, Lim HY, Oertel B, Galve-Roperh I, Ferreiros N, Tegeder I. 2013. Anandamide deficiency and heightened neuropathic pain in aged mice. Neuropharmacology 71:204-215.

Bishay P, Schmidt H, Marian C, Haussler A, Wijnvoord N, Ziebell S, Metzner J, Koch M, Myrczek T, Bechmann I, Kuner R, Costigan M, Dehghani F, Geisslinger G, Tegeder I. 2010. R-flurbiprofen reduces neuropathic pain in rodents by restoring endogenous cannabinoids. PLoS One 5(5):e10628.

Breese NM, George AC, Pauers LE, Stucky CL. 2005. Peripheral inflammation selectively increases TRPV1 function in IB4-positive sensory neurons from adult mouse. Pain 115(1-2):37-49.

Calignano A, La Rana G, Giuffrida A, Piomelli D. 1998. Control of pain initiation by endogenous cannabinoids. Nature 394(6690):277-281.

Caterina MJ, Leffler A, Malmberg AB, Martin WJ, Trafton J, Petersen-Zeitz KR, Koltzenburg M, Basbaum AI, Julius D. 2000. Impaired nociception and pain sensation in mice lacking the capsaicin receptor. Science 288(5464):306-313.

Caterina MJ, Schumacher MA, Tominaga M, Rosen TA, Levine JD, Julius D. 1997. The capsaicin receptor: a heat-activated ion channel in the pain pathway. Nature 389(6653):816-824.

Cavanaugh DJ, Lee H, Lo L, Shields SD, Zylka MJ, Basbaum AI, Anderson DJ. 2009. Distinct subsets of unmyelinated primary sensory fibers mediate behavioral responses to noxious thermal and mechanical stimuli. Proc Natl Acad Sci U S A 106(22):9075-9080.

Chen J, Varga A, Selvarajah S, Jenes A, Dienes B, Sousa-Valente J, Kulik A, Veress G, Brain SD, Baker D, Urban L, Mackie K, Nagy I. 2016. Spatial Distribution of the Cannabinoid Type 1 and Capsaicin Receptors May Contribute to the Complexity of Their Crosstalk. Sci Rep 6:33307.

Clapper JR, Moreno-Sanz G, Russo R, Guijarro A, Vacondio F, Duranti A, Tontini A, Sanchini S, Sciolino NR, Spradley JM, Hohmann AG, Calignano A, Mor M, Tarzia G, Piomelli D. 2010. Anandamide suppresses pain initiation through a peripheral endocannabinoid mechanism. Nat Neurosci 13(10):1265-1270.

Costigan M, Befort K, Karchewski L, Griffin RS, D'Urso D, Allchorne A, Sitarski J, Mannion JW, Pratt RE, Woolf CJ. 2002. Replicate high-density rat genome oligonucleotide microarrays reveal hundreds of regulated genes in the dorsal root ganglion after peripheral nerve injury. BMC Neurosci 3:16.

Cravatt BF, Giang DK, Mayfield SP, Boger DL, Lerner RA, Gilula NB. 1996. Molecular characterization of an enzyme that degrades neuromodulatory fatty-acid amides. Nature 384(6604):83-87.

Cruz CD, Charrua A, Vieira E, Valente J, Avelino A, Cruz F. 2008. Intrathecal delivery of resiniferatoxin (RTX) reduces detrusor overactivity and spinal expression of TRPV1 in spinal cord injured animals. Exp Neurol 214(2):301-308.

Devane WA, Hanus L, Breuer A, Pertwee RG, Stevenson LA, Griffin G, Gibson D, Mandelbaum A, Etinger A, Mechoulam R. 1992. Isolation and Structure of a Brain Constituent That Binds to the Cannabinoid Receptor. Science 258(5090):1946-1949.

Fu J, Gaetani S, Oveisi F, Lo Verme J, Serrano A, Rodriguez De Fonseca F, Rosengarth A, Luecke H, Di Giacomo B, Tarzia G, Piomelli D. 2003. Oleylethanolamide regulates feeding and body weight through activation of the nuclear receptor PPAR-alpha. Nature 425(6953):90-93.

Geurts L, Everard A, Van Hul M, Essaghir A, Duparc T, Matamoros S, Plovier H, Castel J, Denis RG, Bergiers M, Druart C, Alhouayek M, Delzenne NM, Muccioli GG, Demoulin JB, Luquet S, Cani PD. 2015. Adipose tissue NAPE-PLD controls fat mass development by altering the browning process and gut microbiota. Nat Commun 6:6495.

Guasti L, Richardson D, Jhaveri M, Eldeeb K, Barrett D, Elphick MR, Alexander SP, Kendall D, Michael GJ, Chapman V. 2009. Minocycline treatment inhibits

microglial activation and alters spinal levels of endocannabinoids in a rat model of neuropathic pain. Mol Pain 5:35.

Guo Y, Wang H, Okamoto Y, Ueda N, Kingsley PJ, Marnett LJ, Schmid HH, Das SK, Dey SK. 2005. N-acylphosphatidylethanolamine-hydrolyzing phospholipase D is an important determinant of uterine anandamide levels during implantation. J Biol Chem 280(25):23429-23432.

Hammond DL, Ackerman L, Holdsworth R, Elzey B. 2004. Effects of spinal nerve ligation on immunohistochemically identified neurons in the L4 and L5 dorsal root ganglia of the rat. J Comp Neurol 475(4):575-589.

Hargreaves K, Dubner R, Brown F, Flores C, Joris J. 1988. A new and sensitive method for measuring thermal nociception in cutaneous hyperalgesia. Pain 32(1):77-88.

Hudson LJ, Bevan S, Wotherspoon G, Gentry C, Fox A, Winter J. 2001. VR1 protein expression increases in undamaged DRG neurons after partial nerve injury. Eur J Neurosci 13(11):2105-2114.

Jhaveri MD, Richardson D, Kendall DA, Barrett DA, Chapman V. 2006. Analgesic effects of fatty acid amide hydrolase inhibition in a rat model of neuropathic pain. J Neurosci 26(51):13318-13327.

Ji RR, Samad TA, Jin SX, Schmoll R, Woolf CJ. 2002. p38 MAPK activation by NGF in primary sensory neurons after inflammation increases TRPV1 levels and maintains heat hyperalgesia. Neuron 36(1):57-68.

Kelly S, Jhaveri MD, Sagar DR, Kendall DA, Chapman V. 2003. Activation of peripheral cannabinoid CB1 receptors inhibits mechanically evoked responses of spinal neurons in noninflamed rats and rats with hindpaw inflammation. Eur J Neurosci 18(8):2239-2243.

Khasabova IA, Holman M, Morse T, Burlakova N, Coicou L, Harding-Rose C, Simone DA, Seybold VS. 2013. Increased anandamide uptake by sensory neurons contributes to hyperalgesia in a model of cancer pain. Neurobiol Dis 58:19-28.

Khasabova IA, Khasabov S, Paz J, Harding-Rose C, Simone DA, Seybold VS. 2012. Cannabinoid type-1 receptor reduces pain and neurotoxicity produced by chemotherapy. J Neurosci 32(20):7091-7101.

Khasabova IA, Khasabov SG, Harding-Rose C, Coicou LG, Seybold BA, Lindberg AE, Steevens CD, Simone DA, Seybold VS. 2008. A decrease in anandamide signaling contributes to the maintenance of cutaneous mechanical hyperalgesia in a model of bone cancer pain. J Neurosci 28(44):11141-11152.

Kim SE, Coste B, Chadha A, Cook B, Patapoutian A. 2012. The role of Drosophila Piezo in mechanical nociception. Nature 483(7388):209-212.

Kim SH, Chung JM. 1992. An experimental model for peripheral neuropathy produced by segmental spinal nerve ligation in the rat. Pain 50(3):355-363.

Lauckner JE, Jensen JB, Chen HY, Lu HC, Hille B, Mackie K. 2008. GPR55 is a cannabinoid receptor that increases intracellular calcium and inhibits M current. Proc Natl Acad Sci U S A 105(7):2699-2704.

Lawson SN, Harper AA, Harper EI, Garson JA, Anderton BH. 1984. A monoclonal antibody against neurofilament protein specifically labels a subpopulation of rat sensory neurones. J Comp Neurol 228(2):263-272.

Lawson SN, Waddell PJ. 1991. Soma Neurofilament Immunoreactivity Is Related to Cell-Size and Fiber Conduction-Velocity in Rat Primary Sensory Neurons. J Physiol (Lond) 435:41-63.

Leung D, Saghatelian A, Simon GM, Cravatt BF. 2006. Inactivation of N-acyl phosphatidylethanolamine phospholipase D reveals multiple mechanisms for the biosynthesis of endocannabinoids. Biochemistry 45(15):4720-4726.

Lever IJ, Robinson M, Cibelli M, Paule C, Santha P, Yee L, Hunt SP, Cravatt BF, Elphick MR, Nagy I, Rice AS. 2009. Localization of the endocannabinoid-degrading enzyme fatty acid amide hydrolase in rat dorsal root ganglion cells and its regulation after peripheral nerve injury. J Neurosci 29(12):3766-3780.

Liu J, Wang L, Harvey-White J, Huang BX, Kim HY, Luquet S, Palmiter RD, Krystal G, Rai R, Mahadevan A, Razdan RK, Kunos G. 2008. Multiple pathways involved in the biosynthesis of anandamide. Neuropharmacology 54(1):1-7.

Liu J, Wang L, Harvey-White J, Osei-Hyiaman D, Razdan R, Gong Q, Chan AC, Zhou Z, Huang BX, Kim HY, Kunos G. 2006. A biosynthetic pathway for anandamide. Proc Natl Acad Sci U S A 103(36):13345-13350.

Lo Verme J, Fu J, Astarita G, La Rana G, Russo R, Calignano A, Piomelli D. 2005. The nuclear receptor peroxisome proliferator-activated receptor-alpha mediates the anti-inflammatory actions of palmitoylethanolamide. Mol Pharmacol 67(1):15-19.

Luo H, Cheng J, Han JS, Wan Y. 2004. Change of vanilloid receptor 1 expression in dorsal root ganglion and spinal dorsal horn during inflammatory nociception induced by complete Freund's adjuvant in rats. Neuroreport 15(4):655-658.

Mackie K, Hille B. 1992. Cannabinoids inhibit N-type calcium channels in neuroblastoma-glioma cells. Proc Natl Acad Sci U S A 89(9):3825-3829.

Mackie K, Lai Y, Westenbroek R, Mitchell R. 1995. Cannabinoids activate an inwardly rectifying potassium conductance and inhibit Q-type calcium currents in AtT20 cells transfected with rat brain cannabinoid receptor. J Neurosci 15(10):6552-6561.

Mahmud A, Santha P, Paule CC, Nagy I. 2009. Cannabinoid 1 receptor activation inhibits transient receptor potential vanilloid type 1 receptor-mediated cationic influx into rat cultured primary sensory neurons. Neuroscience 162(4):1202-1211.

Malek N, Mrugala M, Makuch W, Kolosowska N, Przewlocka B, Binkowski M, Czaja M, Morera E, Di Marzo V, Starowicz K. 2015. A multi-target approach for pain treatment: dual inhibition of fatty acid amide hydrolase and TRPV1 in a rat model of osteoarthritis. Pain 156(5):890-903.

Matsuda LA, Lolait SJ, Brownstein MJ, Young AC, Bonner TI. 1990. Structure of a cannabinoid receptor and functional expression of the cloned cDNA. Nature 346(6284):561-564.

Michael GJ, Priestley JV. 1999. Differential expression of the mRNA for the vanilloid receptor subtype 1 in cells of the adult rat dorsal root and nodose ganglia and its downregulation by axotomy. J Neurosci 19(5):1844-1854.

Mitrirattanakul S, Ramakul N, Guerrero AV, Matsuka Y, Ono T, Iwase H, Mackie K, Faull KF, Spigelman I. 2006. Site-specific increases in peripheral cannabinoid receptors and their endogenous ligands in a model of neuropathic pain. Pain 126(1-3):102-114.

Nagy B, Fedonidis C, Photiou A, Wahba J, Paule CC, Ma D, Buluwela L, Nagy I. 2009. Capsaicin-sensitive primary sensory neurons in the mouse express N-Acyl phosphatidylethanolamine phospholipase D. Neuroscience 161(2):572-577.

Nagy I, Friston D, Valente JS, Perez JVT, Andreou AP. 2014. Pharmacology of the Capsaicin Receptor, Transient Receptor Potential Vanilloid Type-1 Ion Channel. Prog Drug Res. Vol 68. p 39-76.

Nagy I, Santha P, Jancso G, Urban L. 2004. The role of the vanilloid (capsaicin) receptor (TRPV1) in physiology and pathology. Eur J Pharmacol 500(1-3):351-369.

Okamoto Y, Morishita J, Tsuboi K, Tonai T, Ueda N. 2004. Molecular characterization of a phospholipase D generating anandamide and its congeners. J Biol Chem 279(7):5298-5305.

Overton HA, Babbs AJ, Doel SM, Fyfe MC, Gardner LS, Griffin G, Jackson HC, Procter MJ, Rasamison CM, Tang-Christensen M, Widdowson PS, Williams GM, Reynet C. 2006. Deorphanization of a G protein-coupled receptor for oleoylethanolamide and its use in the discovery of small-molecule hypophagic agents. Cell Metab 3(3):167-175.

Paria BC, Zhao X, Wang J, Das SK, Dey SK. 1999. Fatty-acid amide hydrolase is expressed in the mouse uterus and embryo during the periimplantation period. Biol Reprod 60(5):1151-1157.

Perry MJ, Lawson SN. 1998. Differences in expression of oligosaccharides, neuropeptides, carbonic anhydrase and neurofilament in rat primary afferent neurons retrogradely labelled via skin, muscle or visceral nerves. Neuroscience 85(1):293-310.

Potenzieri C, Brink TS, Simone DA. 2009. Excitation of cutaneous C nociceptors by intraplantar administration of anandamide. Brain Res 1268:38-47.

Richardson JD, Kilo S, Hargreaves KM. 1998. Cannabinoids reduce hyperalgesia and inflammation via interaction with peripheral CB1 receptors. Pain 75(1):111-119.

Rossi F, Siniscalco D, Luongo L, De Petrocellis L, Bellini G, Petrosino S, Torella M, Santoro C, Nobili B, Perrotta S, Di Marzo V, Maione S. 2009. The endovanilloid/endocannabinoid system in human osteoclasts: possible involvement in bone formation and resorption. Bone 44(3):476-484.

Ryberg E, Larsson N, Sjogren S, Hjorth S, Hermansson NO, Leonova J, Elebring T, Nilsson K, Drmota T, Greasley PJ. 2007. The orphan receptor GPR55 is a novel cannabinoid receptor. Br J Pharmacol 152(7):1092-1101.

Santha P, Jenes A, Somogyi C, Nagy I. 2010. The endogenous cannabinoid anandamide inhibits transient receptor potential vanilloid type 1 receptor-mediated currents in rat cultured primary sensory neurons. Acta Physiol Hung 97(2):149-158.

Silverman JD, Kruger L. 1990. Selective neuronal glycoconjugate expression in sensory and autonomic ganglia: relation of lectin reactivity to peptide and enzyme markers. J Neurocytol 19(5):789-801.

Simon GM, Cravatt BF. 2006. Endocannabinoid biosynthesis proceeding through glycerophospho-N-acyl ethanolamine and a role for alpha/beta-hydrolase 4 in this pathway. J Biol Chem 281(36):26465-26472.

Simon GM, Cravatt BF. 2008. Anandamide biosynthesis catalyzed by the phosphodiesterase GDE1 and detection of glycerophospho-N-acyl ethanolamine precursors in mouse brain. J Biol Chem 283(14):9341-9349.

Sousa-Valente J, Andreou AP, Urban L, Nagy I. 2014a. Transient receptor potential ion channels in primary sensory neurons as targets for novel analgesics. Br J Pharmacol 171(10):2508-2527.

Sousa-Valente J, Varga A, Ananthan K, Khajuria A, Nagy I. 2014b. Anandamide in primary sensory neurons: too much of a good thing? Eur J Neurosci 39(3):409-418.

Starowicz K, Makuch W, Korostynski M, Malek N, Slezak M, Zychowska M, Petrosino S, De Petrocellis L, Cristino L, Przewlocka B, Di Marzo V. 2013. Full inhibition of spinal FAAH leads to TRPV1-mediated analgesic effects in neuropathic rats and possible lipoxygenase-mediated remodeling of anandamide metabolism. PLoS One 8(4):e60040.

Starowicz K, Makuch W, Osikowicz M, Piscitelli F, Petrosino S, Di Marzo V, Przewlocka B. 2012. Spinal anandamide produces analgesia in neuropathic rats: possible CB(1)- and TRPV1-mediated mechanisms. Neuropharmacology 62(4):1746-1755.

Starowicz K, Przewlocka B. 2012. Modulation of neuropathic-pain-related behaviour by the spinal endocannabinoid/endovanilloid system. Philos Trans R Soc Lond B Biol Sci 367(1607):3286-3299.

Suarez J, Bermudez-Silva FJ, Mackie K, Ledent C, Zimmer A, Cravatt BF, de Fonseca FR. 2008. Immunohistochemical description of the endogenous cannabinoid system in the rat cerebellum and functionally related nuclei. J Comp Neurol 509(4):400-421.

Sun Y, Alexander SP, Kendall DA, Bennett AJ. 2006. Cannabinoids and PPARalpha signalling. Biochem Soc Trans 34(Pt 6):1095-1097.

Todd AJ. 2010. Neuronal circuitry for pain processing in the dorsal horn. Nat Rev Neurosci 11(12):823-836.

Tominaga M, Caterina MJ, Malmberg AB, Rosen TA, Gilbert H, Skinner K, Raumann BE, Basbaum AI, Julius D. 1998. The cloned capsaicin receptor integrates multiple pain-producing stimuli. Neuron 21(3):531-543.

Tsuboi K, Okamoto Y, Ikematsu N, Inoue M, Shimizu Y, Uyama T, Wang J, Deutsch DG, Burns MP, Ulloa NM, Tokumura A, Ueda N. 2011. Enzymatic formation of N-acylethanolamines from N-acylethanolamine plasmalogen through N-acylphosphatidylethanolamine-hydrolyzing phospholipase D-dependent and -independent pathways. Biochim Biophys Acta 1811(10):565-577.

Twitchell W, Brown S, Mackie K. 1997. Cannabinoids inhibit N- and P/Q-type calcium channels in cultured rat hippocampal neurons. J Neurophysiol 78(1):43-50.

Ueda N, Liu Q, Yamanaka K. 2001. Marked activation of the N-acylphosphatidylethanolamine-hydrolyzing phosphodiesterase by divalent cations. Biochim Biophys Acta 1532(1-2):121-127.

Valente J, Tailor H, Jenes A, Mackie K, Cravatt BF, Buluwala L, Avelino A, Nagy I. Expression of N-acyl phosphotidylethanolamine phospholipase D in rat dorsal root ganglion neurons; 2011; London. Proc Phys Soc. p PC25.

van der Stelt M, Di Marzo V. 2005. Anandamide as an intracellular messenger regulating ion channel activity. Prostaglandins Other Lipid Mediat 77(1-4):111-122.

van der Stelt M, Trevisani M, Vellani V, De Petrocellis L, Schiano Moriello A, Campi B, McNaughton P, Geppetti P, Di Marzo V. 2005. Anandamide acts as an intracellular messenger amplifying Ca2+ influx via TRPV1 channels. EMBO J 24(17):3026-3037.

Varga A, Jenes A, Marczylo TH, Sousa-Valente J, Chen J, Austin J, Selvarajah S, Piscitelli F, Andreou AP, Taylor AH, Kyle F, Yaqoob M, Brain S, White JP, Csernoch L, Di Marzo V, Buluwela L, Nagy I. 2014. Anandamide produced by Ca(2+)-insensitive enzymes induces excitation in primary sensory neurons. Pflugers Arch 466(7):1421-1435.

Vellani V, Petrosino S, De Petrocellis L, Valenti M, Prandini M, Magherini PC, McNaughton PA, Di Marzo V. 2008. Functional lipidomics. Calcium-independent activation of endocannabinoid/endovanilloid lipid signalling in sensory neurons by protein kinases C and A and thrombin. Neuropharmacology 55(8):1274-1279.

Veress G, Meszar Z, Muszil D, Avelino A, Matesz K, Mackie K, Nagy I. 2013. Characterisation of cannabinoid 1 receptor expression in the perikarya, and peripheral and spinal processes of primary sensory neurons. Brain Struct Funct 218(3):733-750.

Vilceanu D, Honore P, Hogan QH, Stucky CL. 2010. Spinal nerve ligation in mouse upregulates TRPV1 heat function in injured IB4-positive nociceptors. J Pain 11(6):588-599.

Wang J, Okamoto Y, Morishita J, Tsuboi K, Miyatake A, Ueda N. 2006. Functional analysis of the purified anandamide-generating phospholipase D as a member of the metallo-beta-lactamase family. J Biol Chem 281(18):12325-12335.

Wang J, Okamoto Y, Tsuboi K, Ueda N. 2008. The stimulatory effect of phosphatidylethanolamine on N-acylphosphatidylethanolamine-hydrolyzing phospholipase D (NAPE-PLD). Neuropharmacology 54(1):8-15.

White JP, Urban L, Nagy I. 2011. TRPV1 function in health and disease. Curr Pharm Biotechnol 12(1):130-144.

Yu L, Yang F, Luo H, Liu FY, Han JS, Xing GG, Wan Y. 2008. The role of TRPV1 in different subtypes of dorsal root ganglion neurons in rat chronic inflammatory nociception induced by complete Freund's adjuvant. Mol Pain 4:61.

Zhang S, Zhao B, Jiang H, Wang B, Ma B. 2007. Cationic lipids and polymers mediated vectors for delivery of siRNA. J Control Release 123(1):1-10.

Zhou Y, Li GD, Zhao ZQ. 2003. State-dependent phosphorylation of epsilon-isozyme of protein kinase C in adult rat dorsal root ganglia after inflammation and nerve injury. J Neurochem 85(3):571-580.

Zygmunt PM, Petersson J, Andersson DA, Chuang H, Sorgard M, Di Marzo V, Julius D, Hogestatt ED. 1999. Vanilloid receptors on sensory nerves mediate the vasodilator action of anandamide. Nature 400(6743):452-457.

Figure legends

Figure 1.

The NAPE-PLD transcript is expressed in adult rat DRG.

(A) Gel image of RT-PCR products which were synthesised from total RNA isolated from the L4-5 DRG of adult rats with primers designed to amplify NAPE-PLD (N, upper panel) and GAPDH (G, lower panel) mRNA. The size of the RT-PCR products is indistinguishable from the predicted size of NAPE-PLD (N; 199bp) and GAPDH (G; 380bp). (B) A microphotograph taken from a DRG section of an adult rat following fluorescent in situ hybridisation with 48 short NAPE-PLD complementary fluorescent dye-tagged probes. The labelling identified only neurons (arrowheads). The great majority of the positive neurons were small diameter cells. Scale bar: 20μm. (C) A microphotograph taken from another rat DRG section. That section was incubated in parallel with the one shown in (B) in identical solutions, except that the specific in situ probes were omitted from the hybridisation buffer.

Figure 2

The NAPE-PLD protein is expressed in adult rat DRG.

(A) The upper panel shows a gel image of immunoblots using an antibody raised against NAPE-PLD (Aviva System Biology) and protein samples prepared from rat DRG (R/DRG), NAPE-PLD$^{-/-}$ mouse brain (KO/BR) or wild type mouse brain (WT/BR). The antibody in addition to recognising a protein with the predicted size of NAPE-PLD (~46kD) in rat DRG and WT mouse brain tissues, also recognised some unknown proteins in all samples. However, the antibody failed to recognise the protein with the predicted size of NAPE-PLD in NAPE-PLD$^{-/-}$ mouse brain. The lower image shows beta actin (42kD) expression as loading control. (B)

Microphotograph of a section cut from a rat dorsal root ganglion. The anti-NAPE-PLD antibody produced staining in a sub-population of primary sensory neurons (arrowheads). In addition, satellite cells visible occasionally around primary sensory neurons also exhibit NAPE-PLD immunopositivity (arrows). However, control experiments revealed that this staining is produced by the TSA reaction if the postfixation time is less than 24 hours. Scale bar: 30μm.

Figure 3.

The NAPE-PLD antibody provides specific and selective staining.

(A_1-A_4) Microphotographs (taken with the Zeiss Axiotome microscope) of a section cut from a WT mouse (NAPE-PLD$^{+/+}$) cerebellum and immunostained using the combination of an anti-NAPE-PLD (A_1, green) and an anti-β-III tubulin (A_2, red) antibody. The section was also stained with DAPI (A_3, blue). A_4 shows the composite image of A_1-A_3. Consistent with previous findings, the perikarya of Purkinje cells show strong immunopositivity for NAPE-PLD (arrowheads). (B_1-B_4) Microphotographs (taken with the Zeiss Axiotome microscope) of a section cut from the cerebellum of a NAPE-PLD$^{-/-}$ mouse and immunoreacted with the mixture of the anti-NAPE-PLD (B_1) and the anti-β-III tubulin (B_2) antibodies. The section was also stained by DAPI (B_3). B_4 shows the composite image of B_1-B_3. Note the complete lack of immunolabelling by the anti-NAPE-PLD antibody. Scale bar: 50μm. (C_1-C_4) Microphotographs (taken with the Zeiss Axiotome microscope) of a section cut from a wild type mouse dorsal root ganglion (DRG) and immunostained with the mixture of the anti-NAPE-PLD (C_1) and the anti-β-III tubulin (C_2) antibodies. The section was also stained by DAPI (C_3). C_4 shows the composite image of C_1-C_3. The immunoreaction produced staining in a sub-population of neurons (arrowheads). (D_1-

D_4) Microphotographs (taken with the Zeiss Axiotome microscope) of a section cut from a NAPE-PLD$^{-/-}$ mouse dorsal root ganglion and immunostained with the mixture of the anti-NAPE-PLD and the anti-β-III tubulin (D_2) antibodies. The section was also stained by DAPI (D_3). D_4 shows the composite image of D_1-D_3. Note complete lack of NAPE-PLD immunopositivity. Scale bar: 50μm. Images of DRG sections are stack images from 8 images of 1.25 μm each. Images of the cerebellum are stack images from 12 images of 1.42 μm each.

Figure 4.

Combined staining with NAPE-PLD in situ probes and the anti-NAPE-PLD antibody reveals a high degree of co-staining.

(A) The microphotograph shows the result of fluorescent *in situ* hybridisation in a rat DRG section using fluorescent dye-tagged probes specific for NAPE-PLD mRNA. The labelling identified a group of neurons (arrowheads). (B) The microphotograph shows the image of the same cells showed in (A) immunolabelled with the anti-NAPE-PLD antibody. Arrowheads point to NAPE-PLD immunopositive cells. (C) Microphotograph of the visual field shown in (A) and (B) but stained with DAPI. (D). Composite image of (A)-(C). Arrowheads point to double labelled cells. In this visual filed the co-staining of neurons is 100%. Scale bar: 20μm.

Figure 5.

The majority of primary sensory neurons expressing NAPE-PLD are small cells.

Cell size distribution of NAPE-PLD immunopositive (green bars) and immunonegative (grey bars) rat dorsal root ganglion neurons. The great majority of the NAPE-PLD immunopositive cells are small cells, though some larger cells also

express NAPE-PLD.

Figure 6.

The majority of primary sensory neurons expressing NAPE-PLD also express markers for nociceptive primary sensory neurons.

(A)-(I) Combined immunolabelling was produced using the anti-NAPE-PLD antibody with an antibody raised against the 200kD neurofilament NF200 (A-C) or with biotinylated IB4 (D-F), or with and antibody raised against CGRP (G-I). (A-C) show a typical combined image (A) and separated images (B and C) of a section incubated with the anti-NAPE-PLD (green; B) and an anti-NF200 (red; C) antibody. NAPE-PLD shows a low degree of co-expression with NF200. (D-F) show a typical combined image (D) and separated images (E and F) of a section incubated with the anti-NAPE-PLD antibody (green; E) and a biotinylated IB4 (red; F). NAPE-PLD shows a high degree of co-expression with the IB4 binding site. (G-I) show a typical combined image (G) and separated images (H and I) of a section incubated with the anti-NAPE-PLD (green; H) and anti-CGRP antibody (red; I). NAPE-PLD also shows co-expression with CGRP. Arrowheads on (D) and (G) indicate NAPE-PLD/IB4-binding site-expressing neurons and NAPE-PLD/CGRP-immunopositive neurons, respectively. Scale bar indicates 50 µm. For quantified data, please see Table 1. All images are single scan images acquired with 20X objective lens (NA: 0.50) and 47 µm pinhole aperture corresponding to 1.29 Airy unit and providing 4,6 µm thin optical sections.

Figure 7.

The majority of primary sensory neurons expressing NAPE-PLD also express

the CB1 receptor, TRPV1 and/or FAAH.

(A-C) show a typical combined image (A) and separated images (B and C) of a section incubated with the anti-NAPE-PLD (green; B) and an anti-CB1 receptor (red; C) antibody. NAPE-PLD shows a high degree of co-expression with the CB1 receptor. (D-F) show a typical combined image (D) and separated images (E and F) of a section incubated with the anti-NAPE-PLD (green; E) and an anti-TRPV1 (red; F) antibody. NAPE-PLD also shows a high degree of co-expression with TRPV1. (G-I) show a typical combined image (G) and separated images (H and I) of a section incubated with the anti-NAPE-PLD (green; H) and an anti-FAAH (red; I) antibody. NAPE-PLD also shows a high degree of co-expression with FAAH. Arrowheads on (A), (D) and (G) indicate NAPE-PLD/CB1 receptor-co-expressing, NAPE-PLD/TRPV1-co-expressing and NAPE-PLD/FAAH-immunopositive neurons. Scale bar indicates 50 µm. For quantified data, please see Table 1. All images are single scan images acquired with 20X objective lens (NA: 0.50) and 47 µm pinhole aperture corresponding to 1.29 Airy unit and providing 4,6 µm thin optical sections.

Figure 8

Peripheral pathological conditions disturb the staining pattern observed in naive animals.

(A) Correlation between NAPE-PLD and CB1 receptor staining intensity of naive rat primary sensory neurons exhibiting co-expression of these two molecules. Note the high correlation between the intensities of two staining. (B) Correlation between NAPE-PLD and TRPV1 immunostaining intensity of naive rat primary sensory neurons exhibiting co-expression of these two molecules. Note the lack of correlation between the intensities of the two staining. (C) Correlation of NAPE-PLD

immunostaining with immunostaining intensities for the CB1 receptor (CB1), TRPV1 (TRPV1) and FAAH (FAAH) in ipsilateral DRG in naive condition (empty bars), following injection of complete Freund's adjuvant (CFA, grey bars) into the paw or following ligation of the spinal nerve (SNL, black bar). Note that the strong correlation between the staining intensities of the NAPE-PLD and CB1 receptor immunostaining observed in naive animals, was significantly reduced by both CFA injection and SNL (asterisks). (D) Ratio between staining intensities on the ipsi- and contralateral DRGs for the various markers (NAPE-PLD, the CB1 receptor, TRPV1 and FAAH) in naive condition (empty bars), following CFA injection (grey bars) and following SNL (black bars). Note that CFA injection significantly (asterisk) increases the ipsilateral-contralateral TRPV1 staining intensity. While SNL appears to have the same effect, due to the reduction in the number of TRPV1 immunopositive cells, the ratio could be established only in two animals and statistical analysis was not performed. All data are expressed as mean ± SEM.

Figure 9.

Both CFA and IFA injection into the hind paw reduce the number of NAPE-PLD-immunolabelled neurons without inducing any change in the number of TRPV1-, CB1 receptor or FAAH-immunolabelled neurons in DRG.

The bar chart shows the relative number of neurons exhibiting immunopositivity for NAPE-PLD, CB1 receptor TRPV1 and FAAH in naive (white bars), IFA-injected (grey bars) and CFA-injected (black bars) animals. Both IFA and CFA injection induce a small but significant reduction in the relative number of neurons exhibiting immunopositivity for NAPE-PLD. The number of immunopositive neurons for the

other markers is not changed either by IFA or CFA injection. Asterisks indicate significant difference from naive (p=0.01 for IFA and p=0.02 for CFA, n=3 both for IFA and CFA; 2-tailed Fisher's exact test). All data are expressed as mean ± SEM.

Figure 10.

Ligation of the L5 spinal nerve induces reduction in the number of neurons exhibiting immunopositivity of NAPE-PLD, TRPV1 and the CB1 receptor, whereas it induces an increase in the number of neurons exhibiting immunopositivity of FAAH in the L5 DRG.

(A) Typical images of DRG sections cut from the ipsilateral (IPSI) L5 DRG of a sham-operated rat (SHAM) and animals subjected to ligation of the L5 spinal nerve (SNL) and incubated in anti-NAPE-PLD-, anti-CB1 receptor-, anti-TRPV1- and anti-FAAH antibodies. The number of cells exhibiting immunopositivity for NAPE-PLD, the CB1 receptor and TRPV1 is reduced following SNL whereas the number of cells exhibiting immunopositivity for FAAH is increased following SNL. (B) Comparison between the number of primary sensory neurons exhibiting immunopositivity for NAPE-PLD, CB1 receptor, TRPV1 and FAAH in the ipsilateral L5 DRG of naive (empty bars), sham-operated (grey bars) and rats subjected to L5 spinal nerve ligation (black bar). Spinal nerve ligation reduces the proportion of neurons expressing NAPE-PLD, TRPV1 and the CB1 receptor and increases the proportion of FAAH in the injured L5 DRG. ($p<0.001$ for TRPV1, $p<0.001$ for TRPV1, $p<0.001$ for the CB1 receptor and $p<0.001$ for FAAH, 2-tailed Fisher's exact test). In addition, the sham injury also reduces the number of neurons exhibiting immunopositivity for NAPE-PLD. Bar=50μm.

INFLAMMATION OF ~~PAINFUL~~ PERIPHERAL TISSUES AND INJURY TO PERIPHERAL NERVES INDUCE DIFERRING EFFECTS IN ~~PATHOLOGIES DISRUPT~~ THE EXPRESSION OF THE~~BALANCE OF AUTOCRINE SIGNALLING BY ANANDAMIDE SYNTHESISED IN A~~ CALCIUM-SENSITIVE ANANDAMIDE-SYNTHESISING ENZYME AND RELATED MOLECULES~~MANNER~~ IN RAT PRIMARY SENSORY NEURONS

Dr João Sousa-Valente[1], Dr Angelika Varga[1,2], Mr Jose Vicente Torres Perez[1], Dr Agnes Jenes[1,2], Dr John Wahba[1], Professor Ken Mackie[3], Professor Benjamin Cravatt[4], Professor Natsuo Ueda[5], Dr Kazuhito Tsuboi[5], Dr Peter Santha[6], Professor Gabor Jancso[6], Dr Hiren~~Hiran~~ Tailor[1], Dr António Avelino[7] and Hon Professor Istvan Nagy[1]

[1]Section of Anaesthetics, Pain Medicine and Intensive Care, Department of Surgery and Cancer, Imperial College London, Chelsea and Westminster Hospital, 369 Fulham Road, London, SW10 9NH, United Kingdom; [2]Department of Physiology, University of Debrecen, Medical and Health Science Center, Nagyerdei krt. 98, Debrecen, H-4012, Hungary; [3]Department of Psychological & Brain Sciences, Gill Center for Biomedical Sciences, Indiana University, Bloomington, IN 47405, USA; [4] The Skaggs Institute for Chemical Biology and Department of Chemical Physiology, The Scripps Research Institute, La Jolla, California, USA; [5]Department of Biochemistry, Kagawa University School of Medicine, 1750-1 Ikenobe, Miki, Kagawa 761-0793, Japan [6] Department of Physiology, University of Szeged, Dóm tér 10, 6720, Szeged, Hungary; [7]Departamento de Biologia Experimental, Faculdade de Medicina do Porto, Rua, Plácido~~Plácido~~ Costa, 4200-450 Porto, Portugal and I3S - Instituto de Investigação e Inovação em Saúde, IBMC - Instituto de Biologia Molecular e Celular, Rua Alfredo Allen, 208 4200-135 Porto, Portugal

Abbreviated title: NAPE-PLD in DRG

Associate Editor: Prof. Gert Holstege

Keywords: cannabinoid type 1 receptor, transient receptor potential vanilloid type 1 ion channel, fatty acid amide hydrolase, pain, inflammation, neuropathy

Formatted: Superscript

Formatted: Font: Font color: Auto

Formatted: Font: Font color: Auto

RRID: Aviva Systems Biology Cat# ARP55927_P050 RRID:AB

Correspondence: Istvan Nagy, MD, PhD, Section of Anaesthetics, Pain Medicine and Intensive Care, Department of Surgery and Cancer, Imperial College London, Chelsea and Westminster Hospital, 369 Fulham Road, London, SW10 9NH, United Kingdom, Phone: (0)20-33158897, Fax: (0)2033155109, email: i.nagy@imperial.ac.uk

Acknowledgements: Part of this work has been supported by a project grant from the Wellcome Trust (061637/Z/06/Z) and the NIH (DA011322 and DA021696). João~~Joao~~ Sousa-Valente has been supported by a PhD studentship from Fundação~~Fundacao~~ para a Ciência~~Ciencia~~ e a Tecnologia (Portugal). Angelika Varga has been supported by a European Union Marie Curie Intra-European Fellowship (254661) and by a Hungarian Social Renewal Operation Program (TÁMOP 4.1.2.E-13/1/KONV-2013-0010). Jose Vicente Torres Perez has been supported by a capacity building grant provided by the Chelsea and Westminster Health Charity. Agnes Jenes has been supported by a British Journal of Anaesthesia / Royal College of Anaesthetists Project Grant. Peter Santha has been supported by a Janos Bolyai Research Fellowship from the Hungarian Academy of Sciences.

Formatted: English (U.S.)

Formatted: English (U.S.)

ABSTRACT

Elevation of intracellular Ca^{2+} concentration induces the synthesis of N-arachydonoylethanolamine (anandamide) in a sub-population of primary sensory neurons. N-acylphosphatidylethanolamine phospholipase D (NAPE-PLD) is the only known enzyme, which synthesises converts N-acylphosphatidylethanolamine into N-acylethanolamines including N-arachydonoylethanolamine (anandamide) in a Ca^{2+}-dependentsensitive manner. NAPE-PLD mRNA, as well as anandamide's, with anandamide's, main targets, the inhibitory cannabinoid type 1 (CB1) receptor and the excitatory transient receptor potential vanilloid type 1 ion channel (TRPV1) and the inhibitory cannabinoid type 1 (CB1) receptor), and the main anandamide-hydrolysing enzyme fatty acid amide hydrolase (FAAH) are all expressed by sub-populations of nociceptive primary sensory neurons. Thus, NAPE-PLD, TRPV1, the CB1 receptor and FAAH could form an autocrine signalling system, which could shape the activity of in various neurons including a major sub-population of nociceptive primary sensory neurons, hence contribute to the development of pain. While the expression patterns of TRPV1, the CB1 receptor and FAAH have been comprehensively elucidated, little is known about NAPE-PLD expression in primary sensory neurons under physiological and pathological conditions. We. Here, we report that NAPE-PLD is expressed by about a third of primary sensoryDRG neurons, the overwhelming majorityand that NAPE-PLD exhibits a high degree of which also express nociceptiveco-expression with cellular markers of nociceptive primary sensory neurons as well as with the CB1 receptor, TRPV1 and FAAH. InflammationFurther, we report that various painful disturbances of the homeostasis of peripheral tissues and injury to peripheral nerves induce differing but concerted changes in the expression pattern of NAPE-PLD, the CB1 receptor, TRPV1 and

Formatted: Font color: Black, English (U.S.)

Formatted: Font color: Black, English (U.S.)

Formatted: Font color: Black, English (U.S.)

Formatted: Font color: Black, English (U.S.)

FAAH. Together these data indicate~~show~~ the existence of the anatomical basis for an ~~endocannabinoid/endovanilloid~~ autocrine signalling system, in a major proportion of nociceptive primary sensory neurons, and that alterations in that autocrine signalling by peripheral pathologies could contribute to the development of both inflammatory and neuropathic pain.

INTRODUCTION

N-arachidonoylethanolamine (anandamide) is a lipid signalling molecule (Devane et al., 1992), which is synthesised both in a Ca^{2+}-insensitive and Ca^{2+}-sensitive manner through respective multiple enzymatic pathways and a single pathway which involves the activity of N-acylphosphatidylethanolamine phospholipase D (NAPE-PLD) ~~N-arachidonoylethanolamine (anandamide; (Devane et al., 1992) is an endogenous agent which acts on a series of target molecules~~ (Goodfellow and Glass, 2009). Although, anandamide acts on a series of molecules, the transient receptor potential vanilloid type 1 ion channel (TRPV1) (Caterina et al., 1997) and the cannabinoid 1 (CB1) receptor ~~. Among those targets, the G protein-coupled cannabinoid 1 (CB1) receptor (Matsuda et al., 1990) and the non selective cationic channel transient receptor potential vanilloid type 1 ion channel (TRPV1)~~ (Caterina et al., 1997) are believed to be anandamide's main targets ~~, which respectively mediate inhibition and excitation in specific neurons~~ (Matsuda et al., 1990; Caterina et al., 1997). While activation of TRPV1 results in the opening of this non-selective cationic channel and subsequent excitation of nociceptive primary sensory neurons, activation of the CB1 receptor is believed to produce an inhibitory effect, which includes the inhibition of L-, P/Q-, and N-type voltage-gated Ca^{2+} channels in neurons including primary sensory neurons ~~are considered as the main neuronal targets for anandamide~~ (Devane et al., 1992; Zygmunt et al., 1999). Intriguingly, the CB1 receptor and TRPV1 are co-expressed by various neurons including a great proportion of nociceptive primary sensory neurons ~~.~~

~~Multiple enzymatic pathways are believed to catalyse the synthesis of anandamide in various cells~~ (Okamoto et al., 2004)~~.~~ This anatomical arrangement enables exogenous

anandamide to control the activity of neurons including a major group of nociceptive primary sensory neurons ~~either in a Ca^{2+} sensitive or Ca^{2+} insensitive manner~~ (van der Stelt et al., 2005; Vellani et al., 2008; Varga et al., 2014).

Anandamide is synthesised in ~~N-acylphosphatidylethanolamine phospholipase D (NAPE-PLD), which is a member of the zinc metallohydrolase family of β-lactamase fold enzymes (Okamoto et al., 2004), is currently the only enzyme known to be involved in Ca^{2+} sensitive anandamide synthesis (Ueda et al., 2001; Okamoto et al., 2004; Wang et al., 2006; Wang et al., 2008).~~

~~In dorsal root ganglia (DRG), a great proportion of nociceptive primary sensory neurons express both TRPV1 and the CB1 receptor (Ahluwalia et al., 2000; Binzen et al., 2006; Mitrirattanakul et al., 2006; Agarwal et al., 2007). Intriguingly,~~ sub-populations of primary sensory neurons both in Ca^{2+}-sensitive and Ca^{2+}-insensitive manners (van der Stelt et al., 2005; Vellani et al., 2008; Varga et al., 2014). In agreement with the ability of a group of primary sensory neurons to synthesise anandamide~~TRPV1-expressing primary sensory neurons produce anandamide either~~ in a Ca^{2+}-sensitive ~~or a Ca^{2+} insensitive~~ manner (van der Stelt et al., 2005; Vellani et al., 2008; Varga et al., 2014) and the role of NAPE-PLD~~. Consistently, several enzymes which are implicated~~ in such~~Ca^{2+} insensitive~~ anandamide synthesis (Liu et al., 2006; Simon and Cravatt, 2006; Liu et al., 2008; Simon and Cravatt, 2008), ~~as well as~~ NAPE-PLD mRNA is expressed by~~have been found in~~ primary sensory neurons (Nagy et al., 2009; Bishay et al., 2010; Varga et al., 2014). Importantly, the~~The~~ majority of the NAPE-PLD mRNA-expressing cells are capsaicin sensitive (Nagy et al., 2009), therefore, they should also ~~appear to~~ express TRPV1, and the

Formatted: Justified, Widow/Orphan control, Adjust space between Latin and Asian text, Adjust space between Asian text and numbers

CB1 receptor –(Nagy et al., 2009). Thus, in addition to exogenous anandamide, anandamide of primary sensory neuron origin could also be able to control TRPV1 and CB1 receptor activity in a major sub-population of nociceptive primary sensory neurons in an autocrine manner (van der Stelt and Di Marzo, 2005; van der Stelt et al., 2005). Importantly, the .

In addition to NAPE-PLD and the CB1 receptor, the great majority of TRPV1-expressing primary sensory neurons also express the main anandamide-hydrolysing enzyme, fatty acid amide hydrolase (FAAH) (Cravatt et al., 1996; Lever et al., 2009). Blocking FAAH activity, through increasing the level of anandamide, also results in regulating the activity of a proportion of nociceptive primary sensory neurons through the CB1 receptor and TRPV1 (Lever et al., 2009). Based on the co-expression pattern ofthese data it has been hypothesised that anandamide-synthesising enzymes, including NAPE-PLD, together with TRPV1, the CB1 receptor, NAPE-PLD and FAAH, and the effects of those molecules, the presence of may form an endocannabinoid/endovanilloid autocrine signalling system built by those molecules has been proposed in a major sub-population(s) of nociceptive primary sensory neurons (van der Stelt and Di Marzo, 2005; Sousa-Valente et al., 2014b; Varga et al., 2014). That autocrine signalling system, through TRPV1- and CB1 receptor-mediated changes in the intracellular Ca^{2+} concentration and subsequent NAPE-PLD-mediated anandamide synthesis, as well as FAAH-mediated anandamide hydrolysis is considered to be prominently suitable to provide a significant control over TRPV1 and CB1 receptor activity in, hence over the excitation of, a major group of nociceptive primary sensory neurons (van der Stelt and Di Marzo, 2005; Sousa-Valente et al., 2014b; Varga et al., 2014). -

The excitation level of nociceptiveNociceptive primary sensory neurons isplay a pivotal forrole in the initiation and maintenancedevelopment of pain experiences including those which are associated both during acute encounter of tissues with peripheral pathologies, suchnoxious impact as inflammation of peripheral tissues and injury to peripheral nerveswell as in pathological conditions (Nagy et al., 2004; Sousa-Valente et al., 2014a). Therefore, the control provided by the endocannabinoid/endovanilloid autocrine signalling system built by the CB1 receptor, TRPV1, NAPE-PLD and FAAH in a major group of nociceptive primary sensory neurons may play an important role in the development and maintenance of pain. While the expression patterns, and the changes in those expression patterns by pathological conditions, of the CB1 receptor, TRPV1 and FAAH have comprehensively been elucidated . While TRPV1 is specifically involved in the development of inflammatory heat hyperalgesia (Caterina et al., 2000; Davis et al., 2000) and peripheral nerve injury-associated heat hyperalgesia and mechanical allodynia (Walker et al., 2003; Vilceanu et al., 2010), activation of the CB1 receptor produces an analgesic effect (Calignano et al., 1998; Richardson et al., 1998; Kelly et al., 2003; Clapper et al., 2010). Hence, the putative anandamide induced autocrine signalling system, particularly its alteration by pathological events could be important in controlling the activity and excitability of a major sub-population of nociceptive primary sensory neurons hence the development of pain in various peripheral pathologies (van der Stelt and Di Marzo, 2005; Sousa-Valente et al., 2014b).

In, little is known about those properties and changes of NAPE-PLD. Accordingly, in order to improve our understanding of the putative autocrine

Formatted: English (U.K.)

Formatted: Justified, Widow/Orphan control, Adjust space between Latin and Asian text, Adjust space between Asian text and numbers

cannabinoid/endovanilloid signalling in primary sensory neurons, here we describe the co-expression patterns of NAPE-PLD with TRPV1, the CB1 receptor and FAAH in naive condition and changes those expression patters by pathological conditionas. Preliminary findings have been reported earlier (Valente et al., 2011). ~~order to gain a better understanding of the role of the anandamide – CB1 receptor – TRPV1 – FAAH mediated putative autocrine signalling system in nociceptive processing in primary sensory neurons, in this study we have characterised the expression of the components of this putative signalling system under physiological conditions and following inflammation of peripheral tissues and injury to peripheral nerves in DRG neurons. Preliminary findings have been reported earlier (Valente et al., 2011).~~

METHODS

Forty two male Wistar rats (250-300 g), 10~~8~~ C57BL/6 wild type (WT) and 10~~8~~ NAPE-PLD$^{-/-}$ (Leung et al., 2006; Tsuboi et al., 2011) adult mice were used in this study. NAPE-PLD$^{-/-}$ mice were generated by the deletion of a sequence (from amino acid 99 to amino acid 313), which contains the catalytic domain of the enzyme (Leung et al., 2006; Tsuboi et al., 2011). Both WT and NAPE-PLD$^{-/-}$ mice have been used for antibody control purposes. All quantitative assessments on NAPE-PLD expression pattern have been performed on rat tissues.

Formatted: Superscript

All procedures were performed according to the UK Animals (Scientific Procedures) Act 1986, the revised National Institutes of Health *Guide for the Care and Use of Laboratory Animals*, the Directive 2010/63/EU of the European Parliament and of the Council on the Protection of Animals Used for Scientific Purposes and the guidelines of the Committee for Research and Ethical Issues of IASP published in Pain, 16

(1983) 109-110. Further, we fully obeyed to Good Laboratory Practice and ARRIVE guidelines. Every effort was taken to minimize the number of animals used.

Rat models of inflammatory and neuropathic pain

Tissue inflammation was induced by injecting 50µl of 50% complete Freund's adjuvant (CFA, Thermo Scientific, USA) or incomplete Freund's adjuvant (IFA, Thermo Scientific, USA) subcutaneously into the plantar aspect of the left hindpaw of adult rats. The injection was performed under isoflurane-induced anaesthesia.

Nerve injury was produced according to previously published protocols (Kim and Chung, 1992)~~(Kim and Chung, 1992)~~. Briefly, rats were deeply anaesthetised by isoflurane and the fifth lumbar (L5) spinal nerve was exposed and identified after partial laminectomy. A tight 4.0 ligature was then placed around the nerve. The nerve was cut about 5mm distal from the ligature and the wound was closed in layers. The sham operation consisted of exposing the L5 spinal nerve without placing the ligature or cutting the nerve.

Testing pain-related behaviour

Inflammation- or nerve injury-induced changes in responses to mechanical stimuli were assessed by using an electrical von Frey apparatus (Ugo Basile, Italy). Briefly, rats were placed in a Perspex chamber with a 0.8 cm-diameter mesh flooring and allowed to acclimatize for 15 min. The tip of the probe was pressed against the plantar surface of the paw at a steadily increasing pressure, until the animal voluntarily withdrew the paw. The paw-withdrawal threshold was defined as the average weight in grams over three applications. Care was given not to repeat testing on the same

paw within 5 minutes. Responses to mechanical stimuli were assessed every day for two days prior to, and three days after, the injection of either CFA or IFA. In animals which were subjected to nerve injury, changes in the sensitivity to mechanical stimulation was assessed every day for two days prior to, and then on the second, fourth and seventh day after, the surgery.

Inflammation- or nerve injury-induced changes in responses to noxious heat stimuli were assessed by the Hargreaves test (Hargreaves et al., 1988)~~(Hargreaves et al., 1988)~~. Briefly, rats~~animals~~ were placed in a Perspex box. After a fifteen minutes acclimatisation period, an infrared beam (Ugo Basile, Italy), which is able to deliver a constantly increasing thermal stimulus, was directed to the plantar surface of the paw. The time until the animal voluntarily withdrew the paw was measured. Again, attention was given not to repeat testing on the same paw within 10 minutes. Responses to heat and mechanical stimuli were assessed on the same days.

Reverse transcriptase polymerase chain reaction (RT-PCR)

Rats were terminally anaesthetised~~anaesthesised~~ with isoflurane and L4 and L5 DRGs were collected in RNAlater (Sigma-Aldrich, USA) and homogenised using QIA shredder columns (QIAGEN, UK). Total RNA was extracted using RNeasy Plus Mini Kit (QIAGEN, UK) according to the manufacturer's instruction. RNA was reverse-transcribed using SuperScript II cDNA synthesis reagents (Invitrogen, USA). Sequences~~Sequence~~ of the primers (Eurofins MWG Operon, Germany) designed to amplify rat NAPE-PLD (NM_199381.1) are: forward: TACCAACATGCTGACCCAGA; reverse: ATCGTGACTCTCCGTGCTTC. Sequences of primers designed to amplify~~and~~ the housekeeping gene, glyceraldehyde-

3- phosphate dehydrogenase (GAPDH, NC_005103) are: forward: ACCCATCACCATCTTCCA; reverse: CATCACGCCACAGCTTTCC. The), annealing temperature was 57°C ~~temperatures, number of cycles~~ and product sizes were 199bp for NAPE-PLD and 380bp for GAPDH.~~are shown in Supplementary Table 1.~~ The PCR mixture was composed of cDNA, primers, 1.5 mM $MgCl_2$, 1× Green Go-Taq Reaction buffer (Promega, USA), 0.2 mM deoxynucleotide mix (Promega, USA) and 1.25 U Go-Taq DNA polymerase (Promega, USA), the number of cycles was 30.) After amplification, PCR products were separated by electrophoresis on 2% agarose gels and visualized with ethidium bromide using Syngene G:BOX (Synoptics Ltd, UK). Images were analysed by Syngene's GeneTools software (Synoptics Ltd, UK).

Western-blotting

Rats and mice~~Animals~~ were terminally anaesthetised~~anaesthesised~~ with isoflurane and L4 and L5 DRGs were collected and homogenized on ice in NP40 cell lysis buffer (Invitrogen, USA) supplemented with protease inhibitors cocktail (Sigma, USA). The protein content of the samples was determined with the BCA Protein Assay Reagent (Pierce Biotechnology, IL, USA). Proteins were denatured at 95 ºC for 10 minutes with 4-times concentrated NuPAGE LDS sample buffer (Invitrogen, USA) after which they were run in a NuPAGE Novex 4-12% Bis-Tris gel (Invitrogen, USA) and blotted onto PVDF membrane using the iBlot® Dry Blotting System (Invitrogen, USA). To visualise NAPE-PLD, the membrane was first incubated in 5% non-fat milk and then in an anti-NAPE-PLD antibody (1:1000, Aviva Systems Biology, USA), overnight at 4 ºC. The anti-NAPE-PLD antibody has been raised against the 71-130 amino acid sequence of the protein

Formatted: English (U.S.)

Formatted: Font: (Default) Times New Roman

(TWKNPSIPNVLRWLIMEKDHSSVPSSKEELDKELPVLKPYFITNPEEAGV). Forty four % of this sequence is missing in NAPE-PLD-/- mice (Leung et al., 2006; Tsuboi et al., 2011).

Following the incubation of the membranes in the anti-NAPE-PLD antibody, they were incubated with Horseradish peroxidase-conjugated goat anti-rabbit secondary antibody (1:1000, Cell Signaling, USA) for an hour at room temperature. Western blotting luminol reagent (Santa Cruz, USA) was used for visualization. Images were captured using Syngene G:BOX (Synoptics Ltd, UK) and were analysed by Syngene's GeneTools software (Synoptics Ltd, UK). Membranes were then stripped with 0.2 M glycine stripping buffer supplemented with 0.5% Tween-20 (pH 3.0) at room temperature for 30 minutes and re-probed with rabbit anti-β-actin as a loading control (1:1000, Cell Signaling Technology, Danvers, MA).

Formatted: Justified

Immunostaining

Animals were terminally anaesthetised by intraperitoneal injection of sodium pentobarbital (60 mg/kg) and perfused through the ascending aorta with 100 ml of 0.9% saline followed by 300 ml of 4% paraformaldehyde in 0.1 M phosphate buffer (PB; pH 7.4). The cerebellum and L4 and L5 DRGs were identified and collected bilaterally. Tissues were post-fixed for 4h-24h at 4°C in 4% paraformaldehyde in 0.1 M PB, cryoprotected in 30% sucrose in 0.1 M PB for 1-2 days at 4°C, embedded in a mounting medium and cut with a cryostat into either 10µm sections for DRG tissue or 30 µm for cerebella which were mounted on Superfrost slides.

Slides were washed with PBS containing 0.3% Triton X-100 (PBST) and then incubated with PBST containing 10% normal donkey serum (Jackson ImmunoResearch Labs, USA) for 1 hour at room temperature. Slides were then incubated in PBST containing 2% NDS and the appropriate primary antibody/antibodies ~~(Supplementary Table 2)~~ for 24 hours at room temperature. The antibodies, in addition to the anti-NAPE-PLD antibody described above included: anti-NF200 (200kD neurofilament) andibody (Sigma-Aldrich): clone NE14; anti-CGRP (calcitonin gene-related peptide) antibody Abcam: AB22560; anti-TRPV1 antibody (A. Avelino laboratory): EDAEVFKDSMVPGEK; anti-CB1 receptor antibody (K. Mackie laboratory): SCNTATCVTHRLAGLLSRSGGVVKDNFVPTNVGSEAF; anti-FAAH antibody (B. Cravatt laboratory): GAATRARQKQRASLETMDKAVQRFRLQNPDLDSEALLTLPLLQLVQKLQSG ELSPEAVFFTYLGKAWEVNKGTNCVTSYLTDCETQLSQAPRQGLLYGVPVSL KECFSYKGHDSTLGLSLNEGMPSESDCVVVQVLKLQGAVPFVHTNVPQSMLS FDCSNPLFGQTMNPWKSSKSPGGSSGGEGALIGSGGSPLGLGTDIGGSIRFPSA FCGICGLKPTGNRLSKSGLKGCVYGQTAVQLSLGPMARDVESLALCLKALLC EHLFTLDPTVPPLPFREEVYRSSRPLRVGYYETDNYTMPSPAMRRALIETKQR LEAAGHTLIPFLPNNIPYALEVLSAGGLFSDGGRSFLQNFKGDFVDPCLGDLIL ILRLPSWFKRLLSLLLKPLFPRLAAFLNSMRPRSAEKLWKLQHEIEMYRQSVI AQWKAMNLDVLLTPMLGPALDLNTPGRATGAISYTVLYNCLDFPAGVVPVT TVTAEDDAQMELYKGYFGDIWDIILKKAMKNSVGLPVAVQCVALPWQEELC LRFMREVEQLMTPQKQPS. In the majority of the experiments, NAPE-PLD immunostaining was amplified by the tyramide signal amplification (TSA) system ~~according to the manufacturer's~~ (PerkinElmer Life and Analytical Sciences, USA)

Formatted: Font: 12 pt

Formatted: HTML Preformatted, Widow/Orphan control, Adjust space between Latin and Asian text, Adjust space between Asian text and numbers, Pattern: Clear (White)

Formatted: Font: 12 pt

Formatted: Font: 12 pt

Formatted: Font: 12 pt

instructions. The immunostaining was visualised by 488nm or 568nm alexa fluor-conjugated streptavidin (1:1000) , Invitrogen, USA) or a fluorophore-conjugated secondary antibodies for an hour. Previously we have extensively tested the specificity and selectivity of the anti-TRPV1-, anti-CB1 and anti-FAAH antibodies (Cruz et al., 2008; Lever et al., 2009; Veress et al., 2013). ~~(Supplementary Table 2).~~

Formatted: Font: Times New Roman, 12 pt

Formatted: Font: 12 pt

For the TSA amplification, following incubation of sections in the primary antibody, a biotinylated~~biotynilated~~ secondary antibody (1:500 biotin donkey anti-rabbit, Jackson ImmunoResearch Labs, USA) was applied. Slides were then incubated with peroxidase containing avidin-biotin complex (1:200, ABC kit, PerkinElmer Life and Analytical Sciences, USA) for an hour. The biotinylated tyramide was detected with fluorescent streptavidin (see above). In order to control for the combined use of two antibodies raised in the same species in combination with the TSA amplification, the following experiments were conducted: a) the primary antibody was omitted; b) a fluorescent secondary antibody, recognising the species the primary antibody was produced in, was added at the end of the TSA reaction to check if any unoccupied primary antibody could generate signal; c) for the same primary antibody, a TSA reaction and primary-fluorescent secondary antibody reaction were done in tandem in adjacent sections to verify whether both types of reactions yield similar results.

In addition to the antibodies, fluorescein-labelled *Griffonia simplicifolia* isolectin B4 (IB4) (Sigma-Aldrich, USA) was used to identify the non-peptidergic sub-population of nociceptive primary sensory neurons (Silverman and Kruger, 1990)~~(Silverman and Kruger, 1990)~~. This was performed by incubating sections in 1:1000 dilution of the fluorochrome-conjugated IB4 for 1 hour during the final incubation step for NAPE-

PLD staining. Slides were mounted in Vectashield medium (Vector Laboratories, USA).

Control experiments

For testing the specificity and selectivity of the anti-NAPE-PLD antibody, first~~,~~ we studied proteins identified by the anti-NAPE-PLD antibody in protein samples prepared from the cerebella of WT~~wild type~~ and NAPE-PLD-/- mice. Further, we also studied the immunostaining generated by the anti-NAPE-PLD antibody in sections cut from DRG and cerebellum of WT~~wild type~~ and NAPE-PLD-/- mice. Finally, we also studied the proportion and size distribution of cells expressing NAPE-PLD mRNA as well as the co-expression pattern between NAPE-PLD mRNA and NAPE-PLD protein (*vide infra*).

Fluorescent in situ hybridisation

Fluorescent *in situ* hybridization was carried out using a Custom Stellaris FISH Probe Kit, which contains 48 fluorescent dye-conjugated NAPE-PLD mRNA complementary short probes (Biosearch Technologies). All material and stock solutions were treated with diethyl pyrocarbonate (DEPC; Sigma), RNase ZAP (Sigma), or kept at -80~~180~~ ^{o}C for 8 hours in order to prevent RNA degradation. The DEPC treatment included adding 2.5 mM of DEPC to all solutions and autoclaving. DRG sections mounted onto coverslips were washed with PBS then permeabilized with 70% ethanol for 1 hour at room temperature. After rinsing in washing buffer, which contained 20% formamide and 2 times concentrated saline sodium citrate (SSC) buffer (which contained sodium chloride and trisodium citrate), slides were incubated with the NAPE-PLD probe (2.5 µM) in hybridization buffer (2 times SSC

buffer, 10 % formamide and 100 mg/ml dextran sulphate) at room temperature for 24 h. The following day, after 1-hour incubation in the washing buffer, slides were immunoreacted with the NAPE-PLD antibody as described above. For control, sections were incubated as described above, but the NAPE-PLD probes were omitted from the hybridisation buffer. Control sections were run in parallel with sections incubated in the presence of the NAPE-PLD probes.

Image analysis and quantification of immunofluorescent DRG cells

Immunofluorescent images were examined using a Leica DMR Fluorescence, a Zeiss Axioscope 40, or a Zeiss LSM 700 Confocal Laser Scanning microscope. With the Leica microscope, imagesImages were taken by a Hamamatsu CCD camera connected to a PC running the QWIN software package (Leica, Germany). The PC connected to the Zeiss Axioscope 40 ran the AxioVision 4.6 software, whereas the PC connected to the ZEISS LSM 700 microscope ran the ZEN software package.

Formatted: Font color: Black

With each microscope, respectiveAll images were taken using identical acquisition parameters were used and raw, unprocessed images were used for analysis with Image J (NIH). Images selected for figures however were subject to contrast and brightness adjustments if we felt they were necessary.

Neurons, which displayed a visible nucleus were identified, and the cytoplasm together with the nucleus of these cells were marked as regionsregion of interestinterests (ROI). The area and mean pixel intensity of the ROIs were then measured. At least 200 cells were sampled in each side of each animal, in serial sections at a distance of ± 10 sections (i.e.100µm) apart from each other to make sure

that each cell with a given staining was included in the analysis only once.

The threshold staining intensity was established using three independent methods. First, with visual inspections we confirmed that sections contained both immunopositive and immunonegative cells. The presence of the 2 types of neurons was also confirmed by the non-normal distribution of the staining intensities in each section (Shapiro-Wilk test). k-clustering is able to separate variables into a defined number of clusters which then exhibit the greatest possible distinction. Therefore, we used k-clustering to define 2 clusters and the intensity values which separate the two groups of neurons in each section.

In the second method, raw intensity values were transformed using a logarithmic equation (LOG(255/(255-value)). These values were ranked and displayed on a scatter plot. The initial and last linear parts of the plots were then fitted with a tangent, and the intensity value at the intersection of the two fitted lines were used as a threshold to separate labelled and non-labelled cells. ~~(Supplementary Figure 1).~~ This initial separation was then used in a discriminant analysis as prediction. This statistical probe also confirmed that the accuracy of the prediction was between 95% and 100%.

Finally, one blinded experimenter examined images of randomly chosen sections from naive animals, and the immunopositivity or immunonegativity judged by that experimenter was noted. These notes were than associated with the staining intensity values measured by Image J. These combined data were then used to determine the threshold of immunopositivity by the receiver operating curve. Importantly, the ratio

of immunopositive and immunonegative cells determined by the three methods did not differ more than 5%. Data presented throughout the manuscript are obtained with the second method.

In addition to establishing the immunopositive and immunonegative cells, intensity values were also used for studying pathology-induced changes in staining intensities of NAPE-PLD-, TRPV1-, CB1 receptor- and FAAH-immunopositivity, as well as pathology-induced changes in the correlation between staining intensities of NAPE-PLD and TRPV1-, CB1 receptor- or FAAH-immunopositivity.

Statistics

In naive animals, data ~~Data~~ from both the left and right sides ~~of naive animals~~ were analysed~~combined~~, and ~~those combined data were~~ used for further statistical analysis. In treated animals, data~~Data~~ obtained from the ipsilateral and contralateral sides of ~~animals with~~ the same treatment group were respectively~~then~~ averaged, tested for normal distribution (Shapiro-Wilk test) and analysed for statistical differences. The statistical analysis of behavioural data was performed between withdrawal responses (on different testing days or between different animal groups on the same testing day) using ANOVA followed by Tukey's test, or using 2-tailed Student's t-test as appropriate. Statistical comparisons between the number of immunostained cells identified in different experimental groups was performed by 2-tailed Fisher's exact test. Differences between sizes of neurons belonging to various populations were compared using 2-tailed Mann-Whitney U test. All data are expressed as a mean ± SEM. "n" refers to the number of repeated measurements~~animals used~~ in each of the experimental groups. A difference was regarded as statistically significant at $p<0.05$.

RESULTS

NAPE-PLD is expressed in primary sensory neurons of DRG

Gel images of RT-PCR products exhibited detectable levels of NAPE-PLD mRNA in L4-5 rat DRG (Figure 1A). The size of the PCR product was indistinguishable from the expected product size of 199 bp (Figure 1A). These findings support previous data that a sub-population of primary sensory neurons expresses NAPE-PLD (Nagy et al., 2009; Bishay et al., 2010).

To confirm that the NAPE-PLD mRNA is expressed in neurons in DRG, we performed fluorescent *in situ* hybridisation in sections cut from rat L4-5 DRG. Analysis of the staining confirmed that NAPE-PLD mRNA is expressed in~~by~~ DRG and that only a sub-population of neurons expresses this transcript (Figure 1B and C).

To find whether the NAPE-PLD protein is also expressed in rat DRG, we performed Western-blotting. The anti-NAPE-PLD antibody (Aviva Systems Biology) we used throughout this study recognised, in addition to some unknown proteins, a protein with the predicted size of NAPE-PLD (~46kDa) in samples prepared from rat DRG (Figure 2A). In addition, the anti-NAPE-PLD antibody also recognised a protein with the predicted size of (~46kDa) in WT mouse brain (together with the ~~, though some~~ apparently same unknown ~~heavier~~ proteins; Figure 2A). However, while the antibody ~~were also~~ recognised the unknown proteins, it ~~(Figure 2B). Nevertheless, the same antibody,~~ did not recognise ~~either~~ the specific ~46kDa protein~~and unknown proteins~~ in samples prepared from the brain of NAPE-PLD$^{-/-}$ mice (Figure 2A).~~2B).~~

To confirm that the NAPE-PLD protein is expressed exclusively by neurons in DRG, we incubated sections cut from rat L4-5 DRGs with~~in~~ the anti-NAPE-PLD antibody and visualised the staining using TSA. Analysis of the immunostaining revealed that the antibody produced a homogenous staining in the cytoplasm of DRG neurons (Figure 2B). In addition to DRG neurons, a fluorescent signal~~immunopositivity~~ was also seen in some satellite cells (Figure 2B~~2C~~). However, our control experiments revealed that this staining is produced by the TSA reaction if the postfixation time is less than 24h hours (data not shown~~Supplementary Figure 2~~).

To obtain evidence that the anti-NAPE-PLD antibody~~,~~ produces a selective and specific immunostaining, we immunoreacted cerebellum and DRG sections of WT and NAPE-PLD$^{-/-}$ mice ~~as well as of rats~~ (Figure 3A-D~~2D-H~~). As expected (Suarez et al., 2008; Nagy et al., 2009) ~~rat and~~ WT mouse Purkinje cells (Figure 3A$_{1-4}$~~and some neurons in the molecular layer of the cerebellum (Figure 2D and E~~) as well as a sub-population of WT mouse DRG neurons (Figure 3C$_{1-4}$~~2G~~) exhibited strong NAPE-PLD immunoreactivity. In contrast, the immunoreaction produced by this antibody was lost in both ~~in~~ cerebella and DRG dissected from NAPE-PLD$^{-/-}$ mice (Figure 3B$_{1-4}$~~2F~~ and 3D$_{1-4}$~~H~~).

To provide further evidence that the anti-NAPE-PLD antibody produces a specific and selective staining, we also combined the immunostaining with *in situ* hybridisation~~histochemistry~~ using fluorescent NAPE-PLD probes (Figure 4~~2I~~). Analysis of this combined staining revealed that 73 of 231 cells (31.6%) showed positivity for the *in situ* probes. The number of cells showing NAPE-PLD immunopositivity was not significantly different from this value (75 of 231 (32.5%),

p=0.9, Fischer's exact test). The proportion of immunopositive neurons was not significantly different from that found in naive animals ~~(n=18)~~ in the rest of the study (37.~~60~~60±0.17%, p=0.13, n=18~~07~~; Fischer's exact test). The combined fluorescent *in situ* hybridisation and immunofluorescent~~immufluorescent~~ staining also revealed that fifty-nine of the total number of neurons showed double staining (25.6%), which represented 80.8% and 78.7% of the *in situ*- and immuno~~immune~~-positive cells, respectively.

NAPE-PLD is expressed in small DRG neurons

Next we analysed the morphology and neurochemical properties of NAPE-PLD-expressing primary sensory neurons. Of the 8129 DRG neurons we analysed, 3056 were NAPE-PLD-immunoreactive (37.60±0.17%, 3056 of 8129 cells in the "ipsilateral" and "contralateral" sides of 9 animals, n=18 repeated measurements; Table 1).~~n=18).~~ The cell-size distribution of NAPE-PLD-immunostained neurons revealed that most of the NAPE-PLD-expressing cells were small neurons, though some large NAPE-PLD-immunopositive cells were also found (Figure 5~~3~~). The area of perikarya of the NAPE-PLD-immunoreactive cells was 923±9 μm^2 (n=3056). This value was significantly smaller than the average area of perikarya of unlabelled cells (1315±10 μm^2, n=5073, 2-tailed Mann Whitney U test, p=0.01).

NAPE-PLD is expressed by both ~~by~~ peptidergic and non-peptidergic nociceptive neurons

The great majority of small diameter primary sensory neurons are nociceptive in function (Nagy et al., 2004).~~(Nagy et al., 2004).~~ While nociceptive primary sensory neurons either contain neuropeptides such as calcitonin gene-related peptide (CGRP)

or express the binding site for the lectin IB4, non-nociceptive neurons express the heavy (200kDa) neurofilament NF200 (Lawson et al., 1984; Lawson and Waddell, 1991). Therefore, to confirm that NAPE-PLD-expressing DRG neurons are indeed nociceptive, we used combined immunofluorescent staining using the anti-NAPE-PLD antibody, an anti-NF200, and an anti-CGRP antibody as well as fluorescein-conjugated isolectin B4 (IB4) on sections cut from L4-5 DRGs. Results of these combined immunoreactions are shown in Table 1 and Figure 64. In summary, 31.28±3.89% (n=63) of the NAPE-PLD immunoreactive neurons expressed NF200 (154 of 502 cells in the left and right sides of 3 animals), (Figure 6A, (Figure 4A-C; Table 1). In contrast, 52.05±2.02% (n=63) of the cells bound IB4 (267 of 512 cells in the left and right sides of 3 animals; Figure 6DFigure 4D-F, Table 1), and 34.58±2.67% (n=63) of the cells exhibited immunopositivity for the neuropeptide, CGRP (174 of 509 cells in the left and right sides of 3 animals; Figure 6GFigure 4G-I, Table 1). Importantly, more NAPE-PLD-expressing cells bound IB4 than contained CGRP (p<>0.001 Fisher's exact test).

NAPE-PLD shows a high level of co-expression with TRPV1, the CB1 receptor and FAAH

To find whether NAPE-PLD could indeed be involved in the formation of an autocrine endocannabinoid/endovanilloid signalling system in a sub-population of primary sensory neurons, we next assessed the co-expression of NAPE-PLD and FAAH, or the CB1 receptor or TRPV1. Data from the analysis of these combined immunoreactions are shown in Figure 75 and Table 1. In summary, we found a very high level of co-expression between NAPE-PLD and all the endocannabinoid/endovanilloid signalling-related molecules (Figure 75; Table 1).

However, significantly more (p=0.029 Fisher's exact test) NAPE-PLD-immunopositive neurons expressed the CB1 receptor (72.71±1.47%, n=6; 349 of 480 cells in 3 animals~~3~~) than TRPV1 (59.89±1.33%, n=6; 304 of 546 cells in the left and right sides of 3 animals).~~3)~~

We also assessed the correlation between the intensities of NAPE-PLD- and the CB1 receptor-, TRPV1- or FAAH~~FAHH~~-immunostaining, respectively. While NAPE-PLD- and CB1 receptor-immunostaining exhibited a high correlation (R=0.76±0.02, n=3; ~~Supplementary~~ Figure 8A~~3A~~), essentially, no correlation was found between NAPE-PLD- and TRPV1-immunostaining (R=0.14±0.07, n=3; ~~Supplementary~~ Figure 8B~~3B~~). Further, a weak correlation (R=0.34±0.06, n=3; data not shown) was found between the intensities of NAPE-PLD- and FAAH-immunoreactivity. ~~(not shown).~~

Both CFA and IFA injection induce changes in NAPE-PLD, TRPV1 and the CB1 receptor immunolabelling pattern

In primary sensory neurons, one of the main functions of anandamide's excitatory target, TRPV1, is to signal peripheral inflammatory events to the central nervous system (White et al., 2011; Nagy et al., 2014).~~(White et al., 2011).~~ To determine whether peripheral inflammation induces changes in NAPE-PLD expression that may be associated with increased TRPV1 activity, following the assessment of behavioural changes, we studied the expression pattern of NAPE-PLD, TRPV1, the CB1 receptor and FAAH after the induction of inflammation in the hind paw~~hindpaw~~.

CFA injection into the hind paw~~hindpaw~~ produced hypersensitivity to both thermal and mechanical stimuli, 3 days after injection which was significantly greater than

that induced by IFA (data not shown). ~~Supplementary Figure 4A and B).~~ The proportion of NAPE-PLD immunostained neurons was significantly reduced by both ~~by~~ CFA and IFA injections on the ipsilateral side (from 37.60±0.17% (3056/8129 cells in the left and right sides of 9 animals; n=18) to 35.18±0.64% (1363/3872 in the ipsilateral side of 3 animals)~~n=3;~~ p=0.01, Fisher's exact test,~~)~~ by IFA, and to 35.40±0.60% (1483/ 4181 cells in the ipsilateral side of 3 animals)~~n=3;~~ p=0.02, Fisher's exact test,~~)~~ by CFA, Figure 9~~6~~; Table 2) but not on the contralateral side. The cell-size distribution of the NAPE-PLD immunopositive cells was not changed either on the ipsilateral side or the contralateral side (data not shown). The high correlation between NAPE-PLD and CB1 receptor immunostaining intensity was significantly reduced both by CFA injection (from 0.76±0.02 (n=3) to 0.48±0.03 (n=3), p<0.001, Student's t-test; Figure 8C) and by IFA injection (from 0.76±0.02 (n=3) to 0.57±0.02 (n=3), p<0.001, Student's t-test; data not shown) on the ipsilateral but not on the contralateral side. Further,~~While~~ the ipsilateral/contralateral ratio of NAPE-PLD-, CB1 receptor- and FAAH-immunostaining were not changed (Figure 8D). However, the ipsilateral/contralateral ~~, this~~ ratio for TRPV1-immunolabelling was increased by both ~~by~~ IFA ~~and CFA~~ injection (from 1±0.03, ~~(~~n=3~~)~~ in naive to 1.21±0.07 ~~(~~n=3 in IFA-injected; p=0.02, Student's t-test; data not shown) and CFA~~) by IFA~~ injection (from 1±0.03, n=3 in naive~~and~~ to 1.16±0.05 in CFA injected, n=3; p=0.03~~(n=3, p=0.03, Student's t-test) by CFA injection; Supplementary Figure 5). Further, the high correlation between NAPE-PLD and CB1 receptor immunostaining intensity was significantly reduced both by CFA injection (from 0.76±0.02 (n=3) to 0.48±0.03 (n=3), p<0.0006, Student's t-test) and by IFA injection (from 0.76±0.02 (n=3) to 0.57±0.02 (n=3), p<0.0007~~, Student's t-test; Figure 8D~~) on the ipsilateral but not on the contralateral side (Supplementary Figure 6~~).

Spinal nerve ligation results in a pronounced reduction of NAPE-PLD immunoreactivity in injured DRG neurons

Nerve injury has been associated with changes in the expression in a large number of proteins including ~~TRPV1 and~~ various components of the endocannabinoid/endovanilloid system(s) as well as in anandamide levels in DRG (Michael and Priestley, 1999; Hudson et al., 2001; Costigan et al., 2002; Agarwal et al., 2007; Zhang et al., 2007b; Lever et al., 2009). Therefore, next we assessed nerve injury-induced alterations in NAPE-PLD, FAAH, TRPV1 and the CB1 receptor expression.

In agreement with previous data (Kim et al., 2012) ligation and transection of the 5th lumbar spinal nerve, but not sham surgery, resulted in the development of reflex hypersensitivity to mechanical and thermal stimuli from two to seven days after the surgery (data not shown).~~Supplementary Figure 4C and D).~~ Both the nerve injury and the sham surgery resulted in a significant reduction in the number of NAPE-PLD-immunostained neurons, in the injured DRG (from 37.60±0.17% (3056 of 8129 cells in the left and right sides of of 9 animals; n=18) to 33.71±2.19% (653 of 1932 cells in 3 sets of samples (i.e. 3 different combined staining) from the ipsilateral side of 3 animals, n=9, p=0.002 Fischer's exact test) by sham surgery, and to 18.50±1.42 (653 of 1932 cells in 3 sets of samples from the ipsilateral side of 3 animals, n=9, p<0.001~~0001~~, Fischer's exact test~~)~~ by SNL; Figure 10~~7~~; Table 3~~2~~) tough the SNL-induced reduction was significantly greater than that produced by the sham injury (p<0.001~~0001~~, Fischer's exact test). SNL but not the sham injury also reduced the number of TRPV1-immunolabelled (from 42.14±0.69% (569 of 1350 cells in the

ipsilateral and contralateral sides of 3 animals, n=6~~n=3~~) to 6.38±6.15% (41 of 695 cells in the ipsilateral side of 3 animals, n=3, p<0.001~~0001~~, Fischer's exact test) and CB1 receptor immunolabelled neurons (from 33.64±0.59% (426 of 1267 cells in the ipsilateral and contralateral sides of 3 animals, n=6~~n=3~~) to 24.64±8.46% (96 of 653 cells in the ipsilateral side of 3 animals, n=3, p<0.001~~0001~~, Fischer's exact test~~))~~ and increased the number of FAAH-immunolabelled neurons (from 34.39±1.24% (501 of 1464 cells in the ipsilateral and contralateral sides of 3 animals, n=6~~n=3~~) to 50.81±6.49% (307 of 614 cells in the ipsilateral side of 3 animals, n=3, p<0.001~~0001~~, Fischer's exact test) in the injured DRG (Figure 10; Table 3). Both the sham injury (data not shown) and SNL significantly reduced the correlation between the intensities of NAPE-PLD and CB1 receptor immunolabelling both on the ipsilateral (Figure 8C) and contralateral sides (data not shown).~~7; Table 2).~~ While the number of TRPV1-immunopositive cells was reduced, the ipsilateral/contralateral ratio of TRPV1 immunolabelling was increased (from 1±0.03 (n=3) to 1.29 (n=2, ~~Supplementary~~ Figure 8D~~5~~), though due to absence of TRPV1-immunolabelled neurons in one animal the significance could not be assessed.~~. Both the sham injury and SNL also significantly reduced the correlation between the intensities of NAPE-PLD and CB1 receptor immunolabelling both on the ipsilateral and contralateral sides (Supplementary Figure 6).~~

Previous data show that primary sensory neurons in the DRG adjacent to the injured DRG also show phenotypic changes (Hudson et al., 2001; Hammond et al., 2004). Therefore, we also assessed NAPE-PLD, TRPV1, CB1 receptor and FAAH immunostaining in the ipsilateral L4 DRG. We found no significant change in the ratio of immunopositive cells for NAPE-PLD (p=0.415), FAAH (p=0.454) and

TRPV1 (p=0.166; 2-tailed Fisher's exact test; Table 4~~data not shown~~). For the CB1 receptor, the significance level for the reduction in the ratio of immunopositive cells was p=0.051 (Fisher's exact test; Table 4)~~data not shown).~~

DISCUSSION

We have found in the present study that about a third of primary sensory neurons in lumbar DRGs expresses NAPE-PLD. Our present data also show that about 2/3 - 3/4 of the NAPE-PLD-expressing neurons could be nociceptive, because the majority of the NAPE-PLD-immunopositive cells are small diameter neurons which are nociceptive in function (Nagy et al., 2004)~~(Nagy et al., 2004)~~, and ~35%, ~50% and ~60% of the NAPE-PLD-expressing cells also express, respectively, the nociceptive markers, CGRP, IB4-binding site and TRPV1 (*nota bene*, CGRP, IB4-binding site and TRPV1 exhibit significant co-expression in DRG (Nagy et al., 2004)~~(Nagy et al., 2004)~~), whereas only ~30% of the cells express the non-nociceptive cell marker heavy weight neurofilament NF200. These data are consistent with recent findings, which show that NAPE-PLD mRNA is expressed in primary sensory neurons, and that the majority of those neurons are sensitive to the archetypical TRPV1 activator, capsaicin (Nagy et al., 2009; Bishay et al., 2010).

Between the two major types of nociceptive primary sensory neurons, NAPE-PLD exhibits preference for IB4-binding cells. IB4-binding and peptidergic primary sensory neurons differ in their peripheral tissue targets, spinal projections, membrane protein expression, responses to painful events, and even in the brain areas where the information they convey is~~are~~ transmitted (Bennett et al., 1996; Perry and Lawson, 1998; Breese et al., 2005; Todd, 2010). Functionally, IB4-binding neurons are

associated primarily with responses to noxious mechanical stimuli and the development of mechanical pain, though they may also significantly contribute to the development of thermal pain following nerve injury (Cavanaugh et al., 2009; Vilceanu et al., 2010). Hence, if NAPE-PLD is involved in nociceptive processing in primary sensory neurons, its activity could contribute, among others, to the regulation of mechanosensitivity and the development of mechanical pain.

Among the putative enzymatic pathways, which are implicated in converting NAPE into N-acylethanolamine (NAEA), including anandamide (Okamoto et al., 2004; Liu et al., 2006; Simon and Cravatt, 2006; Liu et al., 2008; Simon and Cravatt, 2008), the NAPE-PLD-catalysed pathway is the only one known to be Ca^{2+}-sensitive (Ueda et al., 2001; Okamoto et al., 2004; Wang et al., 2006; Wang et al., 2008; Tsuboi et al., 2011). van der Stelt and colleagues ~~(2005)~~ have reported that increasing the intracellular Ca^{2+} concentration results in anandamide synthesis in cultured primary sensory neurons (van der Stelt et al., 2005). These data therefore, indicate that NAPE-PLD is functional in cultured primary sensory neurons.

In addition to anandamide, related molecules including~~NAPE-PLD also catalyses the formation of~~ palmitoylethanolamine (PEA) and oleoylethanolamine (OEA) are also synthesised by NAPE-PLD.~~)~~. Both PEA and OEA (and anandamide) activate the peroxisome proliferator-activated receptor alpha (PPARα; (Fu et al., 2003; Lo Verme et al., 2005; Sun et al., 2006), and the G protein coupled receptor 119 (GPR119; (Overton et al., 2006; Ryberg et al., 2007). Further, PEA (and anandamide) also activates GPR55 (Ryberg et al., 2007; Lauckner et al., 2008). While PPARα is expressed in both small and large diameter cells, GPR55 is primarily expressed in

NF200-expressing large diameter cells (Lo Verme et al., 2005; Lauckner et al., 2008). Hence, the expression pattern of NAPE-PLD we found in the present study suggests that NAPE-PLD in addition to signalling through the CB1 receptor and TRPV1, could also be involved in signalling through PPARα and GPR55 in sub-populations of primary sensory neurons.

Consistent with the view that an autocrine signalling system, which involves anandamide, the CB1 receptor and TRPV1, could exist in a sub-population of nociceptive primary sensory neurons (Sousa-Valente et al., 2014b), we have shown here that NAPE-PLD exhibits a high degree of co-expression ~~both~~ with ~~both~~ TRPV1 and the CB1 receptor. We have also demonstrated here that NAPE-PLD also shows a high degree of co-expression with FAAH, which is expressed in the majority of TRPV1-expressing primary sensory neurons (Lever et al., 2009). Considering the co-expression patterns we found in the present study, together with those published previously on TRPV1 and CB1 receptor-, and on TRPV1 and FAAH co-expression (Ahluwalia et al., 2000; Binzen et al., 2006; Mitrirattanakul et al., 2006; Agarwal et al., 2007; Lever et al., 2009), it appears that the anatomical basis for an anandamide-, TRPV1-, CB1 receptor- and FAAH-mediated autocrine signalling system indeed exists in the majority of nociceptive primary sensory neurons. Importantly, our recent finding that TRPV1 shows a high degree of co-expression with some of the enzymes implicated in Ca^{2+}-insensitive anandamide synthesis (Varga et al., 2014)~~(Varga et al., 2014)~~ suggests that anandamide could be synthesised both in Ca^{2+}-sensitive and Ca^{2+}-insensitive manners in at least some of those primary sensory neurons.

While TRPV1 activation by anandamide results in excitation (Zygmunt et al., 1999; Ahluwalia et al., 2003; Potenzieri et al., 2009), CB1 receptor activation by this agent is generally considered as inhibitory in nociceptive primary sensory neurons (Calignano et al., 1998; Richardson et al., 1998; Kelly et al., 2003; Clapper et al., 2010). The CB1 receptor-mediated inhibitory effect, in those neurons, results *inter alia* in the reduction of TRPV1-mediated responses (Binzen et al., 2006; Mahmud et al., 2009; Santha et al., 2010). By hydrolysing anandamide, FAAH could serve as a brake both in the anandamide-induced TRPV1- and CB1 receptor-mediated effects.

We found recently that while anandamide produced in a Ca^{2+}-insensitive fashion in cultured primary sensory neurons induces TRPV1-mediated excitation, it does not produce a CB1 receptor-mediated inhibitory effect, when the inhibitory effect is assessed by measuring TRPV1-mediated responses (Varga et al., 2014). The finding that Ca^{2+}-sensitive anandamide production in primary sensory neurons results in TRPV1-mediated excitatory effects (van der Stelt et al., 2005) suggests that NAPE-PLD activity could also be associated with~~to~~ TRPV1 activation. However, while we found a strong correlation between NAPE-PLD- and CB1 receptor-immunostaining intensities, the correlation between NAPE-PLD- and TRPV1-immunostaining intensities is very low. These data suggest that NAPE-PLD activity, at least in intact DRG, may be linked to CB1 receptor, rather than to TRPV1 activation. If anandamide produced by Ca^{2+}-sensitive and Ca^{2+}-insensitive manner has indeed differing primary targets in primary sensory neurons, the anandamide-, CB1 receptor-, TRPV1- and FAAH-formed putative autocrine signalling system could exert a very delicate control over the activity of a major proportion of nociceptive cells, hence over the development of pain. Consequently, any change in the expression or activity of any

members of that system could disturb balanced signalling, which may contribute to the development of pain.

Our data indicate that various types of painful disturbances of the homeostasis of peripheral tissues are able to produce such perturbation. While CFA is used to induce a painful inflammatory reaction, IFA is used as its control, though IFA injection itself induces some inflammatory reaction and even hypersensitivity (Billiau and Matthys, 2001) ~~(Billiau and Matthys, 2001)~~. Indeed, IFA injection induced a transient hypersensitivity in the present study. Further, ~~, which~~ similarly to CFA injection it also induced a small nevertheless significant reduction in ~~reduced~~ the number of NAPE-PLD-immunolabelled cells as well as in~~and~~ the high correlation of intensities between NAPE-PLD and CB1 receptor immunolabelling. Both~~Further both~~ IFA and CFA increased the ipsilateral/contralateral intensity ratio of TRPV1 immunolabelling (i.e. increased in intensity of TRPV1 immunolabelling on the ipsilateral side). The slight but significant reduction in the number of CB1 receptor-expressing cells produced by CFA and IFA is surprising as they are opposite to those reported previously (Amaya et al., 2006) ~~(Amaya et al., 2006)~~. Further, the lack of increase in the number of TRPV1-expressing cells is also surprising as it differs from data reported earlier (Ji et al., 2002; Amaya et al., 2004; Luo et al., 2004; Amaya et al., 2006; Yu et al., 2008) but see (Zhou et al., 2003; Bar et al., 2004). These differences could be due to the use of different analysing techniques in the different studies. Nevertheless, the combined effects of the changes we observed suggest that a balanced signalling between anandamide of NAPE-PLD origin and TRPV1 and the CB1 receptor is tipped towards a signalling with increased excitatory and reduced inhibitory components. However, the contribution of this unbalanced signalling ~~to the development of hypersensitivity~~

~~in inflammatory condition~~ could be negligible~~small~~ because while the CFA injection-induced hypersensitivity is significantly greater than that produced by IFA injection, the changes in the expression pattern of the molecules are not.

Formatted: Strikethrough

A different type of perturbation of balanced endocannabinoid/endovanilloid signalling occurs following peripheral nerve injury, because SNL reduces the number of NAPE-PLD-and CB1 receptor-expressing neurons, whereas it increases the number of FAAH-immunolabelled cells. These changes are expected to result in a dramatic reduction of inhibitory signalling between anandamide of NAPE-PLD origin and the CB1 receptor in the affected neurons. The nerve injury-induced down-regulation of NAPE-PLD expression agrees with a recent report which shows that NAPE-PLD mRNA expression is reduced in the injury-affected DRG in another neuropathic pain model, the so called spared nerve injury model (Bishay et al., 2010). Importantly, nerve injury-induced down-regulation of NAPE-PLD expression is associated with a reduction in NAEA content, including that of anandamide, of the affected DRG (Mitrirattanakul et al., 2006; Bishay et al., 2010; Bishay et al., 2013). The nerve injury-induced up-regulation of FAAH expression is also in agreement with previous reports (Bishay et al., 2010), though in our earlier study (Lever et al., 2009), the increase in the proportion of FAAH-expressing neurons did not reach the level of significance. This discrepancy between our present and previous data could be due to the transient nature of up-regulation of FAAH expression, which reaches its peak on the 7th day after the injury (Bishay et al., 2010). Although we assessed nerve injury-induced changes 7 days after the surgery in both studies, due to possible slight differences in surgery techniques used by different persons, the time course of changes could be different. Nevertheless, the changes we found in CB1 receptor

expression is generally in agreement with previous reports (Costigan et al., 2002; Mitrirattanakul et al., 2006; Zhang et al., 2007). Finally, in~~In~~ addition to~~,~~ changes in the proportions of NAPE-PLD-, CB1 receptor- and FAAH-expressing neurons, the proportion of TRPV1-expressing DRG neurons are also dramatically reduced by the spinal nerve ligation. This change is similar to that reported earlier by others using the same neuropathic model (Hudson et al., 2001; Lever et al., 2009). This reduced~~The effect of nerve injury on~~ TRPV1 expression is in agreement~~and CB1 receptor expression in DRG are in agreement with previous findings (Michael and Priestley, 1999; Costigan et al., 2002; Mitrirattanakul et al., 2006; Zhang et al., 2007a; Lever et al., 2009; Bishay et al., 2010) as well as~~ with the limited role of this ion channel~~TRPV1~~ in the development of pain following peripheral nerve injury (Caterina et al., 2000).

In summary, we have shown here that a major proportion of primary sensory neurons express~~expresses~~ NAPE-PLD. We have also shown that NAPE-PLD exhibits a high degree of co-expression with TRPV1, the CB1 receptor and FAAH, which indicates that NAPE-PLD indeed could be involved in an autocrine regulatory mechanism in a major proportion of nociceptive primary sensory neurons. Finally, we have shown that while peripheral inflammation and injury to peripheral nerves induce differing changes in the expression pattern of NAPE-PLD, the CB1 receptor, TRPV1 and FAAH, both sets of changes are highly likely to produce unbalanced signalling in that autocrine regulatory system, and that unbalanced signalling is characterised primarily by reduced anandamide-induced and CB1 receptor-mediated activity hence, reduced inhibition on the activity and excitability of primary sensory neurons.~~inhibition.~~ Similar unbalanced endocannabinoid/endovanilloid signalling due to~~, peripheral~~

~~pathology induced~~ reduction in CB1 receptor-mediated inhibitory effects in primary sensory neurons as well as in the spinal cord has been reported and shown to contribute to the development of pain in various animal models of persistent pain~~previously~~ (Jhaveri et al., 2006; Khasabova et al., 2008; Guasti et al., 2009; Bishay et al., 2010; Khasabova et al., 2012; Starowicz et al., 2012; Starowicz and Przewlocka, 2012; Khasabova et al., 2013; Starowicz et al., 2013).

~~I~~mportantly, the findings we present here provide the first insight into an autocrine signalling system, which is highly likely to play an important role in regulating the excitability of a major group of nociceptive primary sensory neurons. This insight is important because it suggests that pharmacological manipulation of this system may provide a significant reduction in ~~restoring balanced endocannabinoid signalling both at the periphery and the~~ spinal nociceptive input hence reduction in pain associated with peripheral pathologies. However, full utilisation of the putative analgesic potential of this system requires further elucidation of the signalling mechanism. For example, we have shown recently that spatial proximity and protein-protein interactions between TRPV1 and the CB1 receptor may determine how the CB1 receptor affects TRPV1 activity (Chen et al., 2016). Similarly, the spatial relationship between FAAH and TRPV1 and/or the CB1 receptor, which is currently unknown, is of high importance as it determines whether FAAH activity directs ~~cord by increasing the level of~~ anandamide away from the CB1 receptor or TRPV1. Further, although our data suggest that~~produces an analgesic effect (Starowicz et al., 2012; Starowicz et al., 2013). Inhibiting FAAH activity has been considered using to increase tissue level of anandamide (Piscitelli and Di Marzo, 2012; Sousa Valente et al., 2014b).~~

Formatted: Pattern: Clear

Formatted: Pattern: Clear

Formatted: Pattern: Clear

~~However, if indeed~~, anandamide synthesised by NAPE-PLD may preferentially activate the CB1 receptor, this assumption requires further support.

It is also important to note that in order to avoid inducing undesirable effects, manipulation of the endocannabinoid/endovanilloid autocrine signalling system even outside the blood-brain-barrier should occur in a cell specific~~in Ca^{2+} sensitive and Ca^{2+} insensitive~~ manner (i.e. in nociceptive primary sensory neurons), because several components of the endocannabinoid/endovanilloid system exhibit widespread expression pattern. Hence, while the CB1 receptor and TRPV1, outside the central nervous system, are expressed almost exclusively by nociceptive primary sensory neurons (Caterina et al., 1997; Tominaga et al., 1998; Ahluwalia et al., 2000; Binzen et al., 2006; Mitrirattanakul et al., 2006; Agarwal et al., 2007; Veress et al., 2013; Sousa-Valente et al., 2014a), both NAPE-PLD and FAAH are expressed by various cells and involved in various physiological functions (Paria et al., 1999; Guo et al., 2005; Rossi et al., 2009; Alhouayek and Muccioli, 2012; Geurts et al., 2015). Nevertheless, our data indicate that NAPE-PLD could be ~~is associated primarily with CB1 receptor and TRPV1 activation, respectively, increasing anandamide levels through increasing its synthesis could be a more effective approach than reducing its hydrolysis to reduce pain. Based on the considerations discussed above, here we propose that NAPE-PLD could be~~ another important molecule of the endocannabinoid/endovanilloid system(s) which controls nociceptive processing in primary sensory neurons. Therefore, we~~We further~~ propose that ~~since changes in the expression and possibly activity of~~ NAPE-PLD in nociceptive primary sensory neurons~~could contribute to the development of pain in peripheral pathologies, NAPE-~~

Formatted: Pattern: Clear

Formatted: Pattern: Clear

~~PLD~~ could be a valuable novel target ~~molecule~~ for the development of new analgesics.

Formatted: No widow/orphan control, Don't adjust space between Latin and Asian text, Don't adjust space between Asian text and numbers

Formatted: Font color: Custom Color(RGB(33,33,33)), Pattern: Clear (White)

Conflict of Interest Statement
The authors report no conflict of interest associated with this work.

Role of Authors
Dr João Sousa-Valente: Majority of immunolabelligimmunilabellig and data analysis, behavioural experiments, writing up
Dr Angelika Varga: Immunolabelling, Western blotting, PCR, writing up
Mr Jose Vicente Torres Perez: In situ hybridisation-immunolabelling
Dr Agnes Jenes: immunolabelling, statistical analysis, writing up
Dr John Wahba: PCR
Professor Ken Mackie: writing up, finalising the manuscript
Professor Benjamin Cravatt: FAAH antibody, finalising manuscript
Professor Natsuo Ueda: NAPE-PLD-/- mice, finalising manuscript
Dr Kazuhito Tsuboi: NAPE-PLD-/- mice, finalising manuscript
Dr Peter Santha: imaging, statistics, writing up
Professor Gabor Jancso: imaging, statistics, writing up
Dr Hiran Tailor: immunolabelling
Dr António Avelino: project management, writing up
Hon Professor Istvan Nagy: project management, writing up

REFERENCES

Agarwal N, Pacher P, Tegeder I, Amaya F, Constantin CE, Brenner GJ, Rubino T, Michalski CW, Marsicano G, Monory K, Mackie K, Marian C, Batkai S, Parolaro D, Fischer MJ, Reeh P, Kunos G, Kress M, Lutz B, Woolf CJ, Kuner R. 2007. Cannabinoids mediate analgesia largely via peripheral type 1 cannabinoid receptors in nociceptors. Nature Neurosci 10(7):870-879.

Ahluwalia J, Urban L, Bevan S, Nagy I. 2003. Anandamide regulates neuropeptide release from capsaicin-sensitive primary sensory neurons by activating both the cannabinoid 1 receptor and the vanilloid receptor 1 in vitro. European J Neurosci 17(12):2611-2618.

Ahluwalia J, Urban L, Capogna M, Bevan S, Nagy I. 2000. Cannabinoid 1 receptors are expressed in nociceptive primary sensory neurons. Neuroscience 100(4):685-688.

Amaya F, Shimosato G, Kawasaki Y, Hashimoto S, Tanaka Y, Ji RR, Tanaka M. 2006. Induction of CB1 cannabinoid receptor by inflammation in primary afferent neurons facilitates antihyperalgesic effect of peripheral CB1 agonist. Pain 124(1-2):175-183.

Amaya F, Shimosato G, Nagano M, Ueda M, Hashimoto S, Tanaka Y, Suzuki H, Tanaka M. 2004. NGF and GDNF differentially regulate TRPV1 expression that contributes to development of inflammatory thermal hyperalgesia. Eur J Neurosci 20(9):2303-2310.

Bar KJ, Schaible HG, Brauer R, Halbhuber KJ, von Banchet GS. 2004. The proportion of TRPV1 protein-positive lumbar DRG neurones does not increase in the course of acute and chronic antigen-induced arthritis in the knee joint of the rat. Neurosci Lett 361(1-3):172-175.

Bennett DL, Averill S, Clary DO, Priestley JV, McMahon SB. 1996. Postnatal changes in the expression of the trkA high-affinity NGF receptor in primary sensory neurons. Eur J Neurosci 8(10):2204-2208.

Billiau A, Matthys P. 2001. Modes of action of Freund's adjuvants in experimental models of autoimmune diseases. Journal Leukoc Biol 70(6):849-860.

Binzen U, Greffrath W, Hennessy S, Bausen M, Saaler-Reinhardt S, Treede RD. 2006. Co-expression of the voltage-gated potassium channel Kv1.4 with transient receptor potential channels (TRPV1 and TRPV2) and the cannabinoid receptor CB1 in rat dorsal root ganglion neurons. Neuroscience 142(2):527-539.

Bishay P, Haussler A, Lim HY, Oertel B, Galve-Roperh I, Ferreiros N, Tegeder I. 2013. Anandamide deficiency and heightened neuropathic pain in aged mice. Neuropharmacology 71:204-215.

Bishay P, Schmidt H, Marian C, Haussler A, Wijnvoord N, Ziebell S, Metzner J, Koch M, Myrczek T, Bechmann I, Kuner R, Costigan M, Dehghani F, Geisslinger G, Tegeder I. 2010. R-flurbiprofen reduces neuropathic pain in rodents by restoring endogenous cannabinoids. PloS One 5(5):e10628.

Breese NM, George AC, Pauers LE, Stucky CL. 2005. Peripheral inflammation selectively increases TRPV1 function in IB4-positive sensory neurons from adult mouse. Pain 115(1-2):37-49.

Calignano A, La Rana G, Giuffrida A, Piomelli D. 1998. Control of pain initiation by endogenous cannabinoids. Nature 394(6690):277-281.

Caterina MJ, Leffler A, Malmberg AB, Martin WJ, Trafton J, Petersen-Zeitz KR, Koltzenburg M, Basbaum AI, Julius D. 2000. Impaired nociception and pain sensation in mice lacking the capsaicin receptor. Science 288(5464):306-313.

Caterina MJ, Schumacher MA, Tominaga M, Rosen TA, Levine JD, Julius D. 1997. The capsaicin receptor: a heat-activated ion channel in the pain pathway. Nature 389(6653):816-824.

Cavanaugh DJ, Lee H, Lo L, Shields SD, Zylka MJ, Basbaum AI, Anderson DJ. 2009. Distinct subsets of unmyelinated primary sensory fibers mediate behavioral responses to noxious thermal and mechanical stimuli. Proc Natl Acad Sci U S A 106(22):9075-9080.

Clapper JR, Moreno-Sanz G, Russo R, Guijarro A, Vacondio F, Duranti A, Tontini A, Sanchini S, Sciolino NR, Spradley JM, Hohmann AG, Calignano A, Mor M, Tarzia G, Piomelli D. 2010. Anandamide suppresses pain initiation through a peripheral endocannabinoid mechanism. Nature neuroscience 13(10):1265-1270.

Costigan M, Befort K, Karchewski L, Griffin RS, D'Urso D, Allchorne A, Sitarski J, Mannion JW, Pratt RE, Woolf CJ. 2002. Replicate high-density rat genome oligonucleotide microarrays reveal hundreds of regulated genes in the dorsal root ganglion after peripheral nerve injury. BMC Neurosci 3:16.

Cravatt BF, Giang DK, Mayfield SP, Boger DL, Lerner RA, Gilula NB. 1996. Molecular characterization of an enzyme that degrades neuromodulatory fatty-acid amides. Nature 384(6604):83-87.

Davis JB, Gray J, Gunthorpe MJ, Hatcher JP, Davey PT, Overend P, Harries MH, Latcham J, Clapham C, Atkinson K, Hughes SA, Rance K, Grau E, Harper AJ, Pugh PL, Rogers DC, Bingham S, Randall A, Sheardown SA. 2000. Vanilloid receptor-1 is essential for inflammatory thermal hyperalgesia. Nature 405(6783):183-187.

Devane WA, Hanus L, Breuer A, Pertwee RG, Stevenson LA, Griffin G, Gibson D, Mandelbaum A, Etinger A, Mechoulam R. 1992. Isolation and Structure of a Brain Constituent That Binds to the Cannabinoid Receptor. Science 258(5090):1946-1949.

Fu J, Gaetani S, Oveisi F, Lo Verme J, Serrano A, Rodriguez De Fonseca F, Rosengarth A, Luecke H, Di Giacomo B, Tarzia G, Piomelli D. 2003. Oleylethanolamide regulates feeding and body weight through activation of the nuclear receptor PPAR-alpha. Nature 425(6953):90-93.

Goodfellow CE, Glass M. 2009. Anandamide receptor signal transduction. Vitam Horm 81:79-110.

Guasti L, Richardson D, Jhaveri M, Eldeeb K, Barrett D, Elphick MR, Alexander SP, Kendall D, Michael GJ, Chapman V. 2009. Minocycline treatment inhibits microglial activation and alters spinal levels of endocannabinoids in a rat model of neuropathic pain. Mol Pain 5:35.

Hammond DL, Ackerman L, Holdsworth R, Elzey B. 2004. Effects of spinal nerve ligation on immunohistochemically identified neurons in the L4 and L5 dorsal root ganglia of the rat. J Comp Neurol 475(4):575-589.

Hargreaves K, Dubner R, Brown F, Flores C, Joris J. 1988. A new and sensitive method for measuring thermal nociception in cutaneous hyperalgesia. Pain 32(1):77-88.

Hudson LJ, Bevan S, Wotherspoon G, Gentry C, Fox A, Winter J. 2001. VR1 protein expression increases in undamaged DRG neurons after partial nerve injury. Eur J Neurosci 13(11):2105-2114.

Jhaveri MD, Richardson D, Kendall DA, Barrett DA, Chapman V. 2006. Analgesic effects of fatty acid amide hydrolase inhibition in a rat model of neuropathic pain. J Neurosci 26(51):13318-13327.

Ji RR, Samad TA, Jin SX, Schmoll R, Woolf CJ. 2002. p38 MAPK activation by NGF in primary sensory neurons after inflammation increases TRPV1 levels and maintains heat hyperalgesia. Neuron 36(1):57-68.

Kelly S, Jhaveri MD, Sagar DR, Kendall DA, Chapman V. 2003. Activation of peripheral cannabinoid CB1 receptors inhibits mechanically evoked responses of spinal neurons in noninflamed rats and rats with hindpaw inflammation. Eur J Neurosci 18(8):2239-2243.

Khasabova IA, Holman M, Morse T, Burlakova N, Coicou L, Harding-Rose C, Simone DA, Seybold VS. 2013. Increased anandamide uptake by sensory neurons contributes to hyperalgesia in a model of cancer pain. Neurobiol Dis 58:19-28.

Khasabova IA, Khasabov S, Paz J, Harding-Rose C, Simone DA, Seybold VS. 2012. Cannabinoid type-1 receptor reduces pain and neurotoxicity produced by chemotherapy. J Neurosci 32(20):7091-7101.

Khasabova IA, Khasabov SG, Harding-Rose C, Coicou LG, Seybold BA, Lindberg AE, Steevens CD, Simone DA, Seybold VS. 2008. A decrease in anandamide signaling contributes to the maintenance of cutaneous mechanical hyperalgesia in a model of bone cancer pain. J Neurosci 28(44):11141-11152.

Kim SE, Coste B, Chadha A, Cook B, Patapoutian A. 2012. The role of Drosophila Piezo in mechanical nociception. Nature 483(7388):209-212.

Kim SH, Chung JM. 1992. An experimental model for peripheral neuropathy produced by segmental spinal nerve ligation in the rat. Pain 50(3):355-363.

Lauckner JE, Jensen JB, Chen HY, Lu HC, Hille B, Mackie K. 2008. GPR55 is a cannabinoid receptor that increases intracellular calcium and inhibits M current. Proc Natl Acad Sci U S A 105(7):2699-2704.

Lawson SN, Harper AA, Harper EI, Garson JA, Anderton BH. 1984. A monoclonal antibody against neurofilament protein specifically labels a subpopulation of rat sensory neurones. J Comp Neurol 228(2):263-272.

Lawson SN, Waddell PJ. 1991. Soma Neurofilament Immunoreactivity Is Related to Cell-Size and Fiber Conduction-Velocity in Rat Primary Sensory Neurons. J Physiol (Lond) 435:41-63.

Leung D, Saghatelian A, Simon GM, Cravatt BF. 2006. Inactivation of N-acyl phosphatidylethanolamine phospholipase D reveals multiple mechanisms for the biosynthesis of endocannabinoids. Biochemistry 45(15):4720-4726.

Lever IJ, Robinson M, Cibelli M, Paule C, Santha P, Yee L, Hunt SP, Cravatt BF, Elphick MR, Nagy I, Rice AS. 2009. Localization of the endocannabinoid-degrading enzyme fatty acid amide hydrolase in rat dorsal root ganglion cells and its regulation after peripheral nerve injury. J Neurosci 29(12):3766-3780.

Liu J, Wang L, Harvey-White J, Huang BX, Kim HY, Luquet S, Palmiter RD, Krystal G, Rai R, Mahadevan A, Razdan RK, Kunos G. 2008. Multiple pathways involved in the biosynthesis of anandamide. Neuropharmacology 54(1):1-7.

Liu J, Wang L, Harvey-White J, Osei-Hyiaman D, Razdan R, Gong Q, Chan AC, Zhou Z, Huang BX, Kim HY, Kunos G. 2006. A biosynthetic pathway for anandamide. Proc Natl Acad Sci U S A 103(36):13345-13350.

Lo Verme J, Fu J, Astarita G, La Rana G, Russo R, Calignano A, Piomelli D. 2005. The nuclear receptor peroxisome proliferator-activated receptor-alpha mediates the anti-inflammatory actions of palmitoylethanolamide. Mol Pharmacol 67(1):15-19.

Luo H, Cheng J, Han JS, Wan Y. 2004. Change of vanilloid receptor 1 expression in dorsal root ganglion and spinal dorsal horn during inflammatory nociception induced by complete Freund's adjuvant in rats. Neuroreport 15(4):655-658.

Mahmud A, Santha P, Paule CC, Nagy I. 2009. Cannabinoid 1 receptor activation inhibits transient receptor potential vanilloid type 1 receptor-mediated cationic influx into rat cultured primary sensory neurons. Neuroscience 162(4):1202-1211.

Matsuda LA, Lolait SJ, Brownstein MJ, Young AC, Bonner TI. 1990. Structure of a cannabinoid receptor and functional expression of the cloned cDNA. Nature 346(6284):561-564.

Michael GJ, Priestley JV. 1999. Differential expression of the mRNA for the vanilloid receptor subtype 1 in cells of the adult rat dorsal root and nodose ganglia and its downregulation by axotomy. J Neurosci 19(5):1844-1854.

Mitrirattanakul S, Ramakul N, Guerrero AV, Matsuka Y, Ono T, Iwase H, Mackie K, Faull KF, Spigelman I. 2006. Site-specific increases in peripheral cannabinoid receptors and their endogenous ligands in a model of neuropathic pain. Pain 126(1-3):102-114.

Nagy B, Fedonidis C, Photiou A, Wahba J, Paule CC, Ma D, Buluwela L, Nagy I. 2009. Capsaicin-sensitive primary sensory neurons in the mouse express N-Acyl phosphatidylethanolamine phospholipase D. Neuroscience 161(2):572-577.

Nagy I, Santha P, Jancso G, Urban L. 2004. The role of the vanilloid (capsaicin) receptor (TRPV1) in physiology and pathology. Eur J Pharmacol 500(1-3):351-369.

Okamoto Y, Morishita J, Tsuboi K, Tonai T, Ueda N. 2004. Molecular characterization of a phospholipase D generating anandamide and its congeners. J Biol Chem 279(7):5298-5305.

Overton HA, Babbs AJ, Doel SM, Fyfe MC, Gardner LS, Griffin G, Jackson HC, Procter MJ, Rasamison CM, Tang-Christensen M, Widdowson PS, Williams GM, Reynet C. 2006. Deorphanization of a G protein-coupled receptor for oleoylethanolamide and its use in the discovery of small-molecule hypophagic agents. Cell Metabol 3(3):167-175.

Perry MJ, Lawson SN. 1998. Differences in expression of oligosaccharides, neuropeptides, carbonic anhydrase and neurofilament in rat primary afferent neurons retrogradely labelled via skin, muscle or visceral nerves. Neuroscience 85(1):293-310.

Piscitelli F, Di Marzo V. 2012. "Redundancy" of endocannabinoid inactivation: new challenges and opportunities for pain control. ACS Chem Neurosci 3(5):356-363.

Potenzieri C, Brink TS, Simone DA. 2009. Excitation of cutaneous C nociceptors by intraplantar administration of anandamide. Brain Res 1268:38-47.

Richardson JD, Kilo S, Hargreaves KM. 1998. Cannabinoids reduce hyperalgesia and inflammation via interaction with peripheral CB1 receptors. Pain 75(1):111-119.

Ryberg E, Larsson N, Sjogren S, Hjorth S, Hermansson NO, Leonova J, Elebring T, Nilsson K, Drmota T, Greasley PJ. 2007. The orphan receptor GPR55 is a novel cannabinoid receptor. Br J Pharmacol 152(7):1092-1101.

Santha P, Jenes A, Somogyi C, Nagy I. 2010. The endogenous cannabinoid anandamide inhibits transient receptor potential vanilloid type 1 receptor-mediated currents in rat cultured primary sensory neurons. Acta Physiol Hung 97(2):149-158.

Silverman JD, Kruger L. 1990. Selective neuronal glycoconjugate expression in sensory and autonomic ganglia: relation of lectin reactivity to peptide and enzyme markers. J Neurocytol 19(5):789-801.

Simon GM, Cravatt BF. 2006. Endocannabinoid biosynthesis proceeding through glycerophospho-N-acyl ethanolamine and a role for alpha/beta-hydrolase 4 in this pathway. J Biol Chem 281(36):26465-26472.

Simon GM, Cravatt BF. 2008. Anandamide biosynthesis catalyzed by the phosphodiesterase GDE1 and detection of glycerophospho-N-acyl ethanolamine precursors in mouse brain. J Biol Chem 283(14):9341-9349.

Sousa-Valente J, Andreou AP, Urban L, Nagy I. 2014a. Transient receptor potential ion channels in primary sensory neurons as targets for novel analgesics. Br J Pharmacol 171(10):2508-2527.

Sousa-Valente J, Varga A, Ananthan K, Khajuria A, Nagy I. 2014b. Anandamide in primary sensory neurons: too much of a good thing? Eur J Neurosci 39(3):409-418.

Starowicz K, Makuch W, Korostynski M, Malek N, Slezak M, Zychowska M, Petrosino S, De Petrocellis L, Cristino L, Przewlocka B, Di Marzo V. 2013. Full inhibition of spinal FAAH leads to TRPV1-mediated analgesic effects in neuropathic rats and possible lipoxygenase-mediated remodeling of anandamide metabolism. PloS One 8(4):e60040.

Starowicz K, Makuch W, Osikowicz M, Piscitelli F, Petrosino S, Di Marzo V, Przewlocka B. 2012. Spinal anandamide produces analgesia in neuropathic rats: possible CB(1)- and TRPV1-mediated mechanisms. Neuropharmacology 62(4):1746-1755.

Starowicz K, Przewlocka B. 2012. Modulation of neuropathic-pain-related behaviour by the spinal endocannabinoid/endovanilloid system. Philos T Roy Soc B 367(1607):3286-3299.

Suarez J, Bermudez-Silva FJ, Mackie K, Ledent C, Zimmer A, Cravatt BF, de Fonseca FR. 2008. Immunohistochemical description of the endogenous cannabinoid system in the rat cerebellum and functionally related nuclei. J Comp Neurol 509(4):400-421.

Sun Y, Alexander SP, Kendall DA, Bennett AJ. 2006. Cannabinoids and PPARalpha signalling. Biochem Soc T 34(Pt 6):1095-1097.

Todd AJ. 2010. Neuronal circuitry for pain processing in the dorsal horn. Nature Rev Neurosci 11(12):823-836.

Tsuboi K, Okamoto Y, Ikematsu N, Inoue M, Shimizu Y, Uyama T, Wang J, Deutsch DG, Burns MP, Ulloa NM, Tokumura A, Ueda N. 2011. Enzymatic formation of N-acylethanolamines from N-acylethanolamine plasmalogen through N-acylphosphatidylethanolamine-hydrolyzing phospholipase D-dependent and -independent pathways. Biochim Biophys Acta 1811(10):565-577.

Ueda N, Liu Q, Yamanaka K. 2001. Marked activation of the N-acylphosphatidylethanolamine-hydrolyzing phosphodiesterase by divalent cations. Biochim Biophys Acta 1532(1-2):121-127.

Valente J, Tailor H, Jenes A, Mackie K, Cravatt BF, Buluwala L, Avelino A, Nagy I. 2011. Expression of N-acyl phosphotidylethanolamine phospholipase D in rat dorsal root ganglion neurons; Proc Physiol Soc 22 P25.

van der Stelt M, Di Marzo V. 2005. Anandamide as an intracellular messenger regulating ion channel activity. Prostag Oth Lipid M 77(1-4):111-122.

van der Stelt M, Trevisani M, Vellani V, De Petrocellis L, Schiano Moriello A, Campi B, McNaughton P, Geppetti P, Di Marzo V. 2005. Anandamide acts as an intracellular messenger amplifying Ca2+ influx via TRPV1 channels. EMBO J 24(17):3026-3037.

Varga A, Jenes A, Marczylo TH, Sousa-Valente J, Chen J, Austin J, Selvarajah S, Piscitelli F, Andreou AP, Taylor AH, Kyle F, Yaqoob M, Brain S, White JP, Csernoch L, Di Marzo V, Buluwela L, Nagy I. 2014. Anandamide produced by Ca(2+)-insensitive enzymes induces excitation in primary sensory neurons. Pflug Arc Eur J Physiol 466(7):1421-1435.

Vellani V, Petrosino S, De Petrocellis L, Valenti M, Prandini M, Magherini PC, McNaughton PA, Di Marzo V. 2008. Functional lipidomics. Calcium-independent activation of endocannabinoid/endovanilloid lipid signalling in sensory neurons by protein kinases C and A and thrombin. Neuropharmacology 55(8):1274-1279.

Vilceanu D, Honore P, Hogan QH, Stucky CL. 2010. Spinal nerve ligation in mouse upregulates TRPV1 heat function in injured IB4-positive nociceptors. J Pain 11(6):588-599.

Walker KM, Urban L, Medhurst SJ, Patel S, Panesar M, Fox AJ, McIntyre P. 2003. The VR1 antagonist capsazepine reverses mechanical hyperalgesia in models of inflammatory and neuropathic pain. J Pharmacol Exp Ther 304(1):56-62.

Wang J, Okamoto Y, Morishita J, Tsuboi K, Miyatake A, Ueda N. 2006. Functional analysis of the purified anandamide-generating phospholipase D as a member of the metallo-beta-lactamase family. J Biol Chem 281(18):12325-12335.

Wang J, Okamoto Y, Tsuboi K, Ueda N. 2008. The stimulatory effect of phosphatidylethanolamine on N-acylphosphatidylethanolamine-hydrolyzing phospholipase D (NAPE-PLD). Neuropharmacology 54(1):8-15.

White JP, Urban L, Nagy I. 2011. TRPV1 function in health and disease. Curr Pharm Biotechnol 12(1):130-144.

Yu L, Yang F, Luo H, Liu FY, Han JS, Xing GG, Wan Y. 2008. The role of TRPV1 in different subtypes of dorsal root ganglion neurons in rat chronic

inflammatory nociception induced by complete Freund's adjuvant. Mol Pain 4:61.

Zhang F, Hong S, Stone V, Smith PJ. 2007a. Expression of cannabinoid CB1 receptors in models of diabetic neuropathy. J Pharmacol Exp Ther 323(2):508-515.

Zhang S, Zhao B, Jiang H, Wang B, Ma B. 2007b. Cationic lipids and polymers mediated vectors for delivery of siRNA. J Control Release 123(1):1-10.

Zhou Y, Li GD, Zhao ZQ. 2003. State-dependent phosphorylation of epsilon-isozyme of protein kinase C in adult rat dorsal root ganglia after inflammation and nerve injury. J Neurochem 85(3):571-580.

Zygmunt PM, Petersson J, Andersson DA, Chuang H, Sorgard M, Di Marzo V, Julius D, Hogestatt ED. 1999. Vanilloid receptors on sensory nerves mediate the vasodilator action of anandamide. Nature 400(6743):452-457.

Figure legends

Figure 1.

The NAPE-PLD transcript is expressed in adult rat DRG.

(A) Gel image of RT-PCR products which were synthesised from total RNA isolated from the L4-5 DRG of adult rats with primers designed to amplify NAPE-PLD (N, upper panel) and GAPDH (G, lower panel) mRNA. The size of the RT-PCR products is indistinguishable from the predicted size of NAPE-PLD (N; 199bp) and GAPDH (G; 380bp). ~~; please see also Supplementary Table 1).~~ (B) A microphotograph taken from a DRG section of an adult rat following fluorescent in situ hybridisation with 48 short NAPE-PLD complementary fluorescent dye-tagged probes. The labelling identified only neurons (arrowheads). The great majority of the positive neurons were small diameter cells. Scale bar: 20µm. (C) A microphotograph taken from another rat DRG section. That section was incubated in parallel with the one shown in (B) in identical solutions, except that the specific in situ probes were omitted from the hybridisation buffer.

Figure 2

The NAPE-PLD protein is expressed in adult rat DRG.

(A) The upper panel shows a gel~~Gel~~ image of immunoblots using an antibody raised against NAPE-PLD (Aviva System Biology) and protein samples prepared from rat DRG (R/DRG), NAPE-PLD~~). The antibody recognised a protein with the predicted size (~46kD). (B) Gel image of immunoblotts using the antibody used in (A) and protein extracts from the cerebellum (BR) of NAPE-PLD~~$^{-/-}$ mouse brain (KO/BR) or~~ ~~and~~ wild type mouse brain (WT/BR). The~~) mice. While the anti-NAPE-PLD~~ antibody in addition to recognising~~recognised~~ a protein with the predicted size of NAPE-PLD

Formatted: Superscript

(~46kD)~~46kDa), it did not recognise any protein~~ in rat DRG and WT mouse brain tissues, ~~samples from the NAPE-PLD -/- mice. Notably, the anti-NAPE-PLD antibody~~ also recognised some ~~recognises an~~ unknown proteins ~~protein(s), which is not visible~~ in all samples. However, the antibody failed to recognise the protein with the predicted size of NAPE-PLD in NAPE-PLD$^{-/-}$ mouse brain.~~samples isolated from NAPE-PLD -/- mice.~~ The lower image shows beta actin (42kD) expression as loading control. (~~B~~C) Microphotograph of a section cut from a rat dorsal root ganglion. The anti-NAPE-PLD antibody produced staining in a sub-population of primary sensory neurons (arrowheads). In addition, satellite cells visible occasionally around primary sensory neurons also exhibit NAPE-PLD immunopositivity (arrows).~~-~~ However, control experiments revealed that this staining is produced by the TSA reaction if the postfixation time is less than 24 hours. Scale bar: 30µm.

~~(please also refer to Supplementary~~ **Figure 3.**

The NAPE-PLD antibody provides specific and selective staining.

(A_1-A_4) Microphotographs (taken with the Zeiss Axiotome microscope) of ~~2). Scale bar: 50µm. (D) Microphotograph of~~ a section cut from a WT mouse (NAPE-PLD$^{+/+}$) ~~rat~~ cerebellum and immunostained using the combination of an anti-NAPE-PLD (A_1, green) and an anti-β-III tubulin (A_2, red) antibody. The section was also stained with DAPI (A_3, blue). A_4 shows the composite image of A_1-A_3. Consistent with previous findings, the ~~anti NAPE-PLD antibody. The~~ perikarya ~~as well as dendrites~~ of Purkinje cells show strong immunopositivity for NAPE-PLD (arrowheads). (B_1-B_4) Microphotographs (taken with the Zeiss Axiotome microscope)~~. In addition to dendrites of the Purkinje cells, some small perikarya also appear immunopositive for NAPE-PLD in the molecular layer. (E) Microphotograph of a section cut from wild~~

Formatted: Font: Bold

~~type (NAPE-PLD$^{+/+}$) mouse cerebellum and immunostained with the anti NAPE-PLD antibody. The staining pattern is very similar to that seen in the rat cerebellum in (D). (F) Microphotograph~~ of a section cut from the cerebellum of a NAPE-PLD$^{-/-}$ mouse and immunoreacted with the mixture of the anti-NAPE-PLD (B_1) and the anti-β-III tubulin (B_2) antibodies. The section was also stained by DAPI (B_3). B_4 shows the composite image of B_1-B_3. Note the~~anti NAPE-PLD antibody. There is a~~ complete lack of immunolabelling by the anti-NAPE-PLD antibody. Scale bar: 50µm. (C_1-C_4) Microphotographs (taken with the Zeiss Axiotome microscope)~~(G) Microphotograph~~ of a section cut from a wild type mouse dorsal root ganglion (DRG) and immunostained with the mixture of the anti-NAPE-PLD (C_1) and the anti-β-III tubulin (C_2) antibodies. The section was also stained by DAPI (C_3). C_4 shows the composite image of C_1-C_3~~antibody~~. The immunoreaction produced staining in a sub-population of neurons (arrowheads). (D_1-D_4) Microphotographs (taken with the Zeiss Axiotome microscope)~~(H) Microphotograph~~ of a section cut from a NAPE-PLD$^{-/-}$ mouse dorsal root ganglion and immunostained with the mixture of the anti-NAPE-PLD and the anti-β-III tubulin (D_2) antibodies. The section was also stained by DAPI (D_3). D_4 shows the composite image of D_1-D_3. Note~~anti NAPE-PLD antibody. There is a~~ complete lack of NAPE-PLD immunopositivity. Scale bar: 50µm. Images of DRG sections are stack images from 8 images of 1.25 µm each. Images of the cerebellum are stack images from 12 images of 1.42 µm each.

Figure 4.

~~100µm. (I)~~ **Combined staining with NAPE-PLD in situ probes and the anti-NAPE-PLD antibody reveals a high degree of co-staining.**

(A) The microphotograph shows the result of fluorescent *in situ* hybridisation in a rat

Formatted: Font: Bold

DRG section using fluorescent dye-taggedand immunofluorescent staining of rat dorsal ganglion neurons using specific fluorescent in situ probes for the NAPE-PLD mRNA (red) and the anti-NAPE-PLD antibody (green). Blue staining is produced by DAPI. Small diameter primary sensory neurons are stained both by the *in situ* probes specific for NAPE-PLD mRNA. The labelling identified a group of neurons (arrowheads). (B) The microphotograph shows the image of the same cells showed in (A) immunolabelled with the anti-NAPE-PLD antibody. Arrowheads point to NAPE-PLD immunopositive cells. (C) Microphotograph of the visual field shown in (A) and (B) but stained with DAPI. (D). Composite image of (A)-(C). Arrowheads point to double labelled cells. In this visual filed the co-staining of neurons is 100%. and the antibody (arrowheads). Scale bar: 20µm.

Figure 53.

The majority of primary sensory neurons expressing NAPE-PLD are small cells.

Cell size distribution of NAPE-PLD immunopositive (green bars) and immunonegative (greygray bars) rat dorsal root ganglion neurons. The great majority of the NAPE-PLD immunopositive cells are small cells, though some larger cells also express NAPE-PLD.

Figure 64.

The majority of primary sensory neurons expressing NAPE-PLD also express markers for nociceptive primary sensory neurons.

(A)-(I) Combined immunolabelling was produced using the anti-NAPE-PLD antibody with an antibody raised against the 200kD neurofilament NF200 (A-C) or with biotinylated IB4 (D-F-1), or with and antibody raised against CGRP (G-I). (A-C)

show a typical combined image (A) and separated images (B and C) of a section incubated with the anti-NAPE-PLD (green; B) and an anti-NF200 (red; C) antibody. NAPE-PLD shows a low degree of co-expression with NF200. (D-F) show a typical combined image (D) and separated images (E and F) of a section incubated with the anti-NAPE-PLD antibody (green; E) and a biotinylated IB4 (red; F). NAPE-PLD shows a high degree of co-expression with the IB4 binding site. (G-I) show a typical combined image (G) and separated images (H and I) of a section incubated with the anti-NAPE-PLD (green; H) and ~~and~~ anti-CGRP antibody (red; I). NAPE-PLD also shows co-expression with CGRP. Arrowheads on (D) and (G) indicate NAPE-PLD/IB4-binding site-expressing neurons and NAPE-PLD/CGRP-immunopositive neurons, respectively. Scale bar indicates 50 µm. For quantified data, please see Table 1. All images are single scan images acquired with 20X objective lens (NA: 0.50) and 47 µm pinhole aperture corresponding to 1.29 Airy unit and providing 4,6 µm thin optical sections.

Figure 7~~5~~.

The majority of primary sensory neurons expressing NAPE-PLD also express the CB1 receptor, TRPV1 and/or FAAH.

(A-C) show a typical combined image (A) and separated images (B and C) of a section incubated with the anti-NAPE-PLD (green; B) and an anti-CB1 receptor (red; C) antibody. NAPE-PLD shows a high degree of co-expression with the CB1 receptor. (D-F) show a typical combined image (D) and separated images (E and F) of a section incubated with the anti-NAPE-PLD (green; E) and an anti-TRPV1 (red; F) antibody. NAPE-PLD also shows a high degree of co-expression with TRPV1. (G-I) show a typical combined image (G) and separated images (H and I) of a section

incubated with the anti-NAPE-PLD (green; H) and an anti-FAAH (red; I) antibody. NAPE-PLD also shows a high degree of co-expression with FAAH. Arrowheads on (A), (D) and (G) indicate NAPE-PLD/CB1 receptor-co-expressing, NAPE-PLD/TRPV1-co-expressing and NAPE-PLD/FAAH-immunopositive neurons. Scale bar indicates 50 µm. For quantified data, please see Table 1. All images are single scan images acquired with 20X objective lens (NA: 0.50) and 47 µm pinhole aperture corresponding to 1.29 Airy unit and providing 4,6 µm thin optical sections.

Figure 8

Peripheral pathological conditions disturb the staining pattern observed in naive animals.

(A) Correlation between NAPE-PLD and CB1 receptor staining intensity of naive rat primary sensory neurons exhibiting co-expression of these two molecules. Note the high correlation between the intensities of two staining. (B) Correlation between NAPE-PLD and TRPV1 immunostaining intensity of naive rat primary sensory neurons exhibiting co-expression of these two molecules. Note the lack of correlation between the intensities of the two staining. (C) Correlation of NAPE-PLD immunostaining with immunostaining intensities for the CB1 receptor (CB1), TRPV1 (TRPV1) and FAAH (FAAH) in ipsilateral DRG in naive condition (empty bars), following injection of complete Freund's adjuvant (CFA, grey bars) into the paw or following ligation of the spinal nerve (SNL, black bar). Note that the strong correlation between the staining intensities of the NAPE-PLD and CB1 receptor immunostaining observed in naive animals, was significantly reduced by both CFA injection and SNL (asterisks). (D) Ratio between staining intensities on the ipsi- and contralateral DRGs for the various markers (NAPE-PLD, the CB1 receptor, TRPV1

and FAAH) in naive condition (empty bars), following CFA injection (grey bars) and following SNL (black bars). Note that CFA injection significantly (asterisk) increases the ipsilateral-contralateral TRPV1 staining intensity. While SNL appears to have the same effect, due to the reduction in the number of TRPV1 immunopositive cells, the ratio could be established only in two animals and statistical analysis was not performed. All data are expressed as mean ± SEM.

Figure 9~~6~~.

Both CFA and IFA injection into the hind paw~~hindpaw~~ reduce the number of NAPE-PLD-immunolabelled neurons without inducing any change in the number of TRPV1-, CB1 receptor or FAAH-immunolabelled neurons in DRG.

The bar chart shows the relative number of neurons exhibiting immunopositivity for NAPE-PLD, CB1 receptor TRPV1 and FAAH in naive (white bars), IFA-injected (grey bars) and CFA-injected (black bars) animals. Both IFA and CFA injection induce a small but significant reduction in the relative number of neurons exhibiting immunopositivity for NAPE-PLD. The number of immunopositive neurons for the other markers is not changed either by IFA or CFA injection. Asterisks indicate significant difference from naive (p=0.01 for IFA and p=0.02 for CFA, n=3 both for IFA and CFA; 2-tailed Fisher's exact test). All data are expressed as mean ± SEM.

Figure 10~~7~~.

Ligation of the L5 spinal nerve induces reduction in the number of neurons exhibiting immunopositivity of NAPE-PLD, TRPV1 and the CB1 receptor, whereas it induces an increase in the number of neurons exhibiting

immunopositivity of FAAH in the L5 DRG.

(A) Typical images of DRG sections cut from the ipsilateral (IPSI) L5 DRG of a sham-operated rat (SHAM) and animals subjected to ligation of the L5 spinal nerve (SNL) and incubated in anti-NAPE-PLD-, anti-CB1 receptor-, anti-TRPV1- and anti-FAAH antibodies. The number of cells exhibiting immunopositivity for NAPE-PLD, the CB1 receptor and TRPV1 is reduced following SNL whereas the number of cells exhibiting immunopositivity for FAAH is increased following SNL. (B) Comparison between the number of primary sensory neurons exhibiting immunopositivity for NAPE-PLD, CB1 receptor, TRPV1 and FAAH in the ipsilateral L5 DRG of naive (empty bars), sham-operated (grey bars) and rats subjected to L5 spinal nerve ligation (black bar). Spinal nerve ligation reduces the proportion of neurons expressing NAPE-PLD, TRPV1 and the CB1 receptor and increases the proportion of FAAH in the injured L5 DRG. ($p<0.001$~~0001~~ for TRPV1, $p<0.001$~~0001~~ for TRPV1, $p<0.001$~~0001~~ for the CB1 receptor and $p<0.001$~~0001~~ for FAAH, 2-tailed Fisher's exact test). In addition, the sham injury also reduces the number of neurons exhibiting immunopositivity for NAPE-PLD. Bar=50μm.

Table 1

Summary of the proportion of neurons expressing NAPE-PLD and other markers in L4-5 DRG of naive animals.

	Number of cells used for analysis	Percentage of neurons expressing various markers	Percentage of NAPE-PLD-expressing cells expressing various markers	Percentage of neurons expressing various markers together with NAPE-PLD
NAPE-PLD	8129	38±0.3	-	-
NF200	1313	37±0.5	31±3.9	32±3.3
IB4	1361	34±0.6	52±2.0	57±2.1
CGRP	1374	38±0.5	35±2.7	34±2.8
TRPV1	1350	42±0.7	60±1.3	54±2.3
CB1	1267	34±0.6	73±1.5	82±1.6
FAAH	1464	34±1.2	62±2.8	67±3.3

Table 2

Summary of the proportion of neurons expressing NAPE-PLD and other markers in L4-5 DRG from IFA-injected and CFA-injected animals.

		Number of cells used for analysis	Percentage of NAPE-PLD-expressing cells expressing various markers (p value)	Percentage of neurons expressing various markers together with NAPE-PLD (p value)
NAPE-PLD	IFA	3872	35±0.5 (0.09)*	-
	CFA	4181	35±0.6 (0.12)*	-
TRPV1	IFA	1392	42±0.2 (0.92)*	54±6.4 (0.31)*
	CFA	1625	43±2.2 (0.74)*	62±1.6 (0.67)*
CB1	IFA	1006	35±0.7 (0.56)*	61±1.035 (0.40)*
	CFA	1301	33±0.9 (0.66)*	65±6.4 (0.17)*
FAAH	IFA	1474	35±0.5 (0.77)*	76±9.0 (0.16)*
	CFA	1255	36±0.8 (0.52)*	69±10.6 (0.59)*

n=3 for each data point

*** p values determined with 2-tail Fisher Exact test statistical differences from p<0.05**

Table 3

Summary of the proportion of neurons expressing NAPE-PLD and other markers in ipsilateral L5 DRG from sham operated and SNL operated animals.

		Number of cells used for analysis	Percentage of NAPE-PLD-expressing cells expressing various markers (p value)	Percentage of neurons expressing various markers together with NAPE-PLD (p value)
NAPE-PLD	SHAM	1932	34±2.1 (0.04)*	-
	SNL	1962	19±1.4 (0.00)*	-
TRPV1	SHAM	668	39±3.4 (0.48)*	61±8.8 (0.60)*
	SNL	695	6±6.2 (0.00)*	5±10.1 (0.00)*
CB1	SHAM	614	33±1.2 (0.92)*	59±6 (0.04)*
	SNL	653	15±1.8 (0.00)*	49±23.8 (0.00)*
FAAH	SHAM	650	36±2.8 (0.71)*	63±9.6 (1.00)*
	SNL	614	51±6.5 (0.00)*	83±9.5 (0.00)*

n=3 for each data point

*** p values determined with 2-tailed Fisher Exact test showing statistical differences from p<0.05**

Table 4

Summary of the proportion of neurons expressing NAPE-PLD and other markers in ipsilateral L4 DRG from sham operated and SNL operated animals.

		Number of cells used for analysis	Percentage of NAPE-PLD-expressing cells expressing various markers (p value)	Percentage of neurons expressing various markers together with NAPE-PLD (p value)
NAPE-PLD	SHAM	1907	36±1.1 (0.29)*	-
	SNL	1982	38±2.7(0.85)*	-
TRPV1	SHAM	631	41±3.9 (0.82)*	51±8.8 (0.11)*
	SNL	722	36±6.3 (0.12)*	56±6.2 (0.89)*
CB1	SHAM	679	33±0.8 (0.85)*	56±14.9 (0.02)*
	SNL	618	41±1.0 (0.03)*	71±14.6 (0.34)*
FAAH	SHAM	597	37±0.3 (0.37)*	66±3.8 (0.44)*
	SNL	642	38±1.4 (0.96)*	63±10.7 (0.89)*

n=3 for each data point

*** p values determined with 2-tailed Fisher Exact test showing statistical differences from p<0.05**

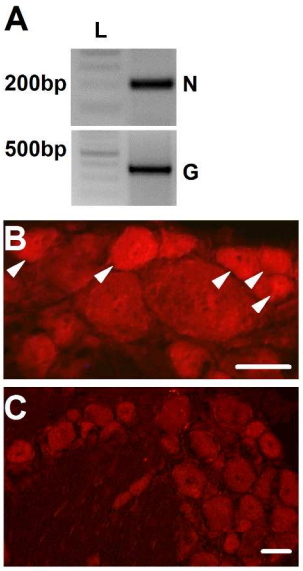

221x286mm (300 x 300 DPI)

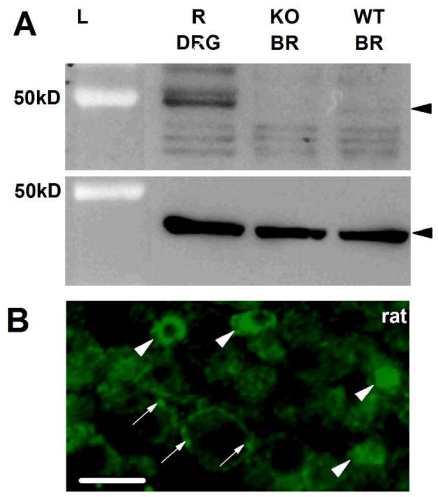

221x286mm (300 x 300 DPI)

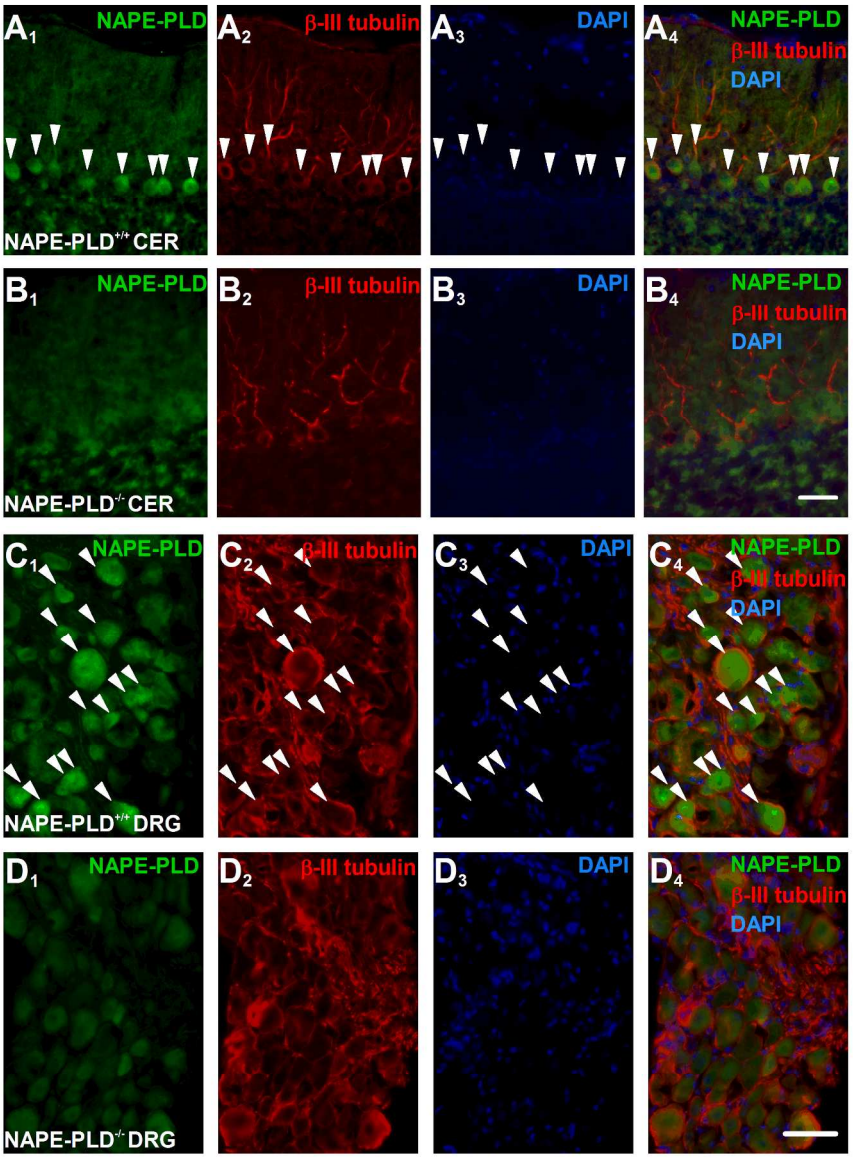

221x286mm (300 x 300 DPI)

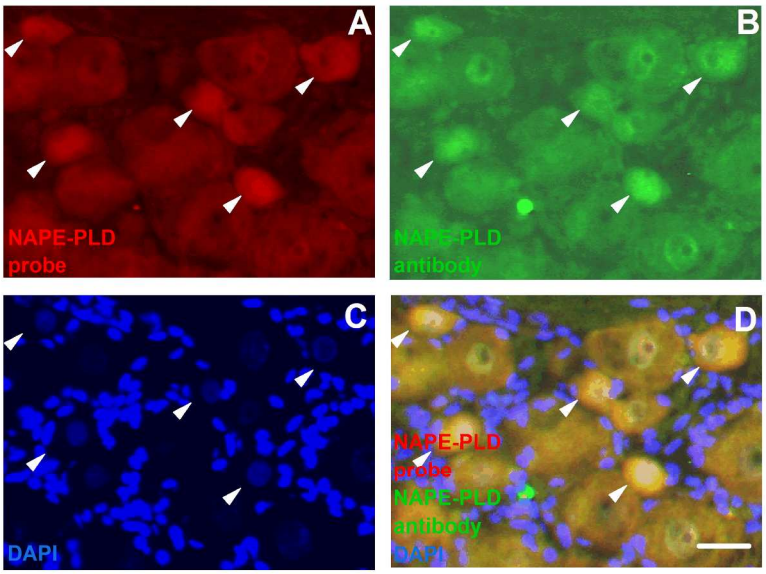

221x286mm (300 x 300 DPI)

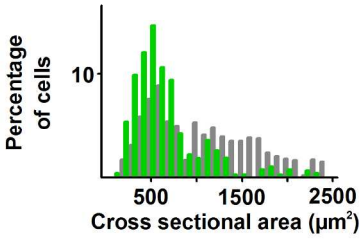

217x280mm (300 x 300 DPI)

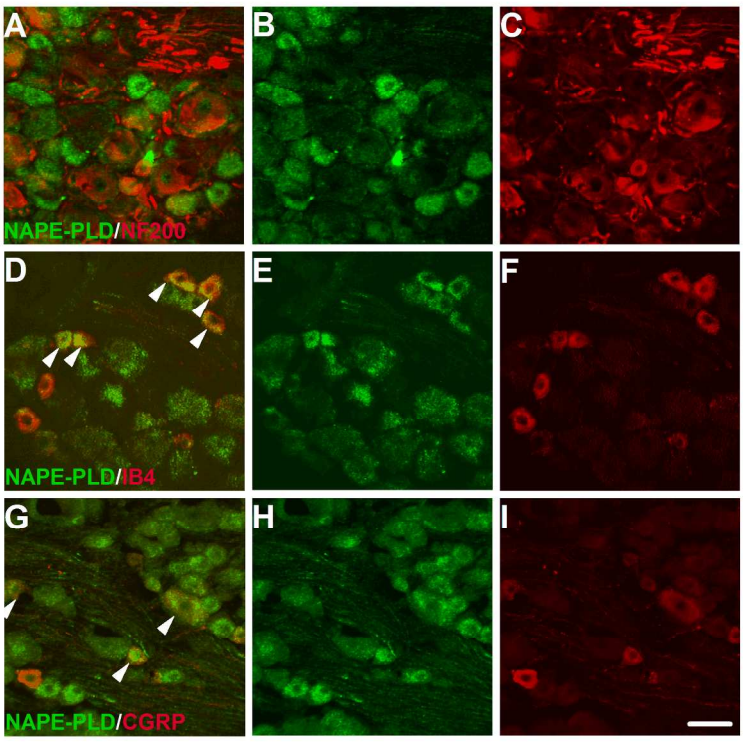

217x280mm (300 x 300 DPI)

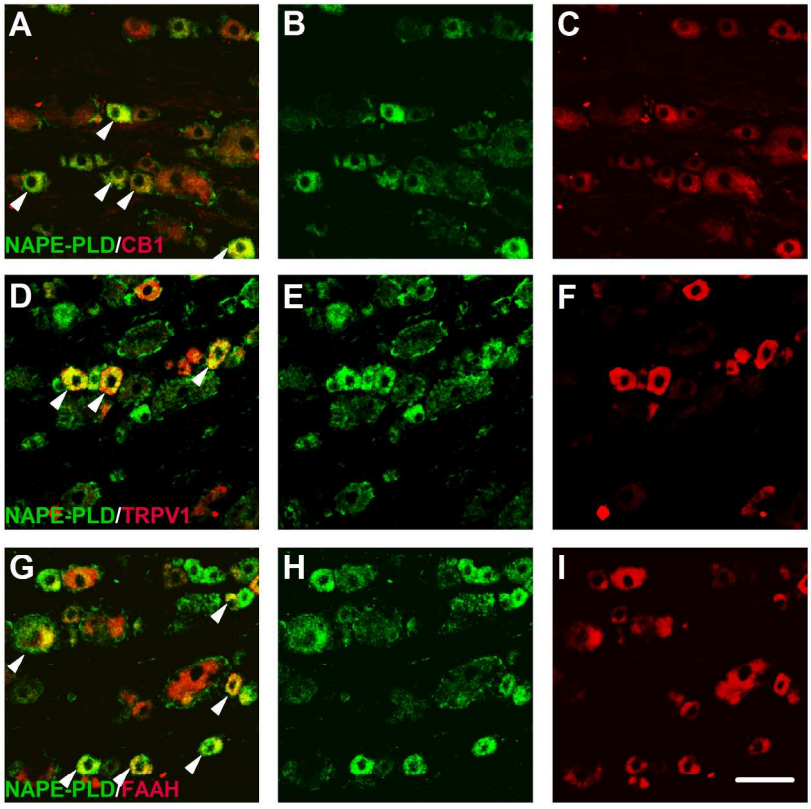

217x280mm (300 x 300 DPI)

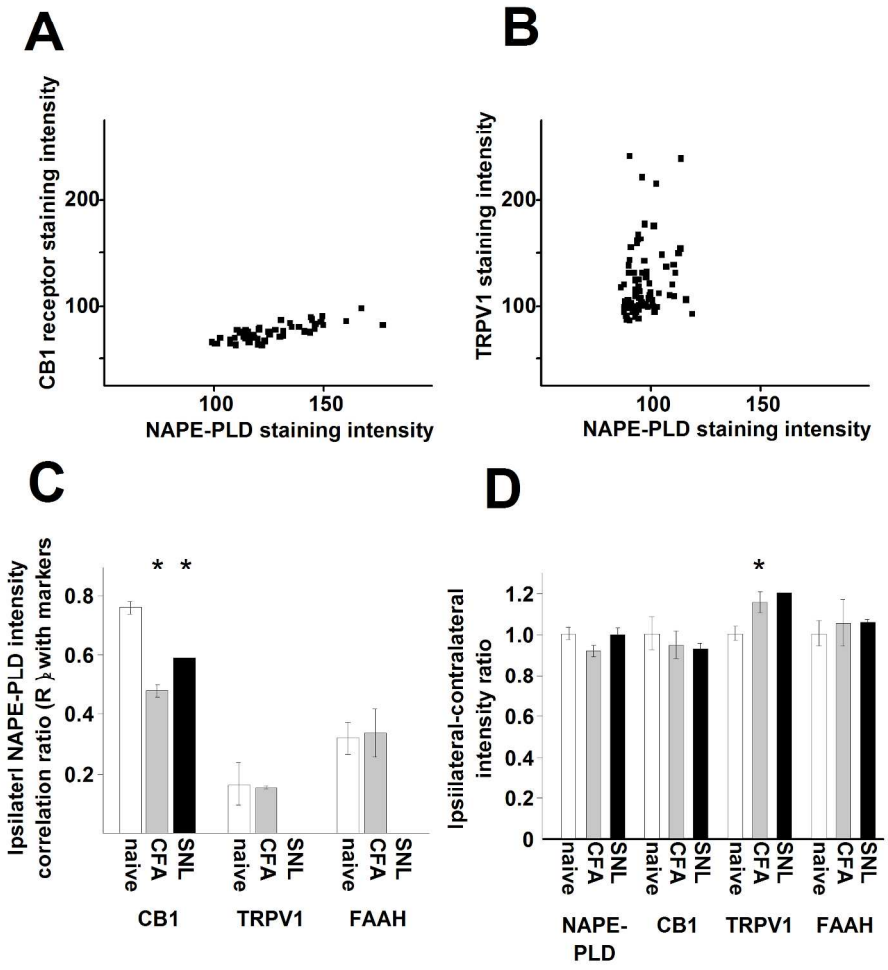

222x287mm (300 x 300 DPI)

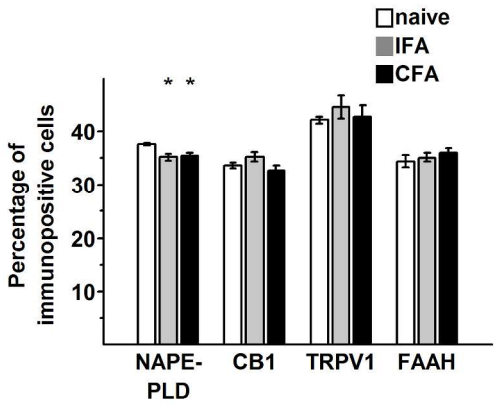

217x280mm (300 x 300 DPI)

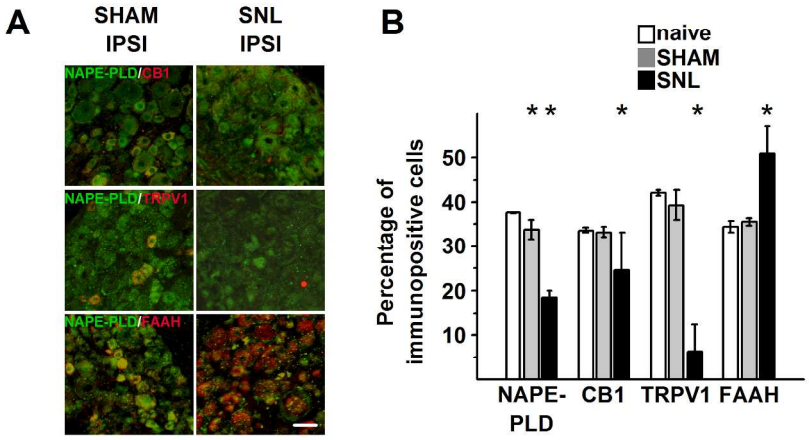

217x280mm (300 x 300 DPI)